Development of innovative composite spoiler for single-aisle aircraft

PURITH POLNIKORN

A THESIS SUBMITTED IN PARTIAL FULFILLMENT OF

THE REQUIREMENTS FOR MASTER OF ENGINEERING

IN MECHANICAL ENGINEERING

FACULTY OF ENGINEERING

BURAPHA UNIVERSITY

2020

การพัฒนาเทคโนโลยีคอมโพสิตสปอยเลอร์ของอากาศยานแบบมีช่องทางเดินเดียว

ภูริต พลนิกร

วิทยานิพนธ์นี้เป็นส่วนหนึ่งของการศึกษาตามหลักสูตรวิศวกรรมศาสตรมหาบัณฑิต
สาขาวิชาวิศวกรรมเครื่องกล
คณะวิศวกรรมศาสตร์ มหาวิทยาลัยบูรพา
2563
ลิขสิทธิ์เป็นของมหาวิทยาลัยบูรพา

Development of innovative composite spoiler for single-aisle aircraft

PURITH POLNIKORN

A THESIS SUBMITTED IN PARTIAL FULFILLMENT OF

THE REQUIREMENTS FOR MASTER OF ENGINEERING

IN MECHANICAL ENGINEERING

FACULTY OF ENGINEERING

BURAPHA UNIVERSITY

2020

The Thesis of Purith Polnikorn has been approved by the examining committee to be partial fulfillment of the requirements for the Master of Engineering in Mechanical Engineering of Burapha University

Advisory Committee   Examining Committee

Principal advisor

------------------------------------   ------------------------------------ Principal
                                                                                   examiner
(Dr. Laurent Patrick Mezeix-varagnat)   (Dr. Natthawat Hongkarnjanakul)

                                          ------------------------------------ Member
Co-advisor   (Associate Professor Dr. Kittipong Boonlong)

                                          ------------------------------------ Member
------------------------------------   ------------------------------------
(Assistant Professor Dr. Pakpong Jantapremjit) (Assistant Professor Dr. Pakpong Jantapremjit)

                                          ------------------------------------ Member
                                          (Dr. Laurent Patrick Mezeix-varagnat)

                                          ------------------------------------ External Member
                                          (Dr. Natthawat Hongkarnjanakul)

------------------------------------ Dean of the Faculty of Engineering
(Assistant Professor Dr. Nayot Kurukitkoson)

This Thesis has been approved by Graduate School Burapha University to be partial fulfillment of the requirements for the Master of Engineering in Mechanical Engineering of Burapha University

------------------------------------ Dean of Graduate School
(Associate Professor Dr. Nujjaree Chaimongkol)

61910019:   MAJOR: MECHANICAL ENGINEERING; M.Eng. (MECHANICAL
ENGINEERING)

KEYWORDS: Composite, Aircraft spoiler, CFRP, Finite Element Analysis, Innovation of
spoiler, Spoiler design

PURITH POLNIKORN : DEVELOPMENT OF INNOVATIVE COMPOSITE
SPOILER FOR SINGLE-AISLE AIRCRAFT. ADVISORY COMMITTEE: LAURENT
PATRICK MEZEIX-VARAGNAT, , PAKPONG JANTAPREMJIT 2020.

The sandwich is being used widely in weight-sensitive structures where high
flexural rigidity is required, such as in the aerospace as flaps, spoiler, cabin floor or rotor.
Sandwich structures consist of thick core material as honeycomb bonded with thin skins as carbon
fibers. When the core material contains closed cells, water ingression must be considered. This
water ingression may significantly increase the weight of the core inducing damages. In this
thesis, a new innovative spoiler design is proposed based on reinforced stiffeners in order to avoid
the use of honeycomb. In the first step, the conceptual design has been proposed by the topology
tool in order to locate the stiffeners. Secondly, the preliminary design (GFEM) has been
performed to extracted reaction force and first rough optimization. Thirdly, detailed design has
been investigated under static and buckling results. Moreover, each ply has to be respected by
aerospace stacking sequence rules. The prototype of a stiffener has been manufactured and tested
under static to validate the bonding between the stiffener and rotation feature. Simulation has
been successfully proposed and used to optimize the bonding by increasing the bonding surface.
Finally, the total mass of the stiffener is 30% higher than honeycomb spoiler.

ACKNOWLEDGEMENTS

TABLE OF CONTENTS

LIST OF TABLES

LIST OF FIGURES

INTRODUCTION

Spoilers are located on the top surface of both wings (Figure 1). They are used for three functions: to brake the aircraft during landing, to assist descent to lower altitudes without picking up speed if they are deployed on both wings. Finally, spoilers can also be used to generate a rolling motion for an aircraft, if they are deployed on only one wing. Typical spoilers on commercial aircraft are a sandwich structure where the upper surface is flat (Figure 2). Most of the problems happened on spoiler is water retention due to many factors. Thus, it is necessary to detect the water that ingress in to the sandwich panel. Therefore, NDT (Non-Destructive Testing) needs to be used to detect the water retention during the maintenance that is difficult and expensive. Indeed, controls need to be performed in hangar (Figure 3) and it is difficult to be performed for large structures especially fuselage. Moreover, NDT required times and high level of expertise.

Figure 1:Spoilers on aircraft

The project presented in this manuscript is realized in collaboration between GISTDA that financially supports it and Burapha University. The topic of the project is provided by AIRBUS. AIRBUS proposed a new design of spoiler that used stiffener instead of honeycomb to reduce the maintenance cost (Figure 4).
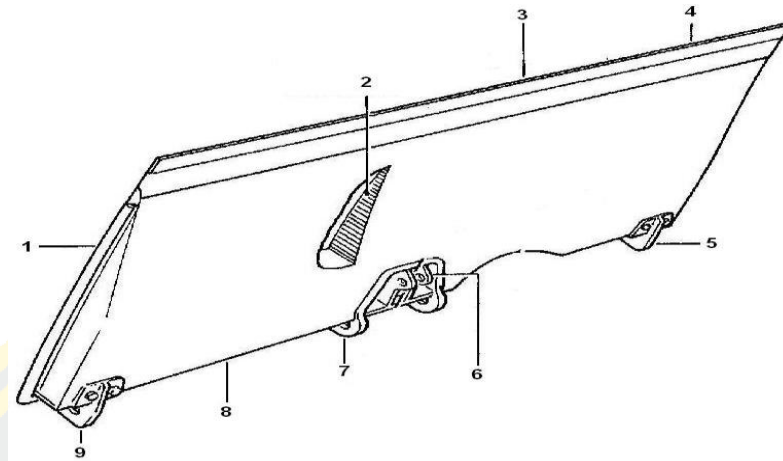
Figure 2:Sandwich structure for spoiler

Therefore, the main goal of this master's thesis is to deliver a concept design a spoiler where honeycomb is replaced by stiffener. The goal is divided into 3 different objectives that are:

I. <u>To investigate the problems of honeycomb-core spoiler</u>. Loading and constrains applied on spoiler have been determined and calculated thanks to the literature. Moreover, aerospace design rules have been identified and composite limitation has been explained.

II. <u>To propose a feasibility of a spoiler for single aisle aircraft</u>. Honeycomb is replaced by composite stiffeners in order to simplify the maintenance during the life cycle. The target is to be lightest as possible.

III. <u>To compare and validate result between simulation and experiment</u>. A stiffener has been extracted and design has been detailed. This stiffener is manufactured and tested and results are compared with the numerical simulation.

Figure 3: Maintenance aircraft in hangar
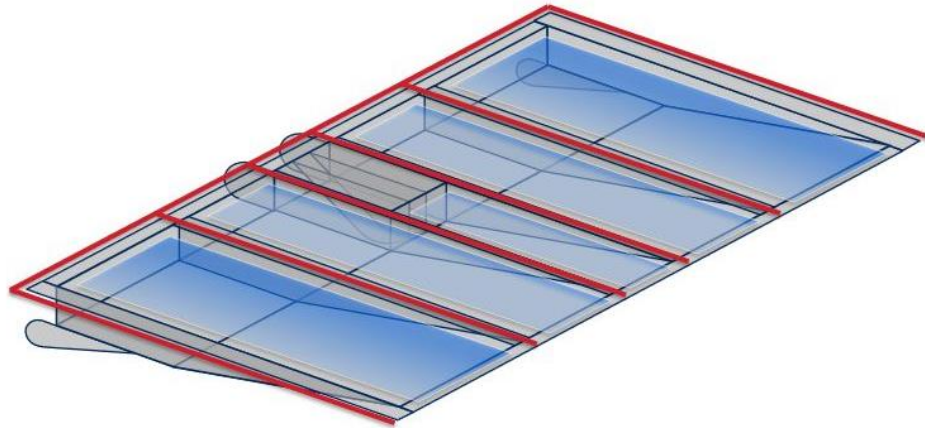
Figure 4: AIRBUS project proposal of spoiler

In order to reach these objectives, the proposed study is divided into step below:

I.   Literature Review will be firstly realized. It will be focus on aircraft spoiler with honeycomb to found problems on it. Then, focus on force and load calculation to find out the learning scope. Composite materials and application will be the next review study. Then, impact and damage tolerance need to be realized to know the design criteria also the aerospace design rules will be considered to respect the aerospace design rules in term of stacking sequence rules and ply drop off. Finally, topology optimization is will be realized and performed to found the exact location of the beam.

II.   Case Study will be described in term of geometry, loadings and materials. Calculation of the mass and the applied load of the selected spoiler will be detailed. Then, design methodology will be explained especially the method to design from the global model to the detailed model.

III.   Design process and optimization of the spoiler will be realized following the methodology and required rules previously detailed. New design will be also compared with the current one for comparison.

IV.   Finally, one stiffener will be selected, and local design will be realized. Stiffener will be manufactured and tested. Result will be compared to the simulation to validate the design.

CHAPTER 1: LITERATURE REVIEW

1.1) Aircraft Spoiler

Spoiler or lift dumper is used for three functions: brake during landing, assist descent to lower altitudes without picking up speed and auxiliary device for roll control (Figure 5a). Typical spoilers on commercial aircraft are a sandwich structure where the upper surface is flat (Figure 5b).
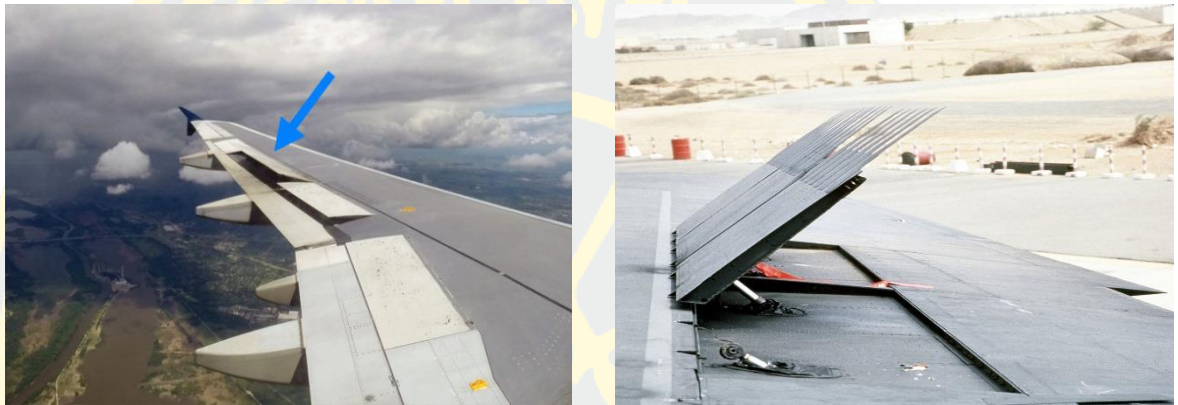
Figure 5:   (a) Spoiler service during flight,   (b) Upper surface of the spoiler

Sandwich structure consists in 2 thin skins separated by a thick core material core bonded together, in the most cases, by a film of resin. In aerospace industry only Nomex or aramid honeycomb is used as core (Figure6).
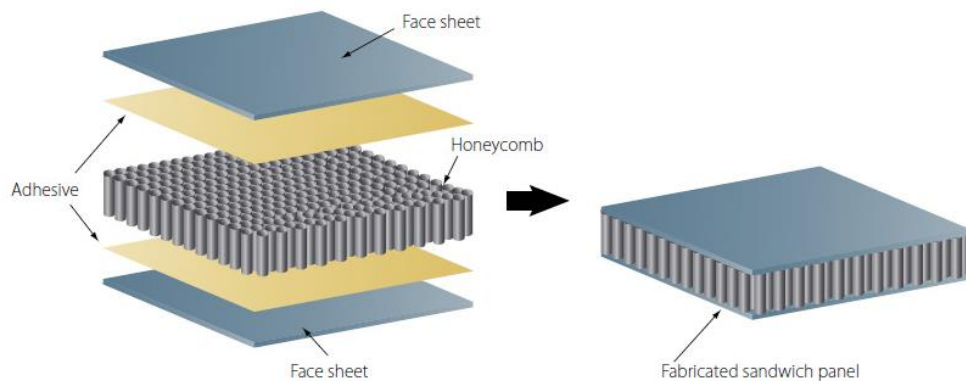
Figure 6: Sandwich structure

Sandwich panel presents a high bending stiffness and strength for a low mass or density. Skins support the in-plane stress and are stabilized to withstand bending and torsion loadings thanks to the core. The core away from the mean line the skins and therefore the flexural rigidity is increased. The increasing of mass is limited by using a low density core material. The sandwich

structure can be compared to an I-beam (Figure 7). In both case, the maximum material is located far from the mean line.
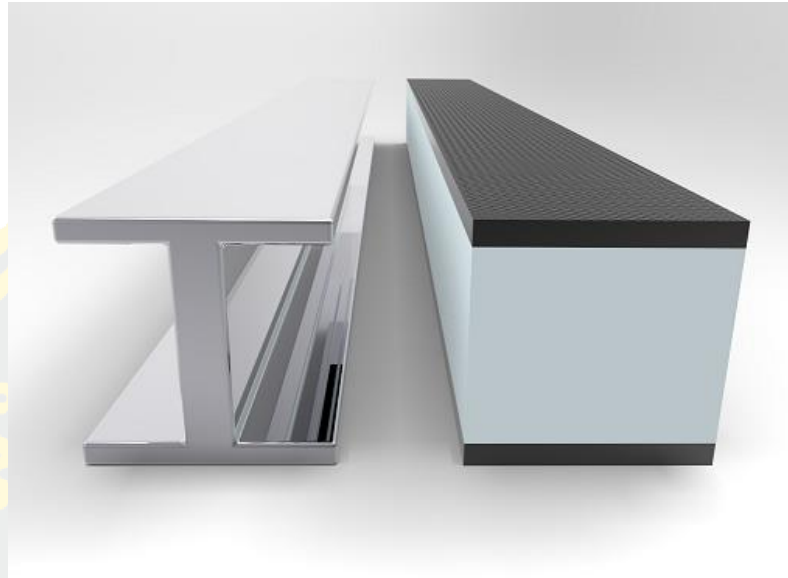
Figure 7: Comparison I beam/ sandwich beam

Sandwich structure allows to increase the rigidity for a little increasing of mass compares with metallic solution (Figure 8) (Table 1).

a)

F = 100 N

Aluminium: E = 70 GPa, r = 2700 kg/m³   5 mm

L = 100 mm

b)

Skin: Aluminium E = 70 GPa, ρ = 2700 kg/m³   F = 100 N   2.5 mm

Aluminium honeycomb: G = 310 MPa, ρ = 50 kg/m³   25 mm

L = 100 mm
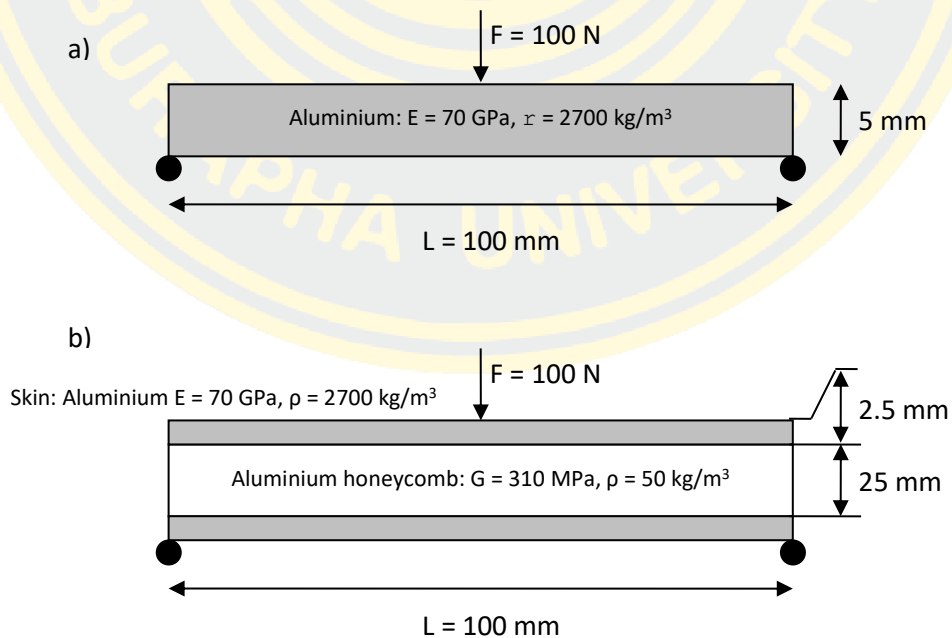
Figure 8: Comparison between beam (a) aluminium and (b) sandwich.

Table 1: Comparison of the mass, bending stiffness and defection of a beam aluminum and sandwich.

	m [g]	EI [N.mm^2]	Deflection [mm]
Aluminium beam	68	3,65E+06	0.57
Sandwich beam	74	8,51E+08	0.06

The major concern with honeycomb sandwich panels is their vulnerability to the water ingress and moisture. Indeed, humidity in the air cause water condensation depending of the flight. From the examples mentioned above, that is why the mass increasing. Failure can be found such as degradation of the adhesive bond and complete failure of panels (LaPlante, Marble et al. 2005). Moreover, the mass of the sandwich increases with the water. Therefore, control of the sandwich structure needs to be performed. For this type of structure, Non-Destructive Testing (NDT) are performed to found the failure inside the honeycomb (Figure 9). Three NDT technic to control the sandwich are available but each of them are difficult to use or results are not enough accurate.

● Ultrasonic methods: In honeycomb core sandwich panels, the signal transmission path through to the panel is limited to the small area until the cell walls. Thus, the received signal is greatly diminished compared to the applied pulse.

● Radiographic methods are based on the partial absorption of penetrating radiation (X-rays for example) as it passes through the object under investigation. This method is not preferred as in situ techniques due to safety restrictions and/or their extremely high cost.

● Thermographic methods are based on the emission of infrared radiation by the surface of the object under investigation. Thermography has been shown capable of detecting water in honeycomb sandwich panels (J.S.R 2000, V. Dattomaa, R. Marcucciob et al. 2001) .However, in the study reported by (J.S.R 2000), an aircraft panel was subjected to a temperature change by thermal soaking of the airplane in a heated hangar for a long period before exposing it to cold outdoor weather. This approach is most likely insufficient in warm conditions.
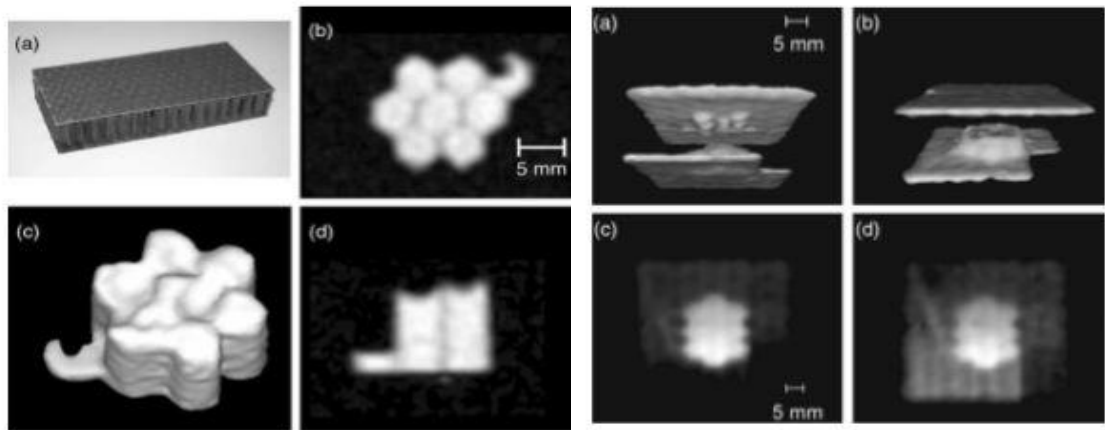
Figure 9: (a) Water inside the cell of honeycomb (b) MR (Magnetic Resonance) image of panel

Another issue is the damage of sandwich structure during the flight or maintenance (Figure 10). As all parts in aircraft damage tolerance needs to be considered and parts need to be controlled during the life cycle. In the case of sandwich, NDT must be performed to check the damage that is difficult. Indeed, Due to the core material NDT must be investigated from both side and high skill level of the inspector is required to interpret the results.

Figure 10: Aircraft inspection

Therefore, sandwich structure is avoided in the latest aircraft, A350, to reduce the maintenance time and cost

Finally, Sandwich are limited due to four main reasons.

- Water ingression

- Moisture ingression

- Impact damage

- NDT control

1.2)   Force Calculation

The spoiler is a part of the wing and while it is using a drag force, F_d is created. It is given by the Equation (1) (Sadraey)

$$F_d = \tfrac{1}{2}\,(\rho \cdot v^2 \cdot A \cdot Cd) \tag{1}$$
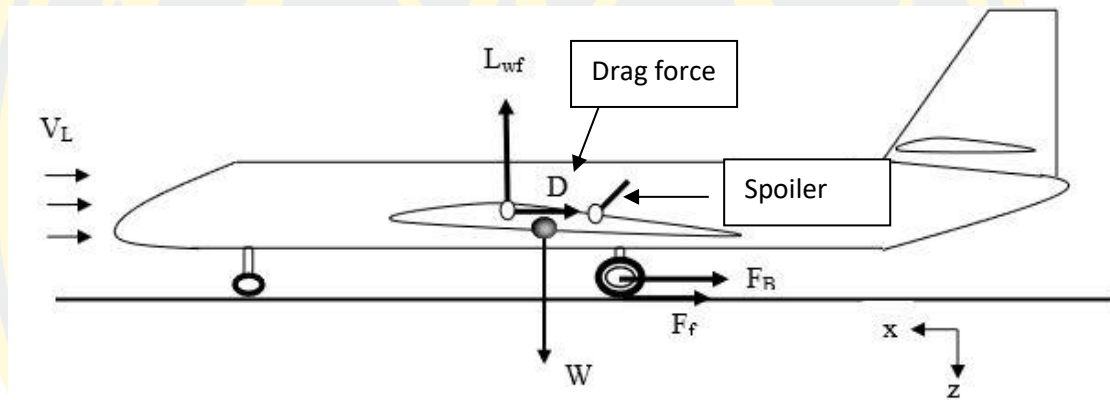
Figure 11: Force during landing operation

Where:

C_d: Drag coefficient

A: Surface of one spoiler

V: Landing Velocity

ρ: Density of air

The spoiler is on the upper surface of the wing and it is used mainly to brake the aircraft during the landing. Therefore, the lift force is not considered. In design, the force used needs to consider a safety factor. Safety factor describes the structural capacity of an aircraft system beyond the expected loads (John W. Rustenburg, Donal Skinn et al. August 1998).

Moreover, for an aircraft Load Factor, LF, is also used. LF depends of the type of aircraft and it is related to the flight and it is given by the V-n diagram (Figure 12). Thus, the V-n diagram is the most important and common plot used due to shows structural load limits as a function of airspeed. This flight envelope is normally defined during the design process. A chart of speed versus load factor (or V-n diagram) is a way of showing the limits of an aircraft's performance. It shows how much load factor can be safely achieved at different airspeeds. In this example the V-n diagram represents airspeed (horizontal axis) against load factor (vertical axis) (Figure 12).
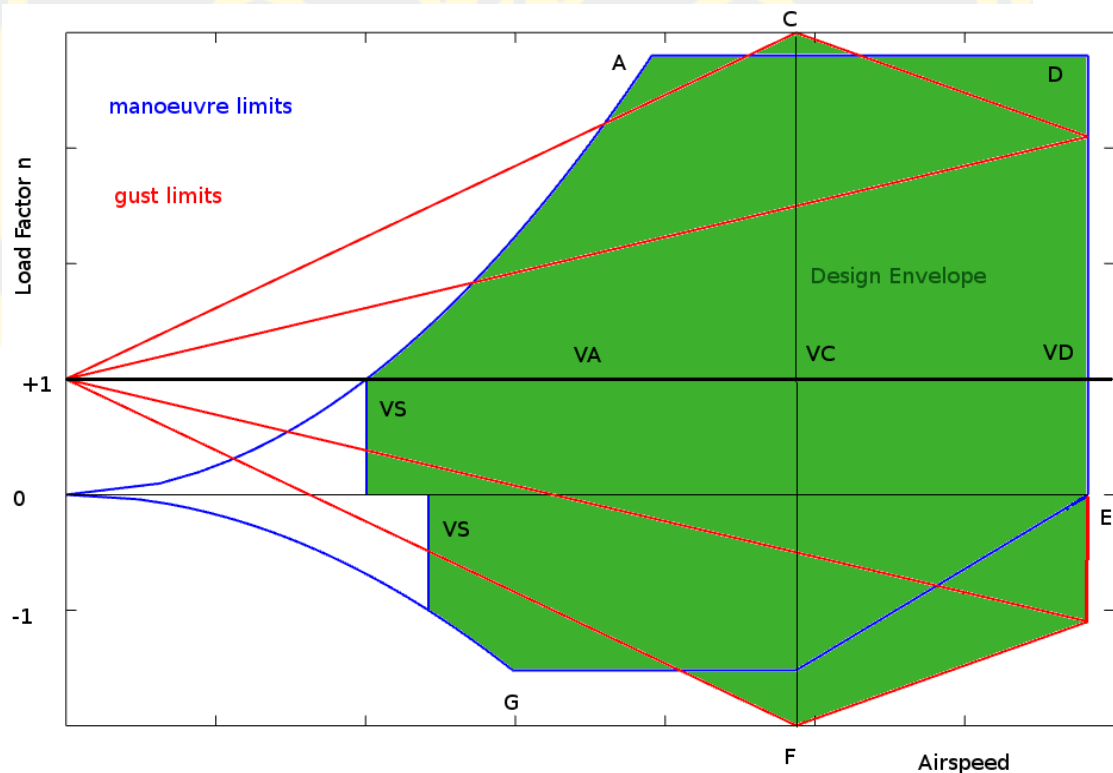
Figure 12: Typical V-n diagram in flight envelope

Finally, the Ultimate Load, UL used to design the spoiler: Equation (2)

$$UL = LL \cdot SF \qquad\qquad (2)$$

When:

LL (Limit Load): F_d * LF

F_d: Drag force on spoiler

SF: Safety factor

LF: Load factor

1.3)   Composite Materials

Composites are engineered products made from two or more different materials. A composite product provides a designed solution that surpasses the performance of the starting materials. While there are many types of composites, the most common engineered composite materials are Fiber Reinforced Polymers (FRP). FRP is often comprised of a reinforcing strong fiber in a weak polymer matrix.

Fiber/Filament Reinforcement   **Matrix**   **Composite**
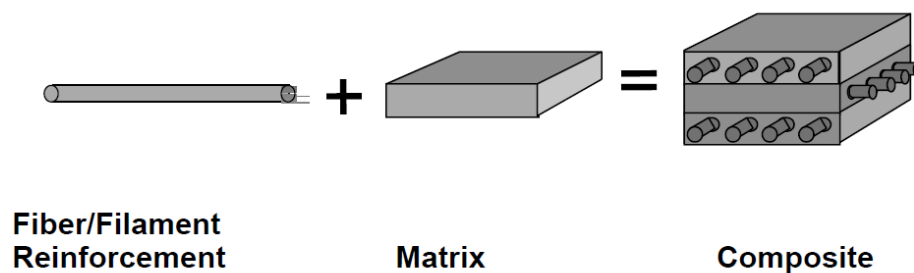
Figure 13: Fiber Reinforced Polymers (FRP)

1.3.1)   Fiber

The reinforcing fibers are commonly glass fiber, aramids, or carbon fibers in function of the applications. (Table 2)

Table 2: Composite Materials Comparison with alloy steel and Aluminum

Materials	Young Modulus (Gpa)	Yield Stress (Strength)	Density (g/cm^3)

		(Gpa)	
Carbon Fiber **(Epoxy Composite)**	300	5.2	1.8
Glass	86	3.2	2.6
Aramid	130	3	1.5
Steel	250	250	7.8
Aluminum	70	276	2.8

Uni-directional fiber

In Uni-Directional fiber, or UD, as it is commonly referred fibers are only in one direction. Since fibers work most effectively if loaded along the axis, fiber orientation becomes a critical aspect as the designer struggles to define load paths.

Woven fiber

A woven fabric contains fibers oriented on at least two axes, in order to provide great all-around strength and stiffness. A sheet of woven fabric once cured can take flexural and tensile loads on multiple axes, and even exhibits good stiffness properties off axis. However, the thickness of woven ply is higher than UD. The real benefits of woven materials, however, come from their behavior in less than ideal circumstances, such as when punctured or exposed to bearing loads. These same properties also result in better toughness, and impact strength than unidirectional material. This is reason to use a woven fiber at the tire seat and outer diameter, where the wheel is most subject to impact and damage (Figure 14).
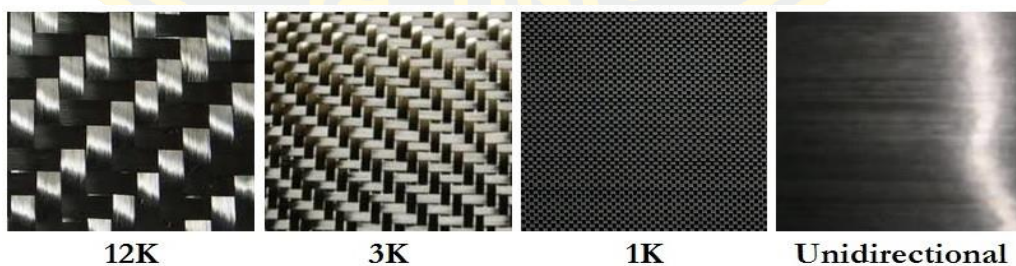
Figure 14: Types of fiber

1.3.2) Matrix

For aerospace applications, polymer matrix is typically a thermosetting resin. Epoxy resin is intensively used in structural application due to its better properties (Table 3).

Table 3: Composite Matrix Materials Comparison (Chehroudi. 2016)

Resin	Density (g/cm^3)	Tensile Strength (Mpa)	Compression Strength (Mpa)
Epoxy	1.92	1190	1001
Polyester	1.80	480-1180	210-480
Acrylic	170	308	292

1.3.3)   Laminate

When there is a single ply or a lay‑up in which all of the layers or plies are stacked in the same orientation, the lay‑up is called a lamina (Figure 15). When the plies are stacked at various angles, the lay‑up is called a laminate. Continuous‑fiber composites are normally laminated materials in which the individual layers, plies, or laminate are oriented in directions that will enhance the strength in the primary load direction (Figure 16). Unidirectional (0°) laminate are extremely strong and stiff in the 0° direction. However, they are very weak in the 90° direction because the load must be carried by the much weaker polymeric matrix. The longitudinal tension and compression loads are carried by the fibers, while the matrix distributes the loads between the fibers in tension and stabilizes the fibers and prevents them from buckling in compression. The matrix is also the primary load carrier for inter‑laminar shear (i.e., shear between the layers) and transverse (90°) tension. The relative roles of the fiber and the matrix in determining mechanical properties are summarized in (Table 3). Because the fiber orientation directly impacts mechanical properties, it seems logical to orient as many of the layers as possible in the main load‑carrying direction. While this approach may work for some structures, it is usually necessary to balance the load‑carrying capability in a number of different directions, such as the 0°, +45°, -45°, and 90° directions.
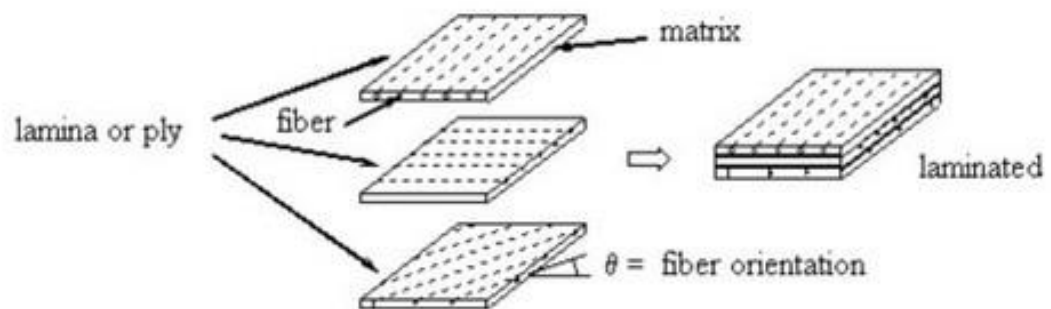
Figure 15: Ply to laminates (Rubem Matimoto Koide, Gustavo von Zeska de França et al. 2012)
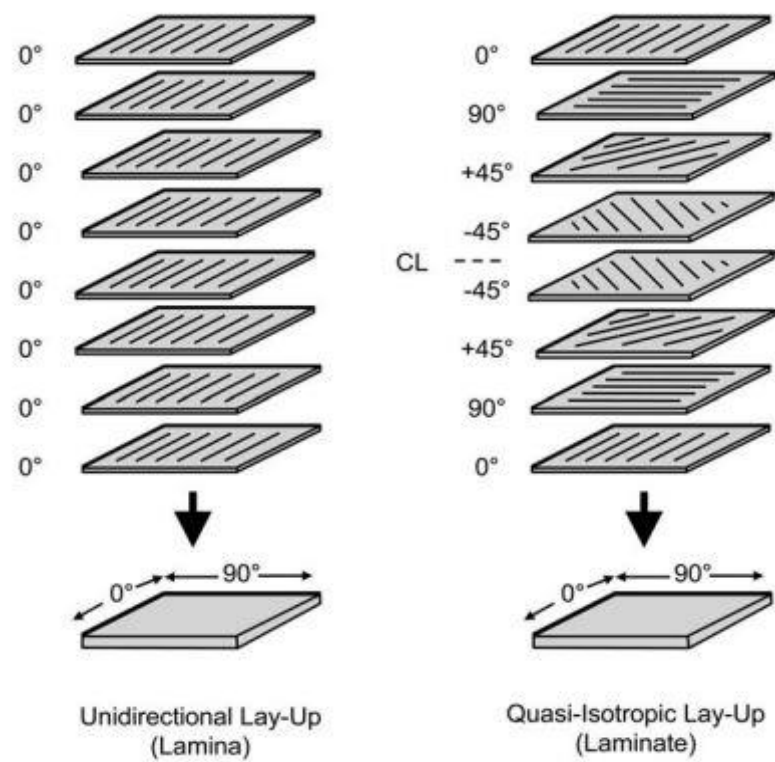
Figure 16: Lamina and Laminate Lay-ups (Campbell 2010)

In function of the application ply are combined together to make the laminates with Different orientation (Table 4).

Table 4: Effect of fiber and matrix on mechanical properties (Campbell 2010)

Mechanical Properties	Dominating composite constituent	
	Fiber	Matrix
Unidirectional		
0° Tension	✓	✗
0° Compression	✓	✓
Shear	✗	✓
90° Tension	✗	✓
Laminate		
Tension	✓	✗
Compression	✓	✓
In-Plane shear	✓	✓
Inter-laminar shear	✗	✓

Advantage

The benefits of using composite materials include:

- High Strength

- Light Weight

- Corrosion Resistance

- Dimensional Stability

- Design Flexibility

- Durability

Most of the time, the use of composite materials on an aircraft structure reduces weight. Fiber-reinforced matrix systems are stronger than traditional aluminum found in most aircraft, and they provide a smooth surface and increase fuel efficiency. Composite materials don't corrode as easily at other types of structures. They don't crack from metal fatigue and they hold up well in structural flexing environments.

Disadvantages

Composite materials don't break easily, but that makes it hard to tell if the interior structure has been damaged at all. In contrast, aluminum bends and dents easily, making it easy to detect structural damage; the same damage is much harder to detect with composite structures. Repairs can also be more difficult when a composite surface is damaged. The resin used in composite material weakens at temperatures as low as 150 degrees, making it important for these aircraft to avoid fires. Fires involved with composite materials can release toxic fumes and micro-particles into the air. Temperatures above 300 degrees can cause structural failure.

Finally, composite materials can be expensive, but the high initial costs are typically offset by long-term cost savings.

1.4)   Applications

In aeronautics, due to the high-performance requirements and to the necessary to reduce the fuel consumption, lightweight structures need to be developed and optimized. One of the ways to reduce the weight of the structures is to adopt composite laminates and sandwich structures (Figure 17). The idea of sandwich for aeronautical structures dates from the 30s. However, their use remains largely restricted to secondary structures as spoiler, floor panels, and interior monuments (Figure 18 and 19).
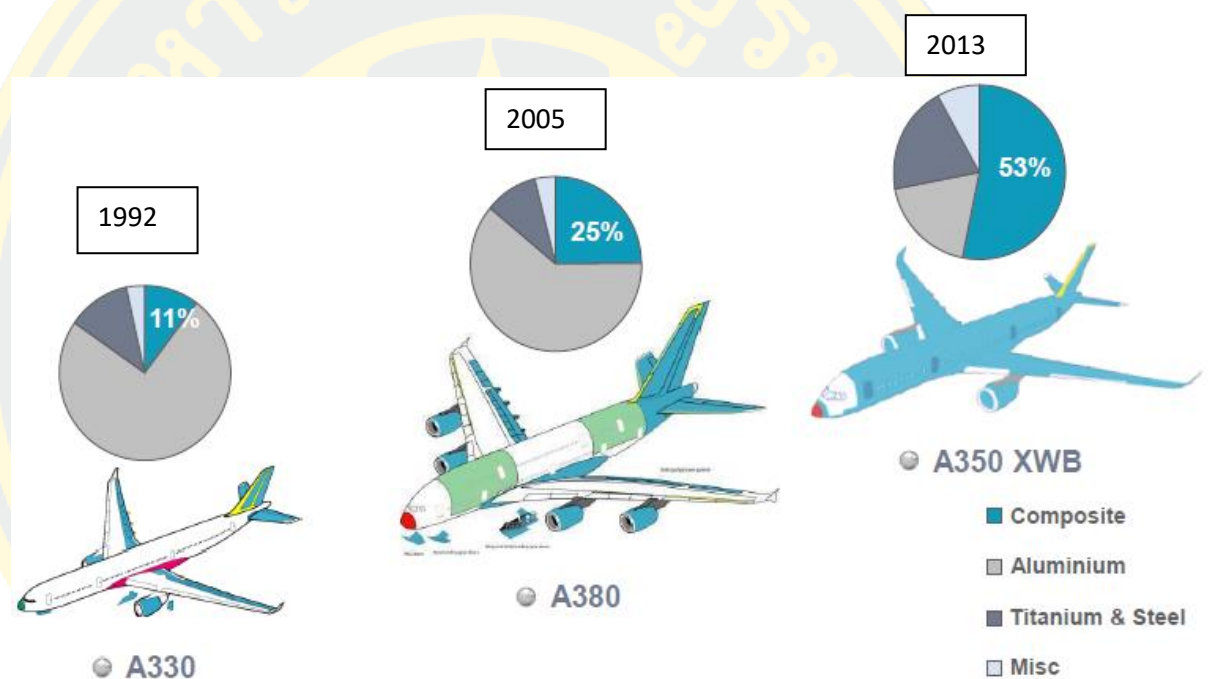
Figure 17: Material comparison, from A330 to A350 [AIRBUS]

Figure 18: Composites used in Aircrafts [AIRBUS]

Figure 19: AECO Americas interior mechanics remove a floor composite panel

1.5)   Impact and Damage Tolerance

In aerospace, composite and sandwich structure can be impacted during the aircraft life: drop tools during the manufacturing and maintenance, removable panel drop, runway debris, ice… It appears that most part of damages occurs during the ground handling (Figure 20).
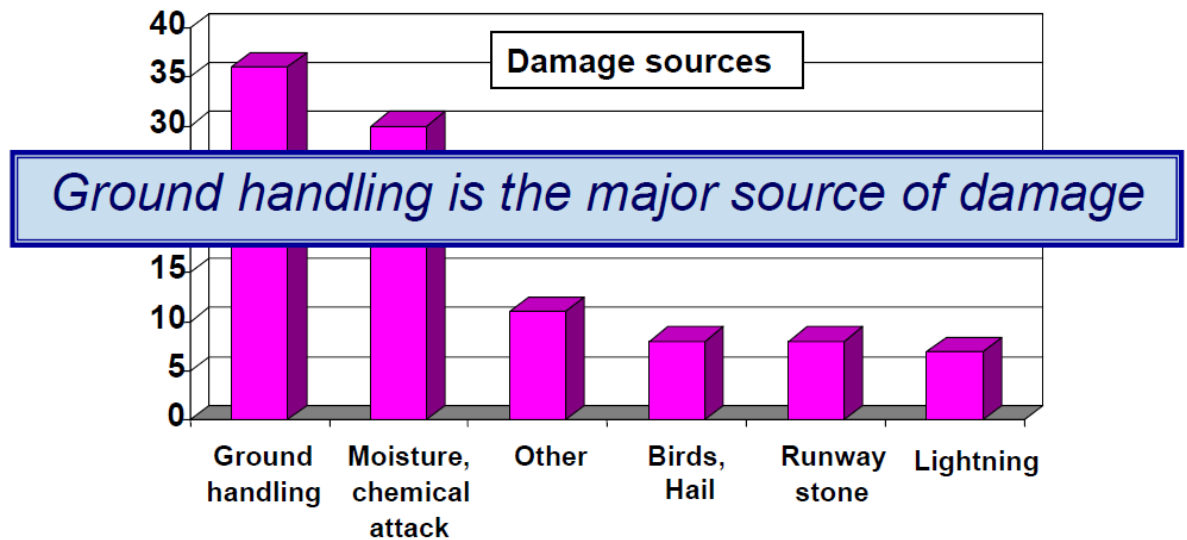
Figure 20: Damage sources [AIRBUS]

These types of impact are called low velocity low energy impact and the damage is not visible on the impact side but the sandwich is strongly damaged. The mechanical strength after impact can be reduced of 50%. For impact, the damage metric used for detectability is the dent depth or permanent indentation. Permanent indentation criterion (BVID) as a damage metric is widely used for composites (Figure 21). It provides a reasonable level of robustness for the structure design. BVID is the minimum impact damage surely detectable by scheduled inspection using typical lighting conditions from a distance of 1.5 meters. It corresponds to a probability of detection of 90% with an interval of confidence of 95% [TROPIS, 1994].

- Typical dent depth: 0.25 mm to 0.5 mm

- 0.3 mm dent depth for a Detailed inspection (DET)

- 1.3 mm dent depth for General Visual Inspection (GVI)

The permanent indentation is not the value determined after the impact. Indeed, there is a relaxation phenomenon that reduces the indentation. This relaxation reduces of 30 % de the indentation after impact.
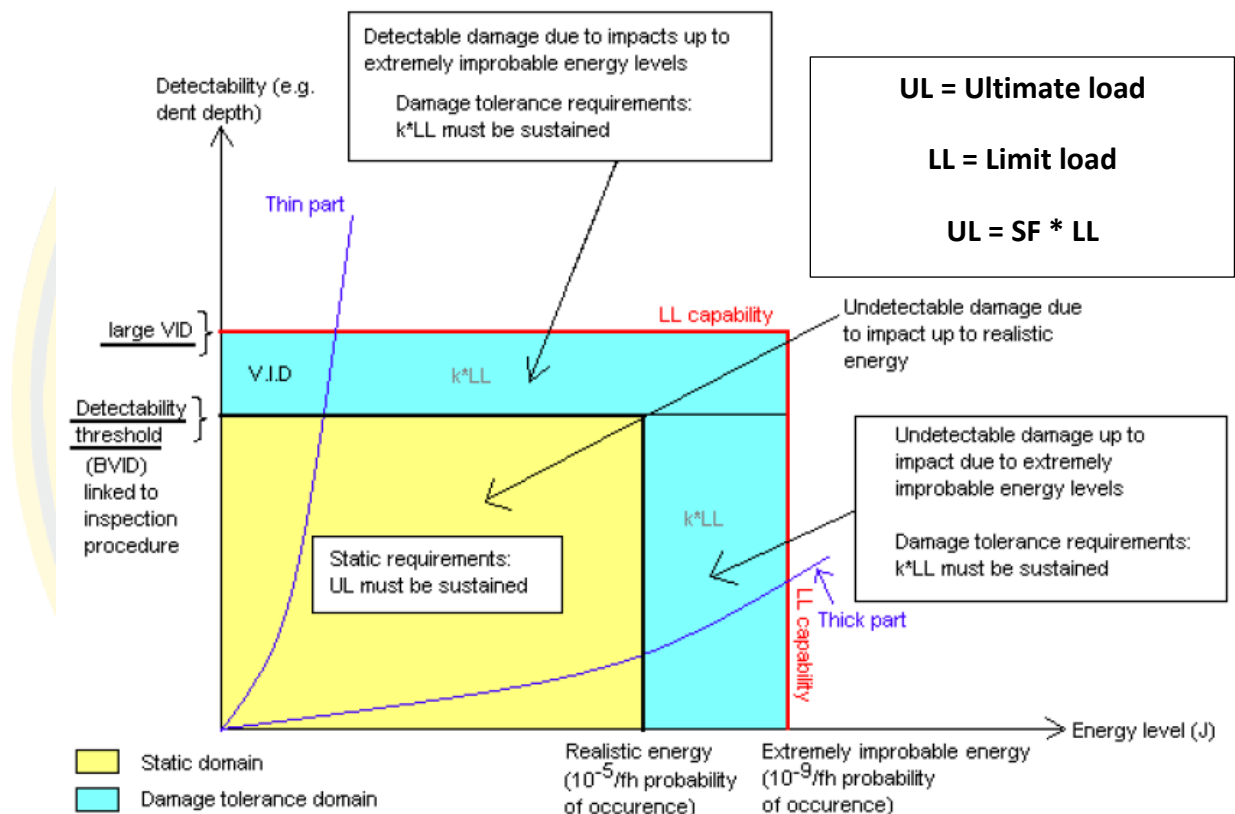
Figure 21: BVID used by AIRBUS.

When the damage has been visibly detected, repairing of the sandwich structure is going to be the next concern. Due to the difficulty of NDT testing, there is including of high cost to hire a very effective inspector to detect the problems as mentioned above in term of maintenance (Figure 22).

Figure 22: Non-Destructive testing maintenance

Sandwich structures are sensitive to impact; even a small velocity and a small energy can damage the skin and the core and reducing until 50% the initial stiffness of the structure (VIZZINI, 2004).

The damages in a sandwich structure made by CFRP and aramid honeycomb can be summarized as follow (VIZZINI, 2004, RAGHU, 2009). The impact damages are different in each part of the sandwich: core shear, delamination, matrix cracking and fibres breakage (Figure 23). Moreover, the skin damages are the same as for laminate only (VIZZINI, 2004). Furthermore, these damages are located in the upper side of the sandwich: upper skin and core material, while the lower part: lower skin, lower core/skin interface are not damaged (Figure 24).
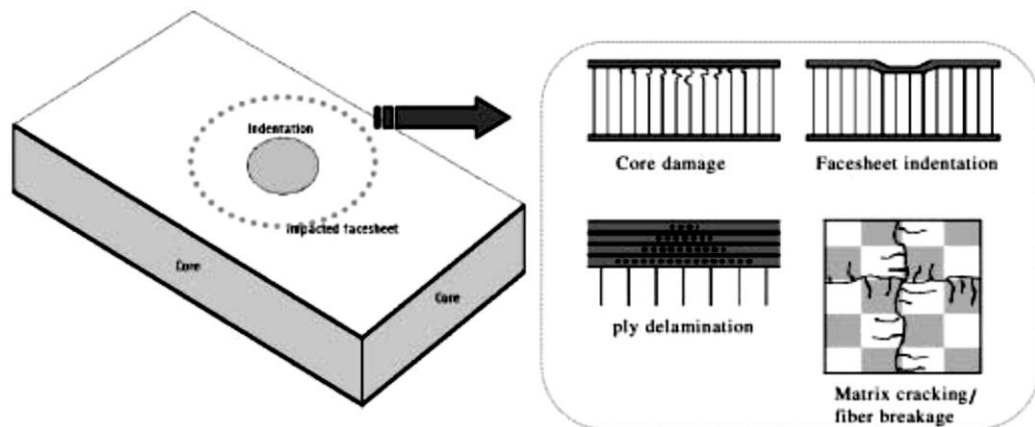
Figure 23. Main damage in an impacted sandwich structure (RAGHU, 2009).
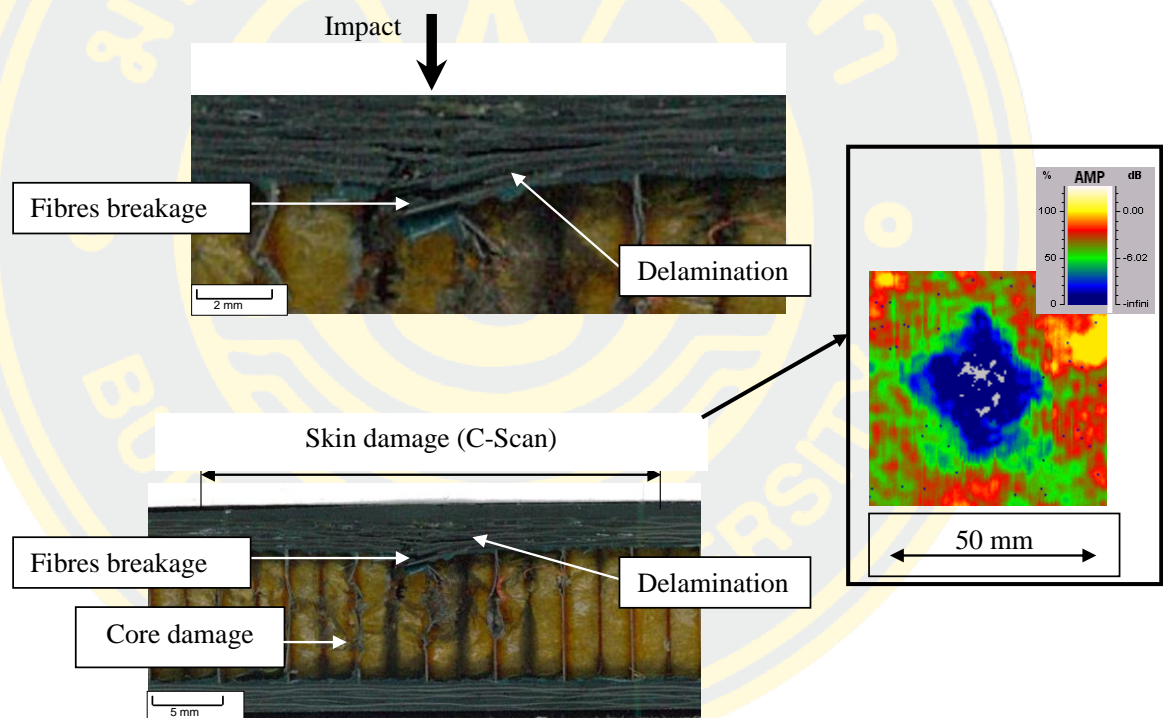
Figure 24. Observation of the damages in a sandwich structure after an impact of 25 J (MEZEIX, 2010).

In this thesis the CFRP (IMA/M21E) it's used with damage tolerance criterion, the strain in compression is therefore -4048 $\mu\varepsilon$ (Figure 25). For example, if the computing result shows that some component has strain value higher than | -4048 | $\mu\varepsilon$ it will be presumed that has a failure. Therefore, this criterion is going to be used to find damage to the result of the simulation.

FAW (gr / m²)	134	194	268	
CPT (mm / ply)	0.127	0.184	0.254	
Density (gr / cm3)		1.58		
Modulus				
Elongitudinal (GPa)		154		
Etension (GPa)		163		
Ecompression (GPa)		145		
Et (GPa)		8.5		
Glt (GPa)		4.2		
ν (Poisson coeff.)		0.35		
Strength				
F11t (MPa)		2610		
F11c (MPa)		-1450		
F22t (MPa)		55		
F22c (MPa)		-285		
F12s (MPa)		105		
Bearing (MPa)		1015		

Strain criterion in compression due to the force applied on upper surface

Damage Tolerance – Edge Impact			
Boxes	**Compression AR/RT (average value)**	-4560με for t<10mm -54.6*t-4014 for 10<t<15mm -4833 for t>15mm For lay-up effect, bending effect and curvature law: see ref 29	B-value KDF = 0.83 t = laminate thickness
	Tension AR/RT(b-value)	10000 με	Given in B-value
Fuselage (including MLGB)	**Compression AR/RT (average value)**	% of 0° fibre ≤ 60%	% of 0° fibre ≥ 60%
		-4084 με	40.93 x % of 0° - 6540
		Bvalue KDF	0.83
	Tension AR/RT (b-value)	9250 με	
	Radius Curvature law	-ε_{comp}*(1+16.95*R$^{-0.75}$) with a max at -6445με (AR/RT – B-value) and ref [32] for door corner	

Figure 25: CFRP (IMA/M21E) datasheet

1.6)   Aerospace design rules

Aerospace design must follow a large number of rules in order to comply with aircraft manufacturer. These rules come from many years of experiences of the main aircraft manufacturer (Airbus and Boeing). These rules must be the most possible respected to avoid manufacturing problems, mechanical failure.

1.6.1)   Stacking Sequence Rules

The following stacking sequence rules must be following to get especially orthotropic laminates or, otherwise, minimize coupling effect and help the manufacturing process.

Rules 1: Symmetry

The stacking sequence should be symmetric around the neutral axis: for each ply in direction $+\theta i$ at a distance Z of the middle plane, exists a ply in direction $+\theta i$ at a distance -Z, θi being the angle with regard to the main load direction

If perfect symmetry is not possible, the "asymmetry" shall be kept as close as possible to the middle plane. These cases should be analyzed to prevent manufacturing deformations.

Table 5: Rule 1 - Symmetry (AIRBUS 2009)

45º	45º
90º	90º
135º	135º
0	0º
Middle	0º
0º	0º
135º	135º
90º	90º
45º	45º
OK	OK

Rules 2: Balanced

The laminate should be balanced: for each ply in direction + θi exists a ply in direction - θi. If perfect balance is not possible, the "Unbalance" shall be kept as close as possible to the middle plane. These cases should be analyzed to prevent manufacturing deformations.

Table 6: Rule 2 – Balancing (AIRBUS 2009)

Angle	Number of Plies	
	20	20
0 º	10	10
45 º	4	6
135 º	4	2
90 º	2	2
	OK	Avoid

However, even for symmetrical and balanced laminates, other mechanical coupling can appear. These coupling can be minimizing with the following rules

Rule 3: plies orientation percentage

For solid laminate part the percentage of the plies laid‑up in each direction should be comprised between 8 percent and 67 percent

Resultant compression load due

Primary Load direction 0

Minimum 8
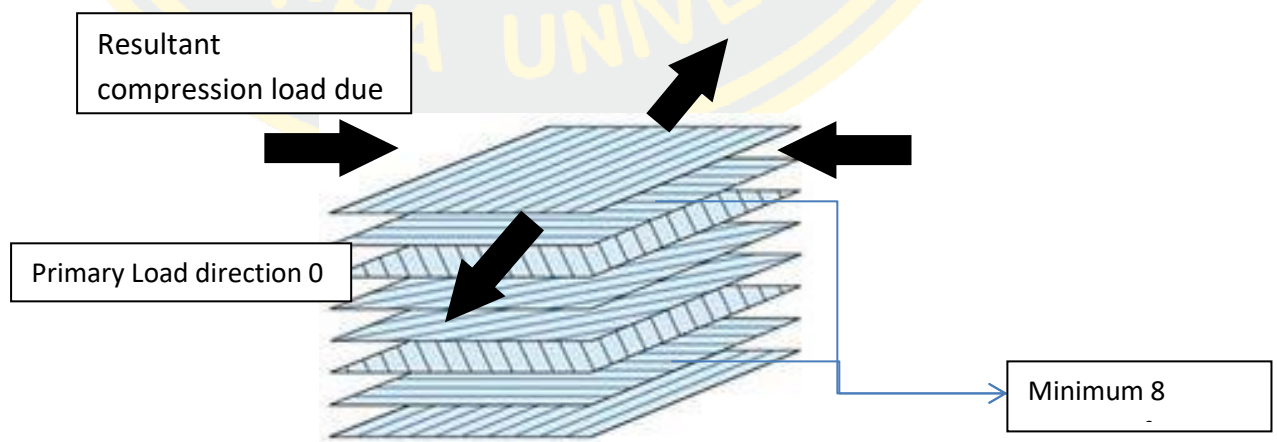
Figure 26: Rule 3 –Plies orientation percentage (AIRBUS 2009)

Rule 4: External Plies

External plies should never be in the direction of the main load. It is recommended to use a 45º/135º pair for the outer plies of the laminate. However, in certain application (CWB), a 90º external ply could be used.

Table 7: Rule 4 – External plies (AIRBUS 2009)

45º	0º
135º	45º
0º	135º
135º	90º
45º	135º
90º	45º
Middle	Middle
90º	45º
45º	135º
135º	90º
0º	135º
135º	45º
45º	0º
OK	AVOID

Rule 5: Regular distribution of layer orientation

The layer with the same orientation should be uniformly distributed throughout the stacking sequence to minimize coupling effect and ensure a homogeneous stress distribution throughout the laminate.

Table 8: Rule: 5 Regular distribution of layer orientation (AIRBUS 2009)

45º	45
135 º	135
90 º	90
135 º	90
45 º	90
0 º	135
45 º	45
135 º	0
90 º	45
45 º	135
135 º	135
0 º	45 º
135 º	0 º
45 º	135 º
90 º	45 º
Middle	Middle
OK	NOT PREFERED

Rule 6: Maximum grouping

The maximum number of plies grouped together in the same direction is limited. This maximum number depends on the ply thickness, using the lower of;

N (max) = 4 plies or t(max) = 1.0 mm

Table 9: Rule 6 – Maximum grouping (AIRBUS 2009)

	45
45	135
135	90
90	135
135	45
45	0
0	0
0	0
0	0
0	0
135	135
45	45
90	90
Middle	Middle
OK	AVOID

However, a maximum of three plies is recommended. In cases where the laminate is especially thick, and under agreement with Stress and Manufacturing, n (max) could be increased.

Rule 7: Improve buckling behavior

In the case of compressive load, placing 0º direction layers as far from the symmetry line as possible increase the buckling allowable. In the other load case (shear and combined), no simplified rules are available with respect to the fiber location to the neutral axis.

1.6.2)   Grouping Plies

These two criteria are rarely used together. The use of one or the other depends on the geometry, laminate thickness. Etc., so a check with stress is highly advisable.

To minimize coupling effects, It is recommended to group the 45º and 135º plies in pairs 45º/   135º.   The   following   stacking   sequence   criterion   is   recommended: (45º/135º/…/135º/45º/…/135º/45º/…/45º/135º/…).

Figure 27: Grouping plies to minimize coupling effects (AIRBUS 2009)

45	45
135	135
0	0
135	135
45	45
90	90
135	135
45	0
0	45
45	45
135	135
0	0
Middle	Middle
OK	Not Preferred

To minimize inter‑ laminar shear effects, it is recommended to lessen the angle between two adjacent plies. 90º direction plies should not be placed adjacent to 0º plies.

Table 10: Grouping plies to minimize inter-laminar shear effect (AIRBUS 2009)

45	45
0	0
135	90
90	135
45	45
0	0
135	135
Middle	Middle
135	135
0	0
45	45
90	135
135	90
0	0
45	45
OK	Not preferred

This recommendation is especially important when several 0º plies are grouped together (up to 4 according to Rule 6).

1.6.3)   Special Laminates for Fastened Areas

In the area where fastened are present, the following rules should be applied to the laminate.

- A minimum of 40% of ± 45º plies is used to improve the bearing stress allowable. When shear strength is the main load case, this percentage should be around 50%

- For cases working mainly in tension/compression, at least 50% of 0º plies is recommended.

- A minimum of 10% of 90º (perpendicular to main load direction) plies minimizes the shear out failure

- For the pull‑Through failure it is advisable to size the joint fir bearing. Using a minimum of 40% of ±45º plies (pad-up, if necessary). Protruding head fasteners, a washer under the collar and wide bearing head fasteners are preferred.

- To maximize fastener strength, apply a pattern as close to quasi‑isotropic (25/50/25) as possible

- When using tape, a local woven fabric fiberglass ply on the outer face to the hole exit is advisable to avoid the risk of delamination during the drill process. This ply can be locally added, i.e. just in the fastener areas, to help reduce weight. Alternatives are being analyzed for drilling in repair.

1.6.4)   Ply Drop offs

Staggering patterns

At the start and end of a ramp, the plies to drop should be those closest to the middle plane to optimize structural behavior.
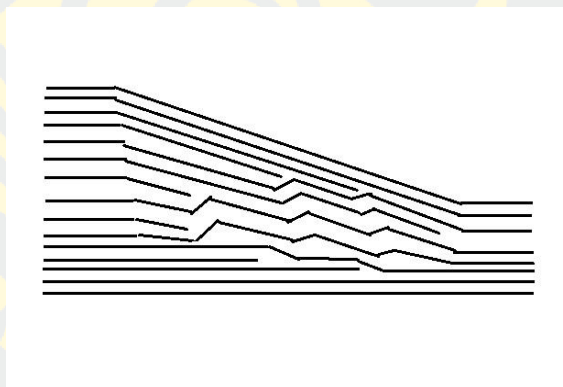
Figure 28: Staggering pattern (AIRBUS 2009)

External plies

At least the two most external plies shall be continuous (see Figure 29.)
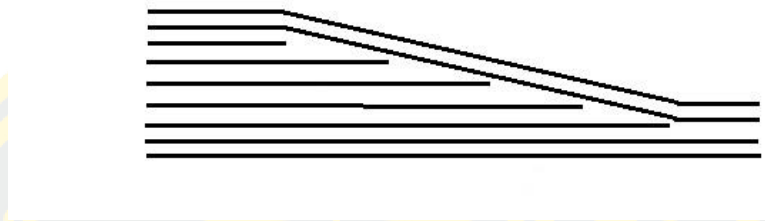
Figure 29: External plies (AIRBUS 2009)

Covering Ply

Every 4 dropped plies there should be, at least, one ply covering those 4 dropped plies (see figure 30.)
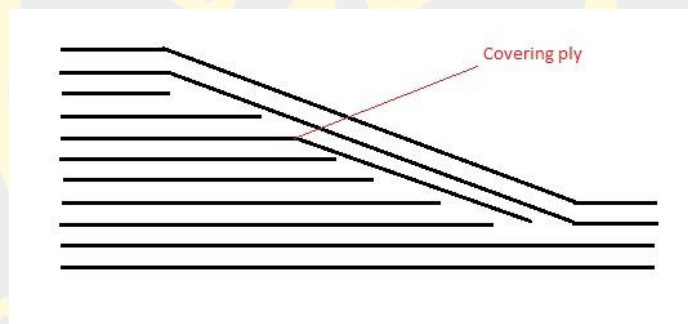
Figure 30: Covering ply (AIRBUS 2009)

Dropping Ply at the same position

Avoid dropping two or more adjacent plies at the same point. The distance between drop offs in adjacent plies should be as big as possible.

OK

Figure 31: Dropping plies at the same position (AIRBUS 2009)

If two plies are dropped at the same position there should be, at least, four plies between them (see Figure 32). However, dropping several plies at the same position is not recommended for drop offs with ramp in only one side
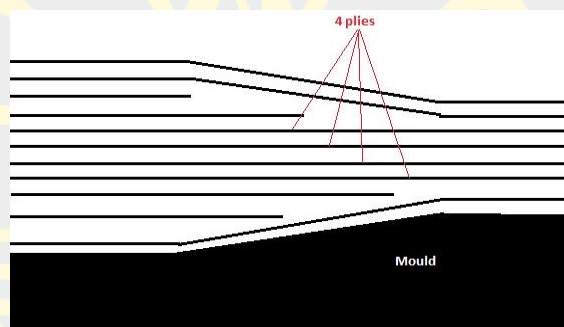
Figure 32: Drop of 2 plies (AIRBUS 2009)

1.6.5) Bonding rules

The bond line and the interface, as well as the adherents in the bond line areas should not be the weakest link of the structure. The reliability and the endurance are the key design targets of the bonded structures. Strength is the key parameter to achieve the highest performance bonding. It is recommended to get stress and manufacturing involved to define bonded structures. As the first approximation, the following parameters are recommended for bond line length, l_{min}:

- Double lap joint: 30-40 t

- Single lap joint: 80-100 t

Figure 33: Bonding Rules (AIRBUS 2009)

1.6.6)   Radius Rules

The following radii have been validated with manufacturing through practice, and should be taken as a minimum. There are, though, cases where it is advisable to increase the value depending on the stress level, functionality (e.g. stringer, "unfolded angle"), etc.

The values for radius depend on material, laminate thickness and manufacturing tooling. As a general rule for pre-preg material, the values to apply are shown in the following scheme.
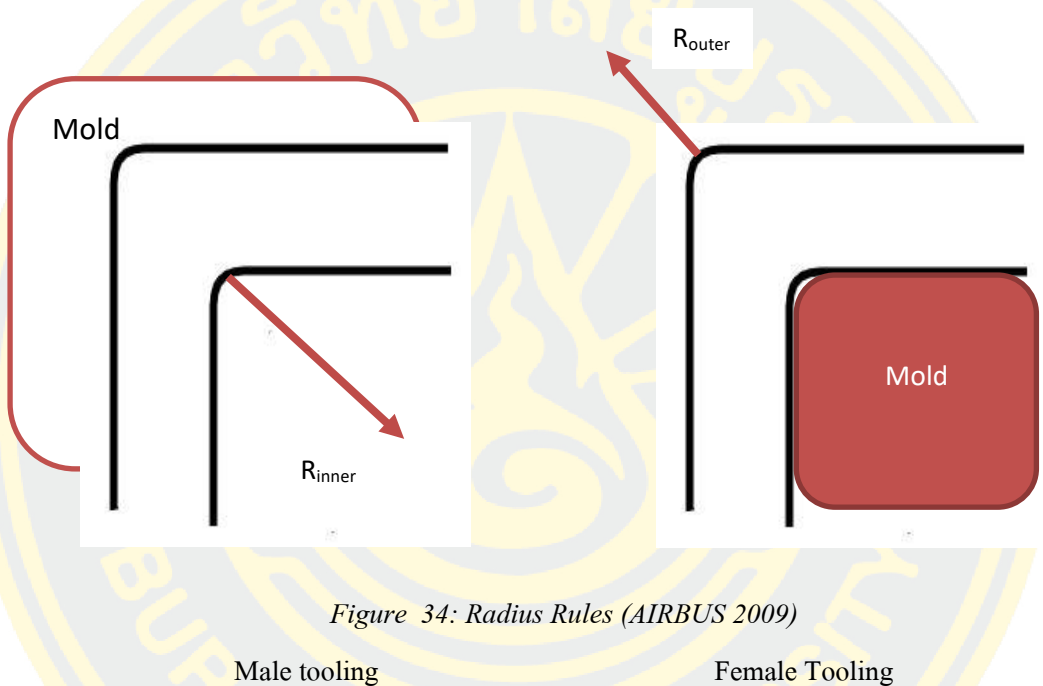
Figure 34: Radius Rules (AIRBUS 2009)

Male tooling   Female Tooling

Table 11: Radius Rules [10]

	Male tooling	**Female tooling**
t < 2.5 mm	$R_{inner} \geq$ max of [2t, 2.0 mm]	
t $\geq$ 2.5 mm	$R_{inner} \geq$ max of [t, 5 mm]	$R_{outer} \geq$ 2t+1.5 mm

1.7) Topology optimization

Structural optimization

Weight minimization is the main design objective in aerospace industry in order to reduce cost of manufacturing, maintenance. One way to saving weight is structural optimization methods, this method is often applied to find an optimized component design. Therefore, mathematical technique is used by this method to iteratively calculate to find a (local) optimal solution to an optimization problem, which in this case would be to find the lightest structure that does not fail under the applied loads.

To formulate the structural optimization problem, an objective function, design variables and state variables needs to be introduced as described in .

- The objective function (f), represents an objective that could either be minimized or maximized. A typical objective could be the, stiffness or volume of a structure. Furthermore, some structural design domain (or area) and state variables associated to the objective function needs to be defined.

  - Objective Function: Any response function of the system to be optimized. The response is a function of the design variables. Ex. Mass, Stress, Displacement, Moment of inertia, Frequency, Center of gravity, Buckling factor, etc.
  - Constraint Functions: Bounds on response functions of the system that need to be satisfied for the design to be acceptable.

- The design variables (x) describes the design of the structure, which are the parameters that describe the design, and which one varies in search of an optimized design. Design variables can be, for example, the cross-sectional area and length of a truss. All allowable variations of the design variables form the design area.

- The state variables (y) represents the structural response which can for example be recognized as stress, strain or displacement. Furthermore, the state variables depends on the design variables y(x). The objective function is subjected to the design and state variable constraints to steer the optimization to a sought solution.

  - Design Variables: System parameters that are to optimize system performance.
  - Design Space: Selected parts which are designable during optimization process: For example, material in the design space of a topology optimization.

$$\begin{cases} \min\limits_{x} & f\big(x, y(x)\big) \\ subject\ to & \begin{cases} design\ constriant\ on\ x \\ state\ constraint\ on\ y(x) \\ wquilibrium\ constraint \end{cases} \end{cases}$$

(LARSSON 2016)

Example: A cantilever beam is modeled with 1 D beam elements and loaded with force F=2400 N. (Figure 35) Width and height of cross-section are optimized to minimize weight such that stresses do not exceed yield. Further the height h should not be larger than twice the width b. (Altair, Optistruct concept design, 2008)
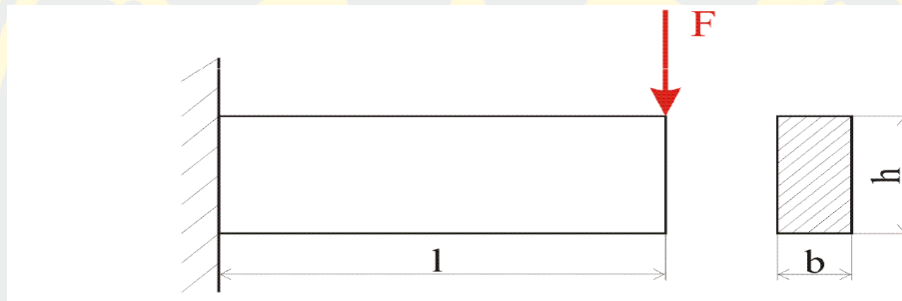
Figure 35: Cantilever beam

20 < b < 40
30 < h < 90

Figure 36: Design variables

So, the optimization can be summarize as:

$$\sigma(b,h) \leq 70\ MPa$$
$$\tau(b,h) \leq 15\ MPa$$
$$h \geq 2*b$$

$$min\ \textbf{Weight(b,h)}$$

(a)   (b)

Figure 37: (a) Objective Function   (b) Constraint Function

It can be written also by:

- Objective
  - Weight: *min m(b,h)*
- Design Variables
  - Width: $b^L < b < b^U$,   *20 < b < 40*
  - Height: $h^L < h < h^U$,   *30 < h < 90*
- Design Region: *All beam elements*
- Design Constraints:

$$\sigma(b,h) \leq \sigma max,\ with\ \sigma max = 160\ MPa$$
$$\tau(b,h) \leq \tau max,\ with\ \tau max = 60\ MPa$$
$$h \geq 2*b$$

(Altair, Optistruct concept design, 2008)

For another examples
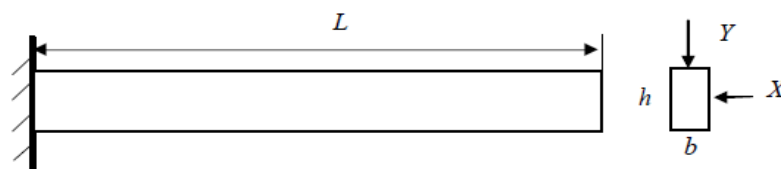
Figure 38: Another cantilever beam

The objective of the problem is to minimize the weight or equivalently the cross-sectional area, d,
As the density ρ is constant, so the objective is to minimize and L is fixed.

$$f(d) = bh,$$

Where b and h are width and height of the crss-section, respectively, and the design variables are **d = (b,h)**

Two constraint are considered. The first constraint is that maximum stress at the fixed end of the cantilever beam is less than the yield strength S = 35,000 psi. The stress constraint is given by

$$g_1(d) \quad = \quad \frac{6L}{bh}\left(\frac{X}{b}+\frac{Y}{h}\right)\text{-}S\leq0$$

where X= 500 lb and Y = 1,000 lb are external forces: L = 100 is the length of the beam. The second constraint is that the tip displacement does not exceed an allowable value D_0.

$$g_2(d) \quad = \quad \frac{4L^3}{E}\sqrt{\left(\frac{X}{b^3h}\right)^2+\left(\frac{Y}{bh^3}\right)^2}\text{-}D_0\leq0.$$

Where D_0 = 2.5" and E = 29e6 psi is the material modulus of elasticity
The bounds for the design variables are $1 \leq b \leq 10$ and $1 \leq h \leq 20$, respectively
The optimization model is then given by

$$
\left\{
\begin{array}{c}
\min\limits_{d=(b,h)} f(d) \\
subject\ to \\
g1(d) = \dfrac{6L}{bh}\left(\dfrac{X}{b}+\dfrac{Y}{h}\right)\text{-}S\leq0 \\
g2(d) = \dfrac{4L^3}{E}\sqrt{\left(\dfrac{X}{b^3h}\right)^2+\left(\dfrac{Y}{bh^3}\right)^2}\text{-}D_0\leq0. \\
1 \leq b \leq 10 \\
1 \leq h \leq 20
\end{array}
\right.
$$

Based on what geometrical feature that is parametrized, the structural optimization problem can be classified into: (Figure 39)

- Sizing optimization allows varying the geometric dimensions such as height and length.

- Shape optimization allows varying the shape of the structure which is typical achieved by defining certain control points on the boundary.
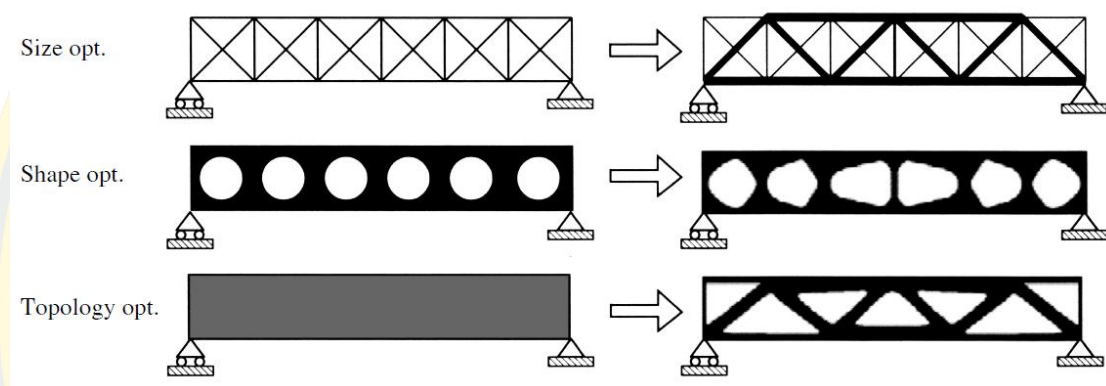
- Topology optimization.

Figure 39: Structural optimization methods

Density-based topology optimization

To have a concept design, topology is a powerful optimization tool definition of topology optimization is to find an optimal distribution of materials within a specify design domain without making any a priori assumptions about the geometry and shape of the final design itself. In recent years, aerospace industry is striving used topology optimization to design parts. For example, Airbus has used topology tools and shape optimization to redesign A380 leading edge ribs, fuselage door intercostals etc (Verbart Alexander, Van Keulen Fred et al. 2015, LARSSON 2016) . (Figure 39)

For topology optimization, commercial softwares determine an optimal placement of a given isotropic material of a reference domain in space. Topology optimization is generally formulated and solved by considering the material distribution approach. In a defined domain, each finite element is assigned a variable density variable ρ. During optimization process, this variable density variable is assigned a value that ranges from 0 to 1. Elements with density variables having a value assigned as $\rho=0$ means voids at those locations in the initially designed domain. This is called a

material distribution topology optimization problem based on maximum stiffness formulation or minimum global compliance. The optimization problem formulated can be written as:

$$\begin{cases} \min\limits_{x} & f(\rho) \\ subject\ to & \begin{cases} 0 \leq \rho \leq 1 \\ state\ function\ constraint \\ Manufacturing\ constrints \end{cases} \end{cases}$$

A possibility to maximize the global stiffness of a structure is to minimize its compliance. A stiff structure is one that has the least possible displacement when given certain set of boundary conditions. A global measure of the displacements is the strain energy (also called compliance) of the structure under the prescribed boundary conditions. The lower the strain energy the higher the stiffness of the structure. So, the problem statement involves the objective functional of the strain energy which has to be minimized:

$$\text{Objective} \qquad \min_{\rho} \int_{\Omega} \frac{1}{2} \sigma : \varepsilon d\Omega$$

With:

$$\sigma = C : \varepsilon$$

And $C(\rho)$ is the stiffness tensor and it is function of the density.

The double dot tensor product is defined as:

$$T : U = T_{ij} U_{ij}$$

The strain energy is defined as the energy stored in a body due to deformation. The strain energy per unit volume is known as strain energy density and the area under the stress-strain curve towards the point of deformation. When the applied force is released, the whole system returns to its original shape. It is usually denoted by U.

$$U = \frac{1}{2} \cdot V \cdot \sigma \cdot \in$$

The design space (Ω). This indicates the allowable volume within which the design can exist. Assembly and packaging requirements, human and tool accessibility are some of the factors that need to be considered in identifying this space. With the definition of the design space, regions or components in the model that cannot be modified during the course of the optimization are considered as non-design regions.

Validated topology by basic problems has been performed in order to prove that topology can use to design the location of the web of the stiffener. The validation model was done by load applied on upper surface and fixed boundary condition. Moreover, extrusion function was used in order to give constraint to the model.
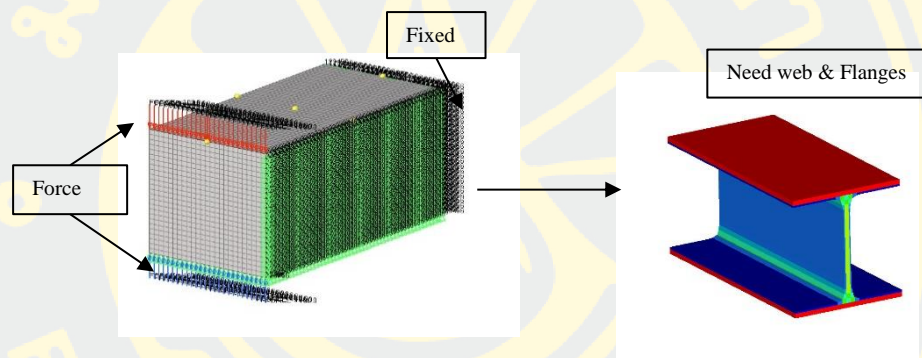

Figure 40: Validated topology by basic problem

Conclusion: Topology was validated by basic problems due to the load applied on upper surface. Composite design needs used in aerospace were identified in order to be respected in this project. Optimization and topology is going to be used in next chapter.

CHAPTER 2: CASE STUDY

2.1) Geometry

Spoiler of A320 aircraft is used in this thesis. One aircraft A320 have 10 panel spoilers that means 5 panels on the left wing and 5 panels on the right (Figure 42). In this study will be focus on one spoiler due to the same geometry of spoilers.

Figure 41: A320 spoilers

The smallest spoiler has been selected as case study in order to reduce computing time (Table 12). The largest dimensions are 1.55 x 0.06 x 0.58 m^3 (Figure 41).

Table 12: Dimension and materials of A320 spoiler

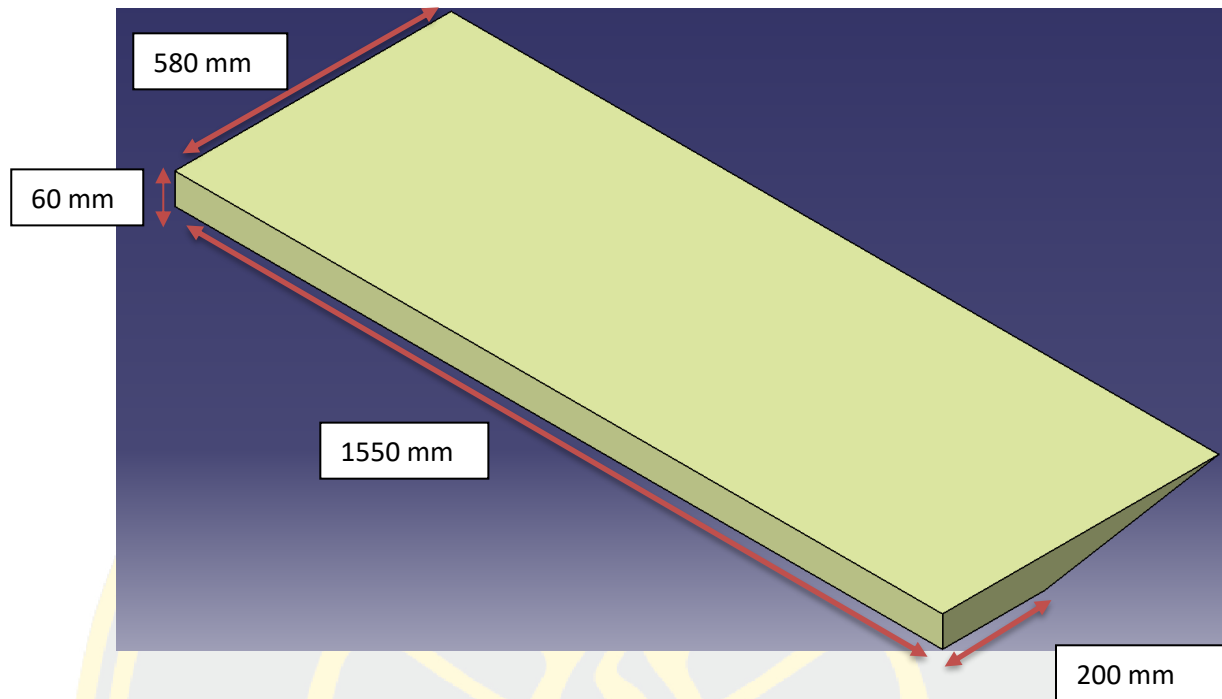| Pictorial view	Dimension (L x W)	Materials
	1.55 x 0.58 (m)	Honeycomb core Carbon skin

Figure 42: Dimension of A320 spoiler in model

2.2) Mass calculation

In order to determine the mass the spoiler needs to reach, the mass of the current spoiler is estimated. The material references used are detailed in the following table 13.

Table 13: List of material reference used in the current spoiler

Item	Material	Reference	Density
1	Carbon epoxy	UD 914C-T300H	1580 kg/m^3
2	Adhesive Redux	319 A	0.24 kg/m^2
3	Core splice foam	FM410	240 kg/m^3
4	Honeycomb Nomex	Hexcel	48 kg/m3

By determining the volume of each components of the sandwich, the mass can be calculated.

Firstly, the volume of the honeycomb was estimated as full spoiler. The volume was calculated from rectangular volume and triangle volume base on geometry. And the density of honeycomb Nomex of Hexcel was selected. Thus, the mass is:

Volume honeycomb	0.044	m^3
ρ	48*	kg/m^3
Mass	2.1	kg

Then, the skins were calculated. To respect the aerospace design rules, the smallest number of plies the sandwich can be made is 8 to get the following staking: [45,0,-45,90,90,-45,0,45]. Therefore, the mass is:

Surface skin	1.55 x 0.6	m^2
	= 0.992	m^2/skin
2 Skins	1.984	m^2
Thickness of CFRP	0.127 mm x 8 Plies (minimum lay-up*)	
	= 1.016	mm/skin
Volume of the skin	1.984 x 0.001016	m^3
	= 0.002015744	m^3
Density	1580	kg/m^3
Mass	3.1	kg

To bond the skins to the honeycomb, epoxy film or Redux is used. The mass is:

Epoxy Redux film (2 skins)	2.124	m^2
Area weight	0.24	kg/m^2
Mass	0.51	kg

Due to the border of the honeycomb core (Figure 43). To avoid the damage the core splicing needs to be considered.

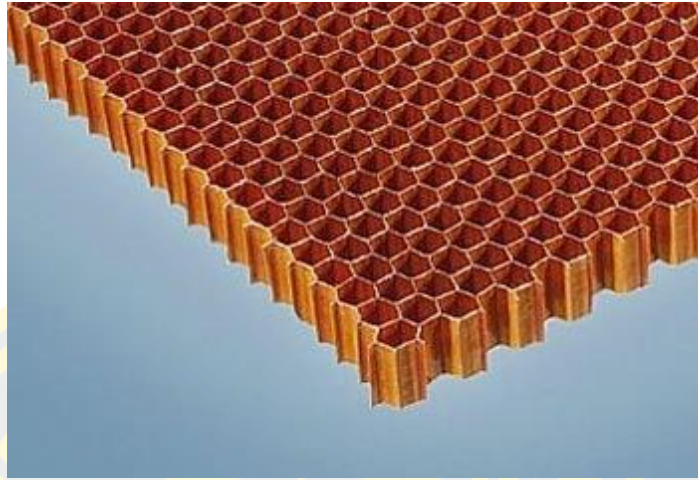*Figure 43: Honeycomb core border*

Epoxy splicing	0.25	m^2
Thickness	0.64	mm
Density	240	kg/m^3
Mass	0.04	kg

Finally, the mass is estimated to 5.85 kg that is the minimum mass of the spoiler. Indeed, many parameters are unknown and therefore the lowest mass is estimated (Table 14).

Table 14: Summary of the calculated mass of sandwich spoiler

Component	Materials	Mass (Kg)
Honeycomb	Nomex	2.1
Skins	Carbon fiber	3.2
Epoxy Adhesive Redux film	Epoxy	0.51
Epoxy splicing	Epoxy	0.04
Total		5.85

2.3)   Force calculation

       The drag force is given by the Equation (1). For the single aisle aircraft, the landing velocity is about 225 km/h (FAA, 2016). The surface of the studied spoiler (Figure 41) is 1 m^2. The drag coefficient of a spoiler was supposed to be the same as a flat plate perpendicular to flow (3D) (NASA, 2013)

$$F_d = \tfrac{1}{2} \, (\rho \cdot v^2 \cdot A \cdot Cd) \qquad\qquad (1)$$

Where:

      C_d: Drag coefficient   =   1.3

      A: Surface of 1spoiler   =   1   m^2

      V: Landing Velocity   =   86.64 m/s

      ρ: Density of air   =   1.225 kg/m^3

      The drag force, F_d = 6,842.22 N.

      The force used to design the spoiler is given by the Equation (2). In aerospace, the safety factor, SF is usually 1.5 (Bristow and Irving 2007). The load factor, LF for a single aisle aircraft is 3 (John W. Rustenburg, Donald A. Skinn et al. 2002)Therefore, the Ultimate Load, UL used to design the spoiler is

$$UL = LL \cdot SF = 30{,}790 \ N \qquad\qquad (2)$$

When:

LL (Limit Load): F_d * LF

F_d: Drag force on spoiler = 6,842.22 N

SF: Safety factor = 1.5

LF: Load factor = 3

2.3)   **Design methodology**

Usually aeronautics standard has three steps to perform the design by following this process (Figure 44).

Conceptual design → Preliminary design (GFEM) → Detailed design

Figure 44: Design methodology

● Conceptual design

As the objective is to replace the honeycomb by stiffeners, there is a large number of solutions of the location. Concept design consist in determining the location of stiffener by using topology tool. The best solution is defined in term of mass and stiffeners, mean to minimize the mass for higher stiffness.

● Preliminary design

In preliminary design, the structure is simulated. The geometry of stiffeners are not detailed, i.e. flanges are not modeled. The basic stacking was used [0,45, -45,90]. Optimization is defined as thickness of plies (Macro plies) (Figure 45). In this step, only static is analyzed.

(blue)	-45
(yellow)	90
(green)	45
(red)	0
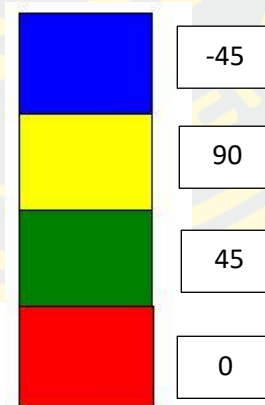
Figure 45: Macro ply

• Detailed design

Detailed design consists in optimization of all stiffeners and skins each ply was defined (Figure 46). Moreover, the geometry is detailed by adding the flange and the corner, radius… The objective is to complete the optimization by local optimization. Contact with external structure or environment as bolts, rivets can be simulated if required. Static and buckling analysis are both performed.
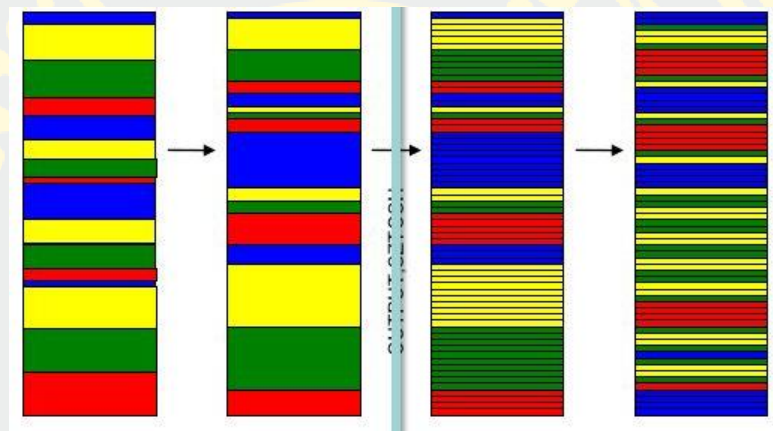

Figure 46: Detailed design of the ply

CHAPTER 3: CONCEPTUAL DESIGN

3.1) Conceptual design

3.1.1) Model construction

Spoiler model has been modelled thanks to the FEA software. Model construction will be expressed into three simple formats following these topics.

- Half spoiler

- Boundary condition

- Loading

Half spoiler

Due to the symmetry of the structure, half of the spoiler will be investigated in order to reduce the time of computing. Therefore, symmetry constraint at the border will be created (Figure 47).
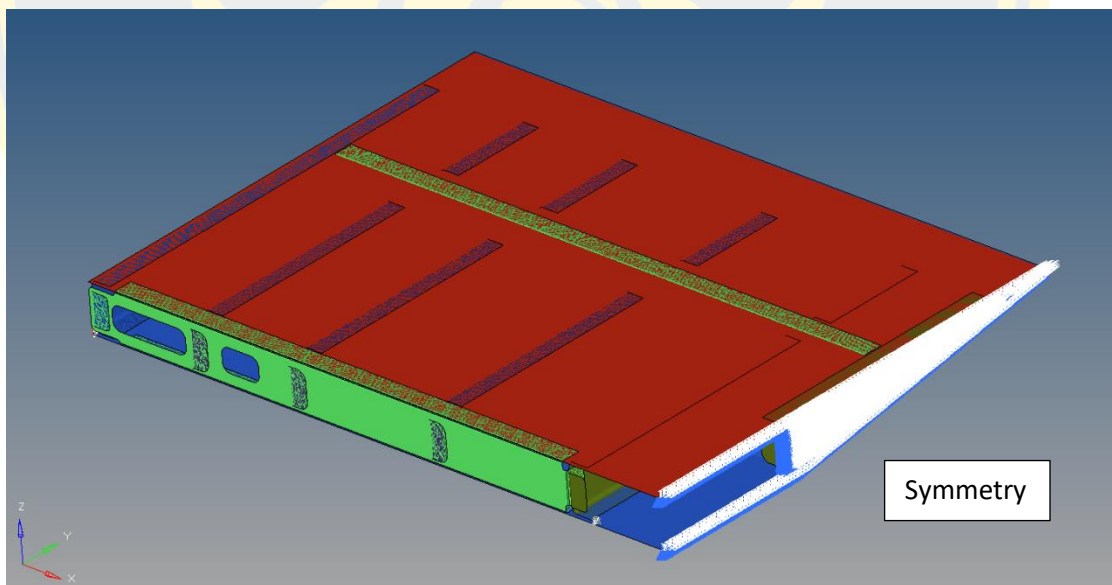
Figure 47: Half spoiler model

Boundary condition

The half spoiler has two common boundary condition which is fix and symmetry. Rotation mechanism (aluminum material) is considered as rigid (Figure 49) Therefore, fix condition was applied (Figure 48). As mentioned above in "half spoiler" symmetry boundary condition was used in order to reduce the time on computing.
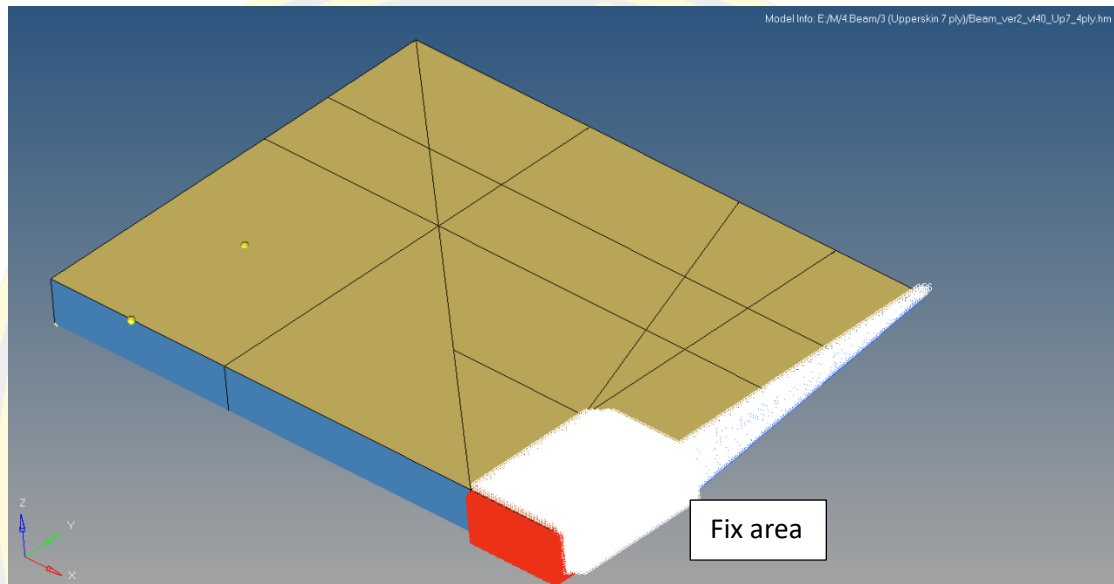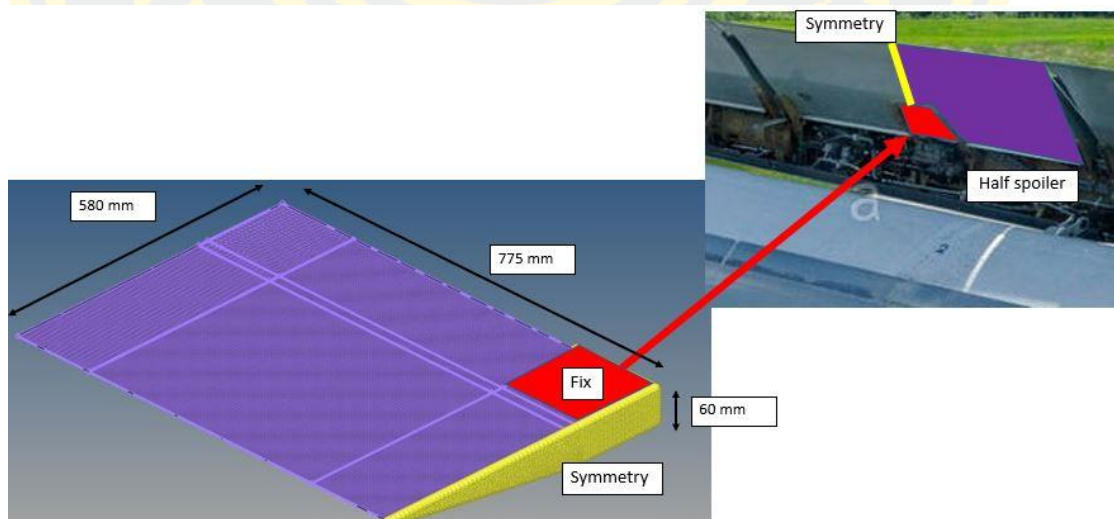

Figure 48: Fix area boundary condition

Figure 49: Rotation mechanism

Loading

The loading was applied on the upper surface of spoiler which is 15,395 N thanks to the calculation by Equation (1) (Figure 50).
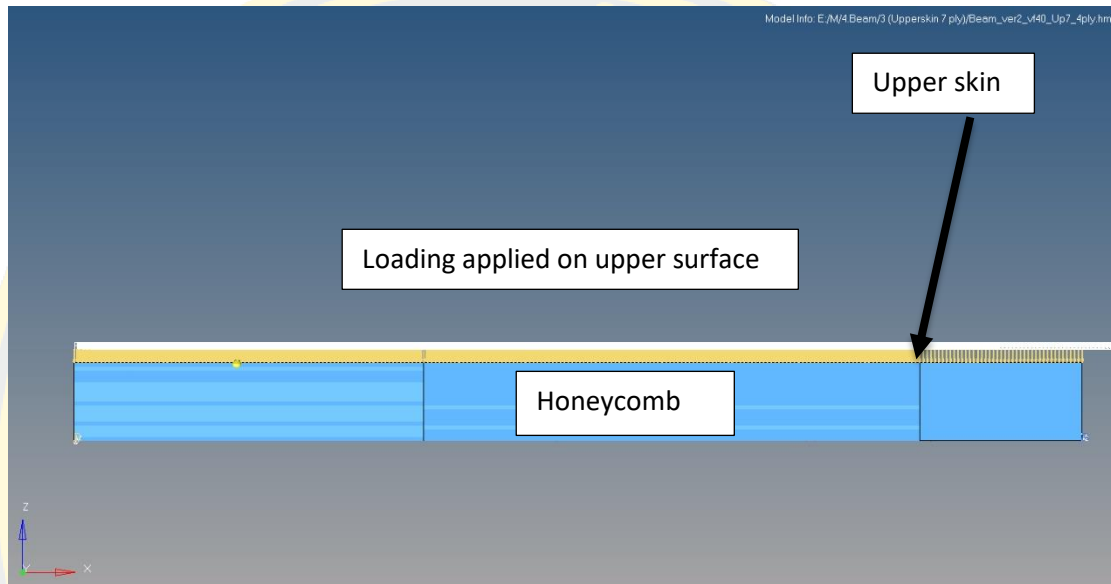
Figure 50: Load applied on upper surface on the half spoiler

The honeycomb spoiler

To validate the model construction (boundaries conditions, loading, mesh…) model of honeycomb spoiler has been firstly created (Figure 51). The mesh size is 1.5 mm for the skins and 2 mm for the core.

CFRP (IMA/M21E) will be selected as the material of the skins and the stacking sequence of the two skins is [45, 0, -45, 90, 90, -45, 0, 45] (8 plies). Indeed, to respect aerospace rules (Figure 26) 8 plies is required. Honeycomb nomex core from Hexcel will be used as the materials of the core (Table 13).
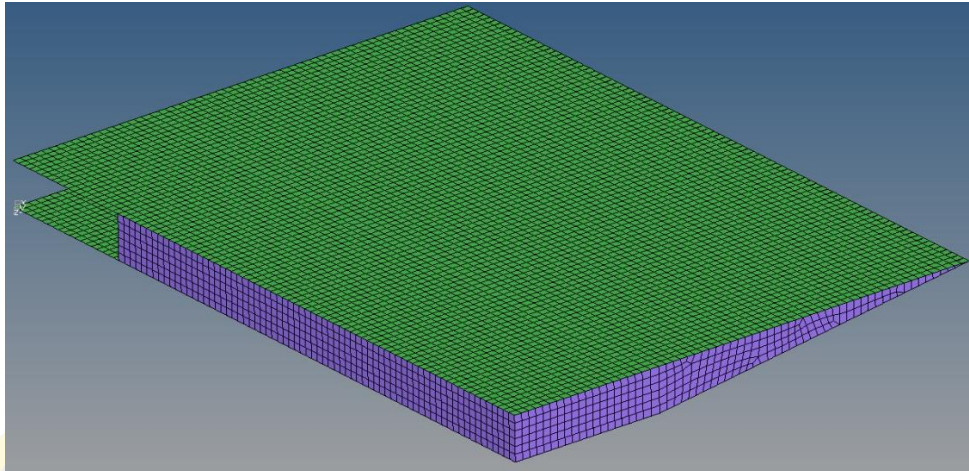
Figure 51: Honeycomb spoiler

Result of the honeycomb model

The result shows by the minimum strain on the skins (Figure 52). The minimum strain observed is -3,720 μDef that is closed to the allowable, i.e. -4000μDef with damage tolerance criterion used in aerospace. Therefore, the reserve factor, RF, is 0.93. RF of 1 is the failure of the structure. In aerospace mass is the main criteria and so to minimize the mass parts are designed to have RF equal to 1. Therefore, as 0.93 has been calculated, model construction can be validated, and the model can be used for topology.

ε = -3720 µDef --> Spoiler

ε_0 = -4000 µDef --> Criterion

RF = ε/ ε_0

RF= 0.93 (Close to 1)

Means model it's work !
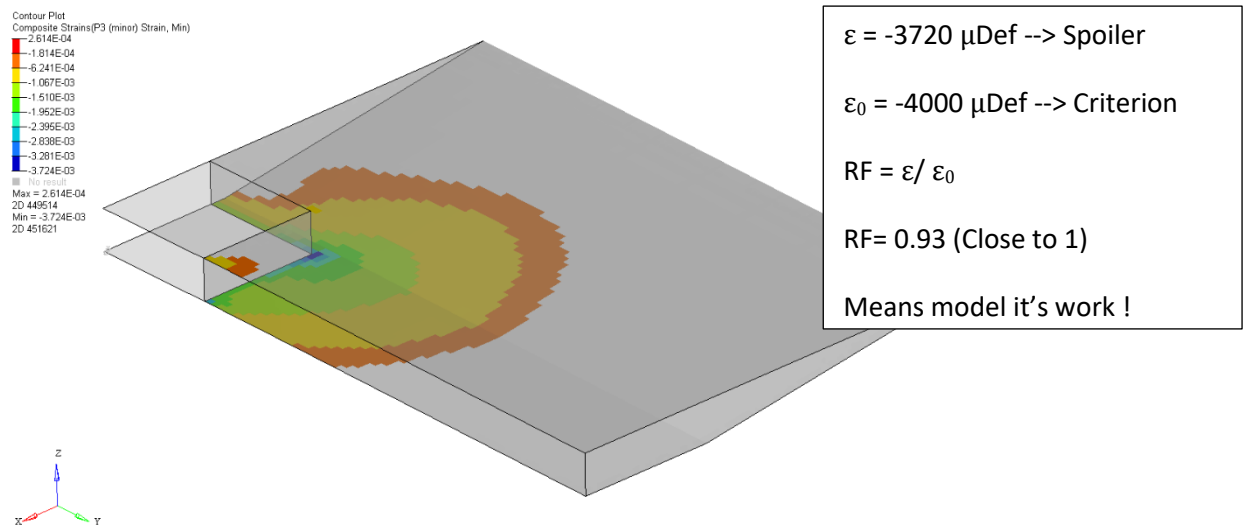
Figure 52: Result of honeycomb spoiler

3.2)   Topology optimization

3.2.1)   Mesh

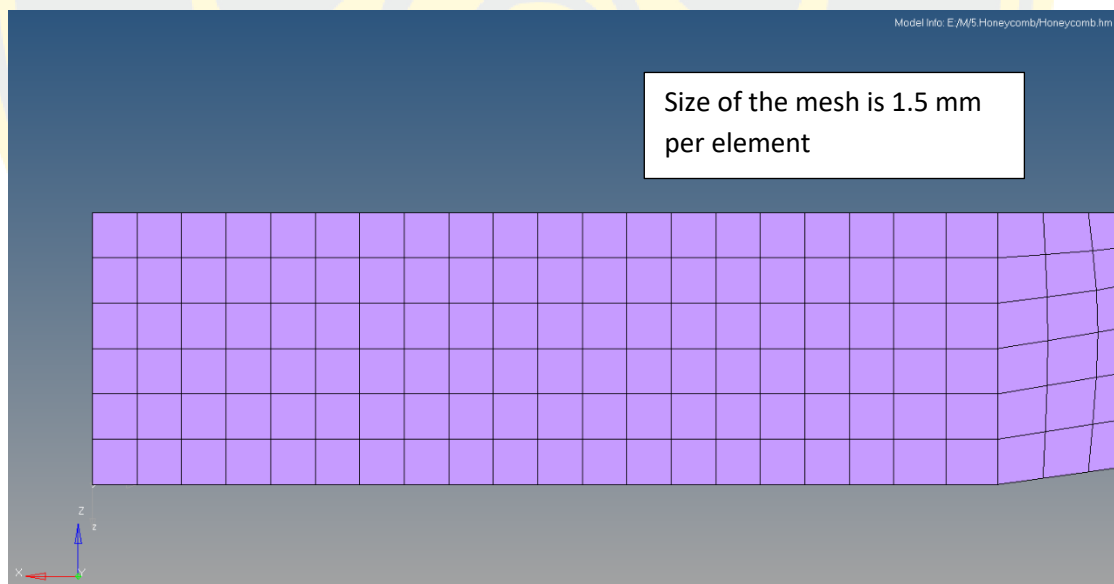Same mesh size as usedin model construction is applied for topology (Figure 53).

Size of the mesh is 1.5 mm per element

Figure 53: Fine mesh in Topology

3.2.2) Design and Non-Design area

The objective is to locate the stiffeners location and so topology is applied to the core of the spoiler. As skins are necessary and cannot be removed, skins have been defined as non-design area (Figure 54 and Figure 55).
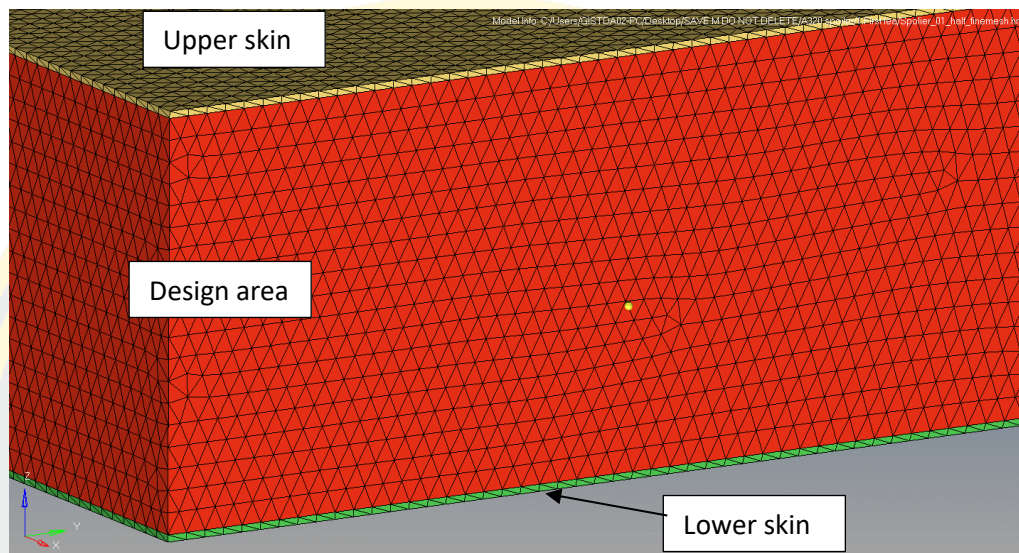
Figure 54: Design and Non-Design area in isometric view
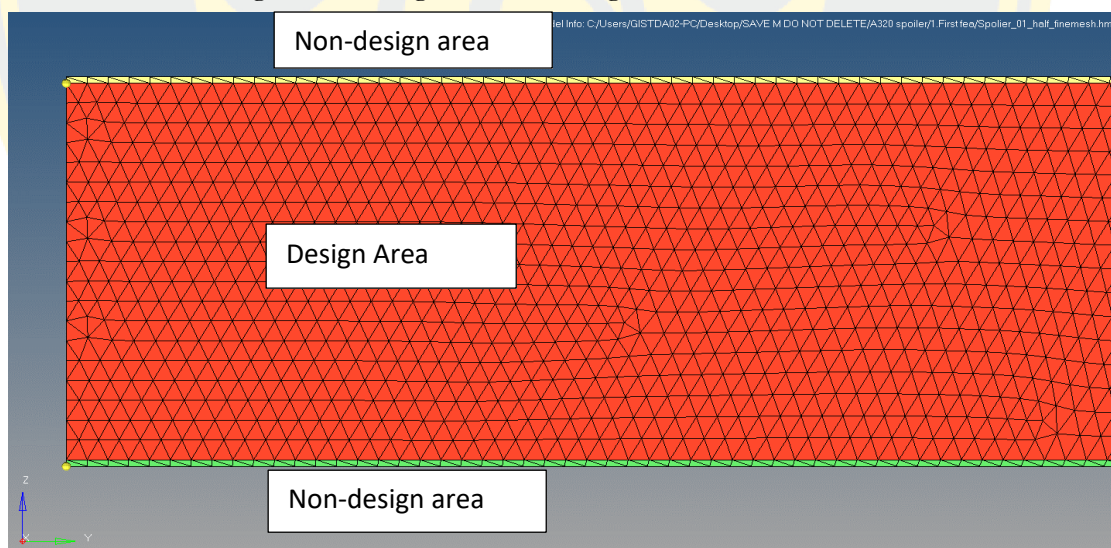
Figure 55: Design and Non-Design area in right side view

3.2.3)   Extrusion function

The objective is to replace honeycomb by stiffeners. Many stiffeners geometry is available (Table 15) such as L-Beam, C-Beam, I-Beam and Omega. Topology is used to locate the web of the stiffeners. With no constrain on material distribution topology provides a non‑manufacturing solution (Figure 56). Therefore, "Extrusion function" is applied in the topology tool in order to constraint the material distribution (Figure 55 and Figure 57). Extrusion direction is assigned perpendicular to the skins in order to locate stiffener webs (Figure 56). Finally, topology gives the web location, flanges do not need to be considered in this step.

Table 15: Table of common beams

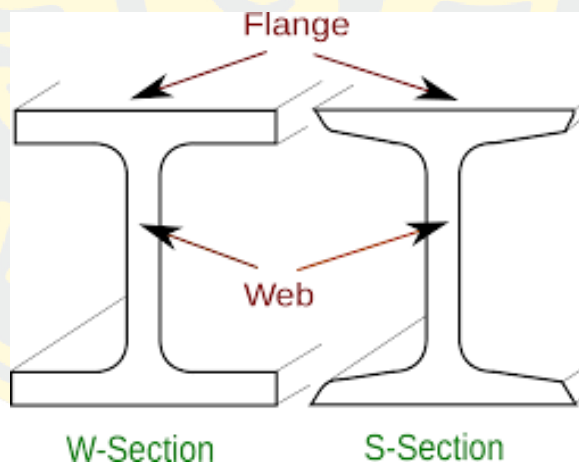| Type of common beam					

Figure 56: typical web in beam

Following figure (Figure 567 shows the simple topology give the layout it is the optimal shape it can be. But cannot manufacturing and design by composite materials
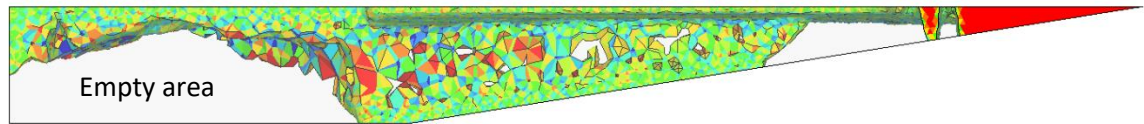

Figure 57: Density element with no-extrusion

Finally, the shape layout has been extracted thanks to the extrusion function (Figure 58). For an easy look the shape layout can see at figure 59.
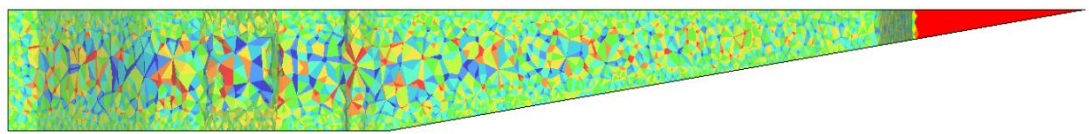

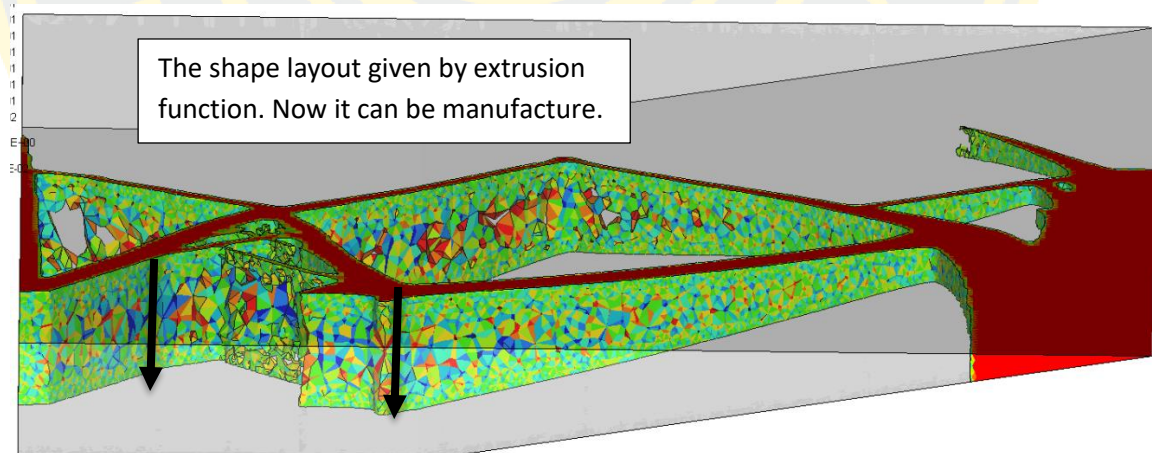*Figure 58: Density element with extrusion*

Figure 59: Extrusion result shows by direction of stiffener

3.2.4)   Objective of optimization

Minimizing the weight compliance has been used as topology objective with volume fraction, VF, as constrain. Four VF has been studied in order to identify the location of the stiffeners. Finally, as composite stiffeners will be manufactured restriction has been simulated though maximum thickness and extrusion direction.

3.3)   Results

Summary of each volume fraction

From many results of volume fraction were analyzed 4 volume fractions were studied and it can give the conclusion about the location of the stiffener thanks to the software. The following figures expressed different volume fraction result for positioning of the stiffener for example comparison between VF 25% and 10% describes that which stiffener it is must be appeared on that location due to the lowest mass
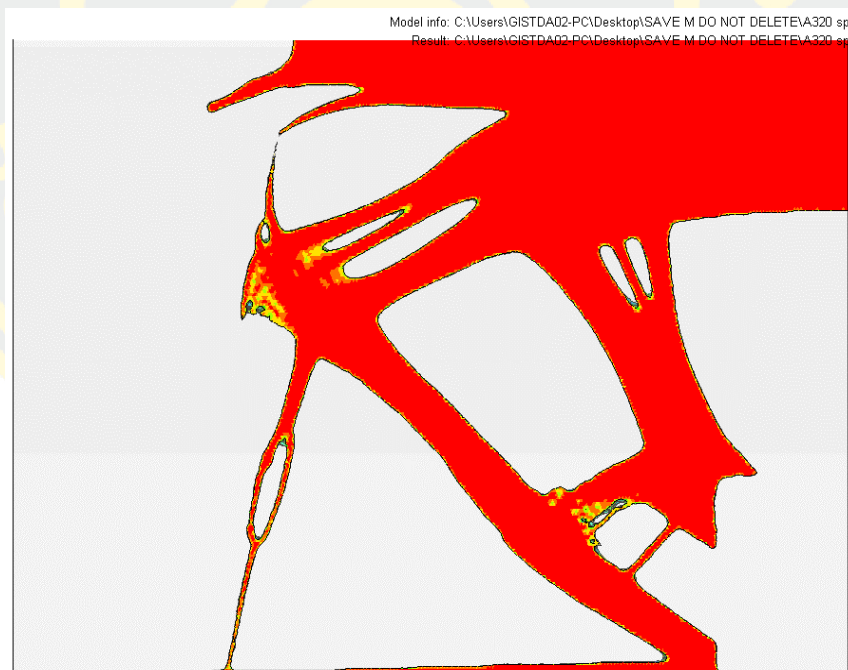

Figure 60: Top view of spoiler Density element VF result of 25% constraints
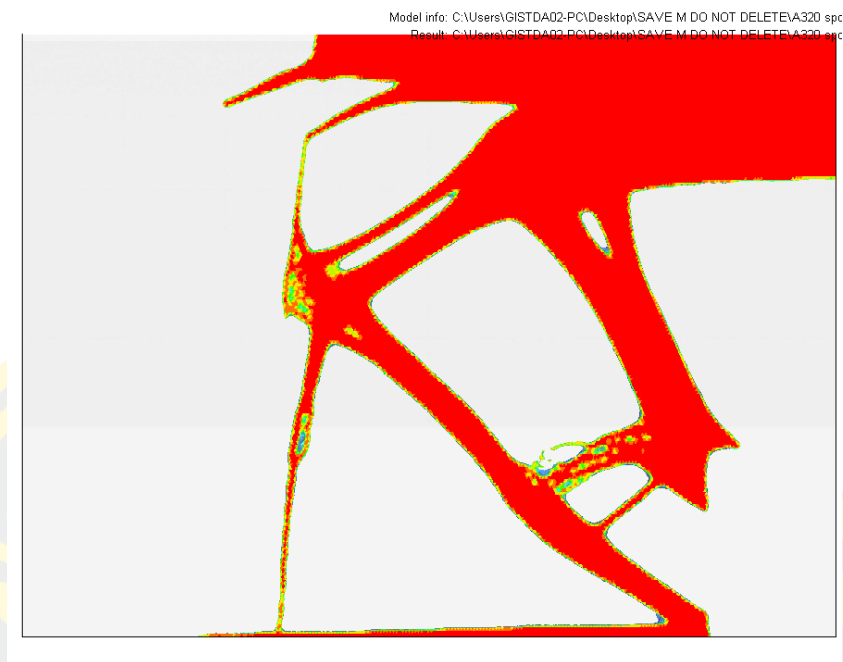
Model info: C:\Users\GISTDA02-PC\Desktop\SAVE M DO NOT DELETE\A320 spo
Result: C:\Users\GISTDA02-PC\Desktop\SAVE M DO NOT DELETE\A320 spo

Figure 61: Top view of spoiler Density element VF result of 20% constraints

Model info: C:\Users\GISTDA02-PC\Desktop\SAVE M DO NOT DELETE\A320
Result: C:\Users\GISTDA02-PC\Desktop\SAVE M DO NOT DELETE\A320
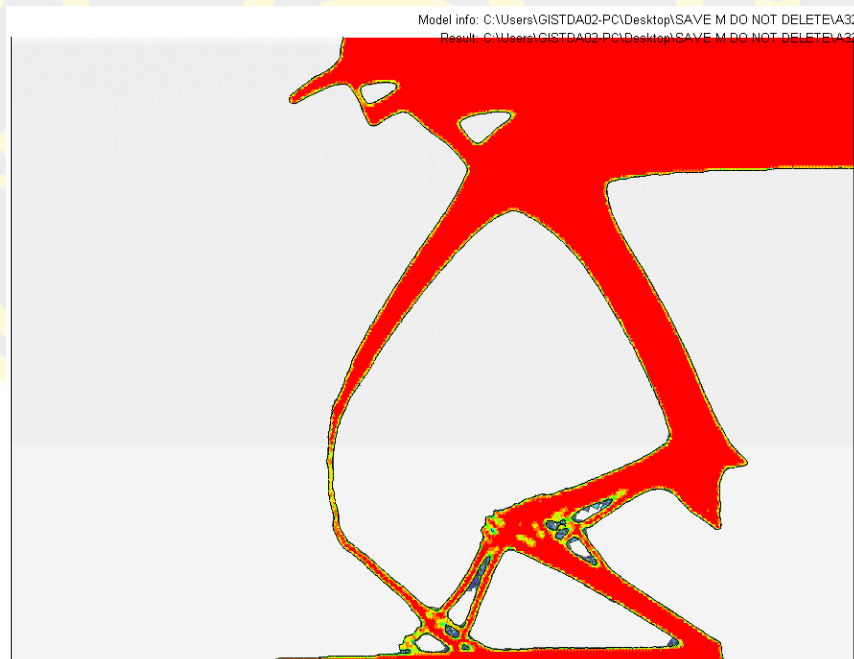
Figure 62: Top view of spoiler Density element VF result of 15% constraints
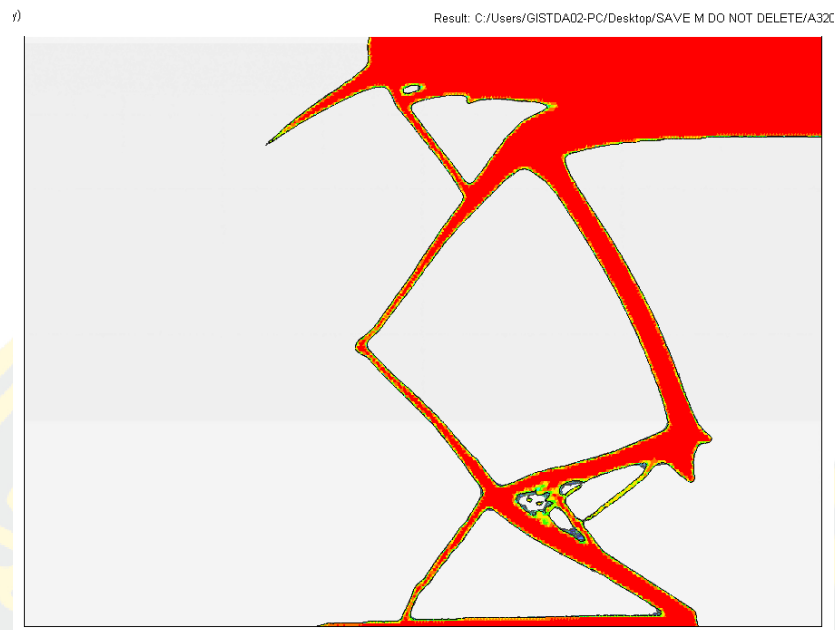
Figure 63: Top view of spoiler Density element VF result of 10% constraints

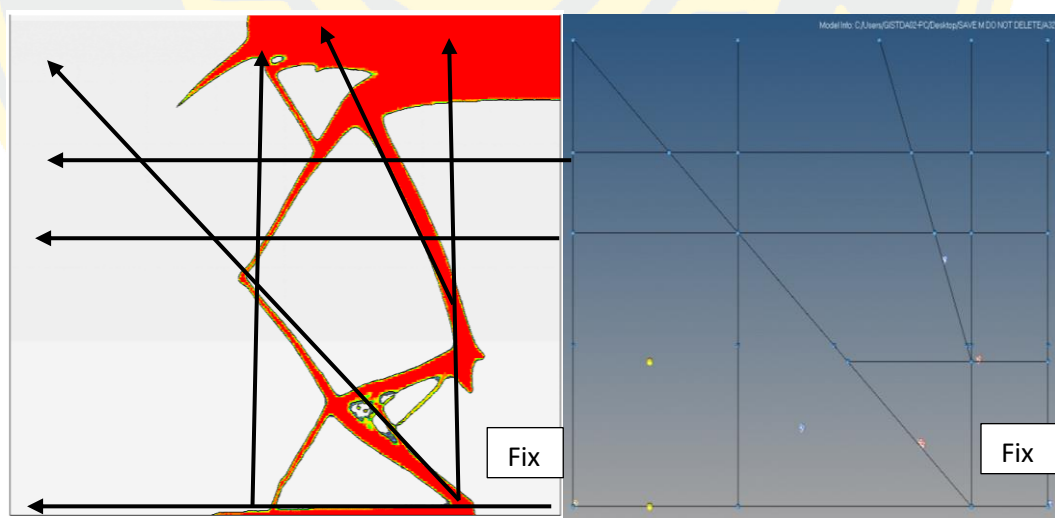By comparing the results, stiffeners location can be determined (Figure 64).

Figure 64: Location of the beam from topology

From the distribution layout of the topology result the beams has been located.

Finally, conceptual design has been done. Spoiler need to be closed by the end stiffener. Therefore, minimum plies will be used on this stiffener (Figure 65).
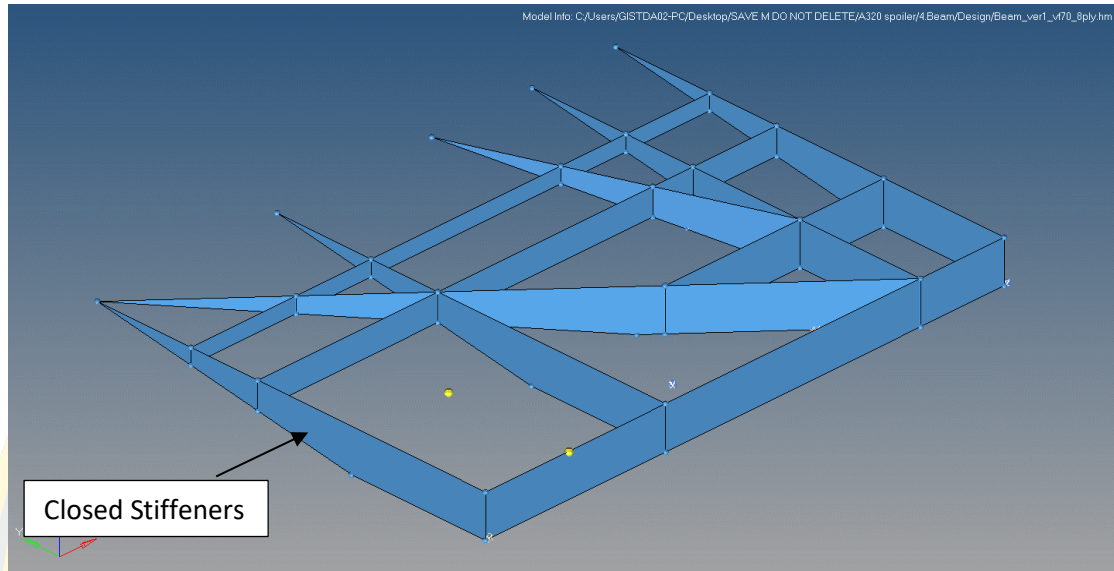

Figure 65: GFEM model after topology optimization

Conclusion: Model was built and validated on the current spoiler. Model was used to determine the stiffeners location by topology. Extrusion was used to find the stiffener web location. Stiffener location was defined, and CAD model prepared for the GFEM.

CHAPTER 4: PRELIMINARY DESIGN (GFEM)

4.1)   Introduction

In preliminary design, will be focus on GFEM (Generalize Finite Element Methods) and optimization of macro plies. In a first step, GFEM will be explained including with boundary condition, loadings, mesh and folding problems from the result and then methods of this studies will be shows in order to reach the preliminary design process and comparison of the studies result will be performed. After that Hollowing of the component will be the next step in order to reduce the mass of the structure after optimization of macro plies. Finally, reaction force will be extracted from GFEM in order to calculating the size of the flanges.

GFEM was performed by Topology result due to the best position of the stiffeners in a first step boundary condition will be recalled from concept design process also load applied and mesh and folding problems was found due to the first numerical analysis of GFEM (Figure 66).
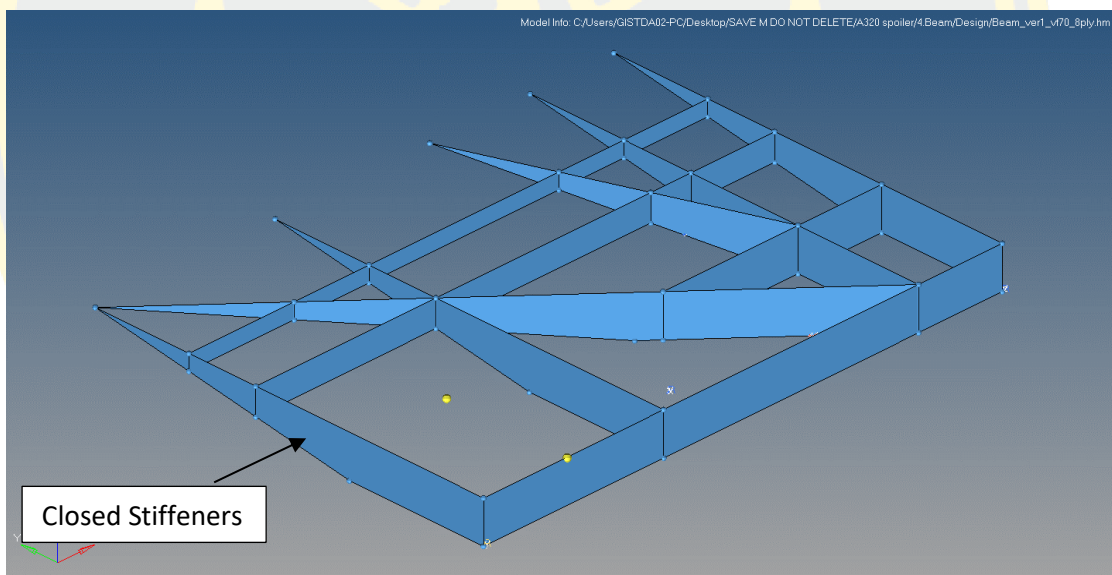

Figure 66: GFEM model after topology optimization

4.2) Boundary condition

Due to the symmetry, the half spoiler will be performed (Figure 67) in order to reduce the time of computing and. Therefore, symmetry constraint at the border will be created to decreasing time as mention above.
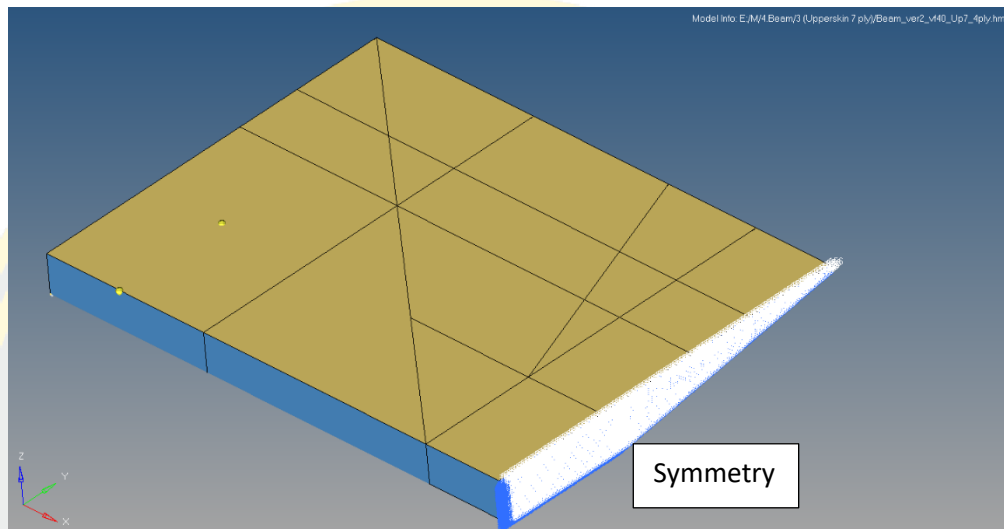

Figure 67: Half spoiler model

The half spoiler has two common boundary condition which is fix (Figure 68) and symmetry (Figure 69). Rotation mechanism is considered as rigid Therefore, fix condition was applied. As mentioned above in "half spoiler" symmetry boundary condition was used in order to reduce the time on computing.
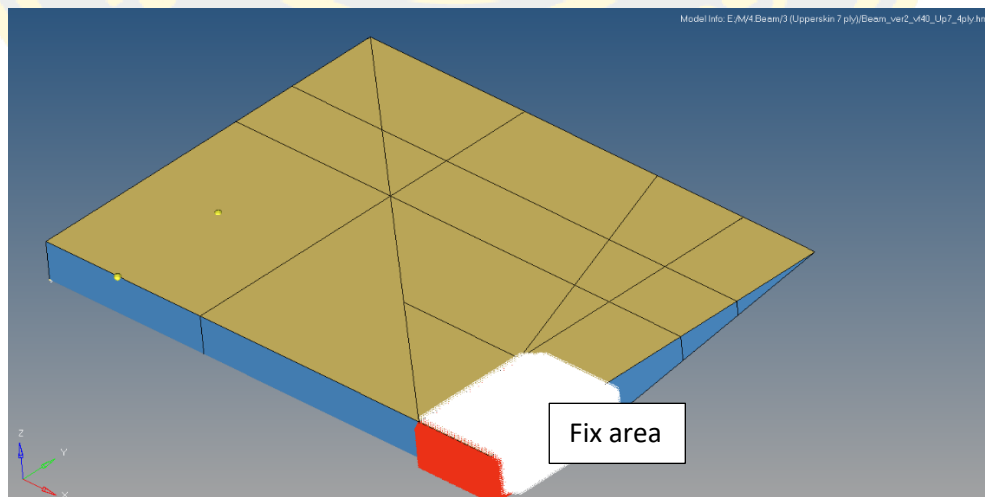

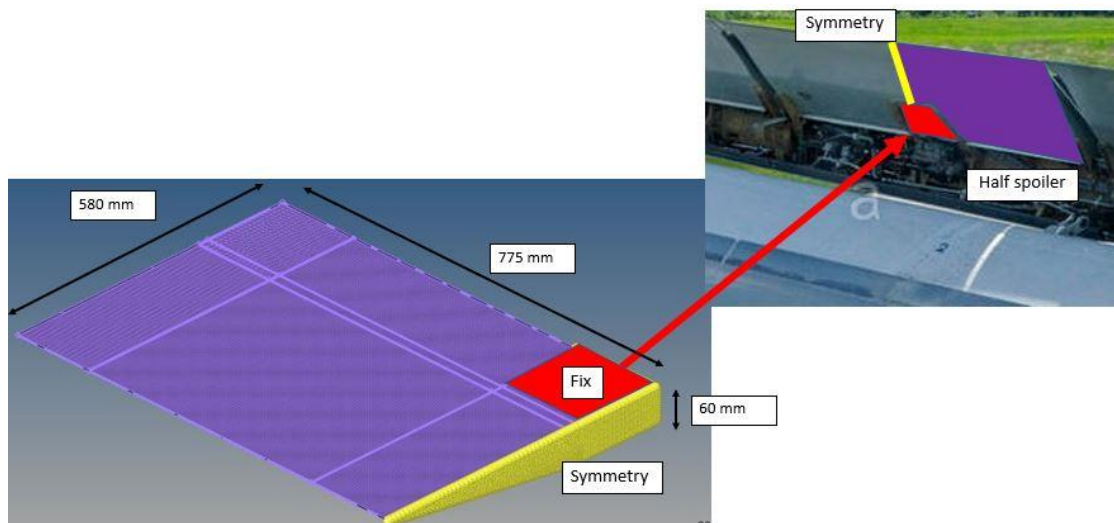*Figure 68: Fix area boundary condition*

Figure 69: Rotation mechanism

4.3) Loading

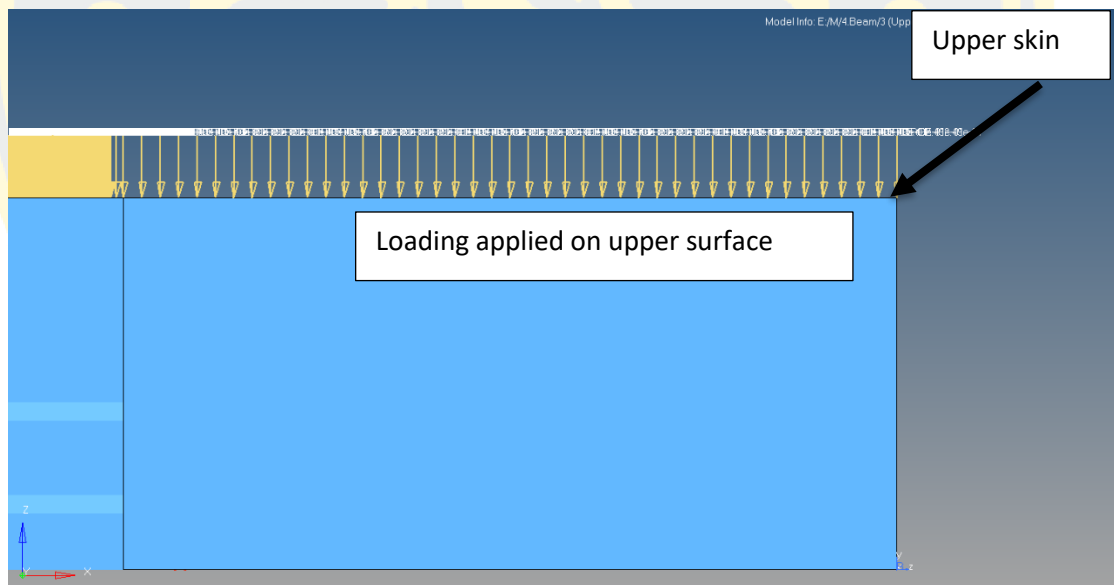The loading was applied on the upper surface of spoiler which is 15,395 N thanks to the calculation. (Figure 70)

Figure 70: Load applied on upper surface on the half spoiler

4.4)   Mesh

The model of spoiler in this thesis, mesh size 1.5 mm per element was selected in order to combine accuracy and computing time (Figure 71).
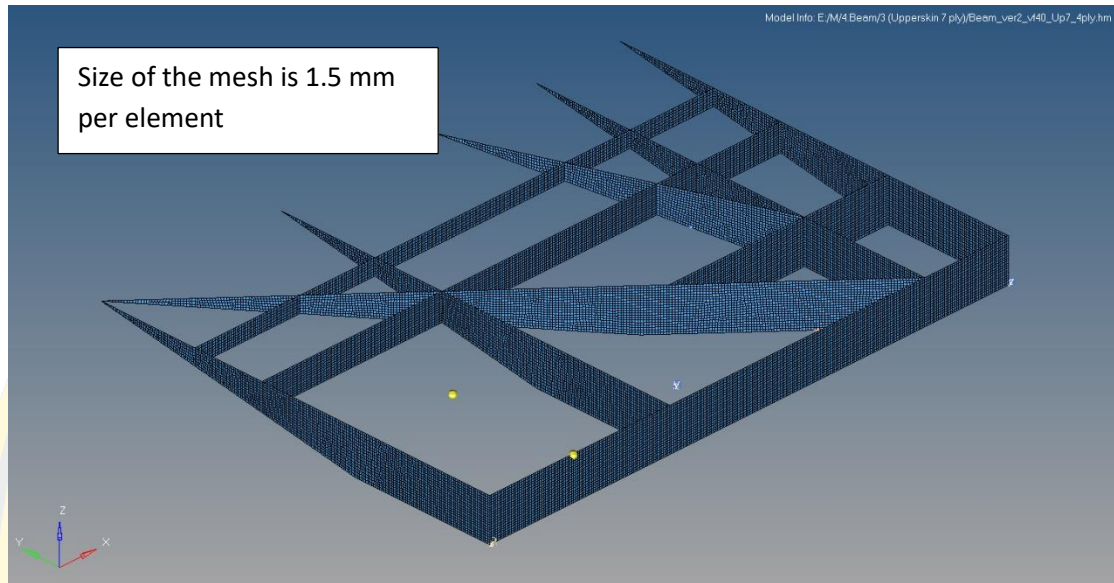

Model Info: E:/M/4.Beam/3 (Upperskin 7 ply)/Beam_ver2_vf40_Up7_4ply.hm

Size of the mesh is 1.5 mm per element

Figure 71: Fine mesh in model

4.5)   Folding

Folding problems has been found after GFEM was performed. First result shown folding on the upper skin (Figure 72). Therefore, more stiffeners are required in order to avoid the folding.
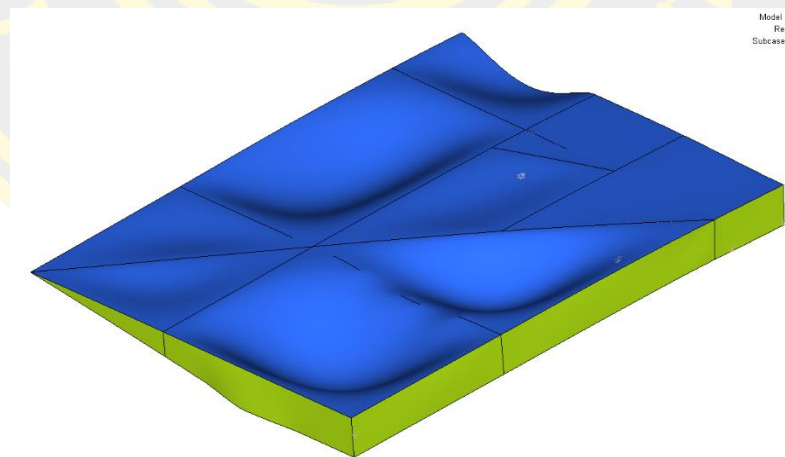

Model info:
Result:
Subcase 1 (c

Figure 72: Folding problems

4.6)   Method of the optimization

In this topic will show the process of the optimization. Firstly, the different plies of the stiffeners will be express in to 12/10/8/6/4/2 plies for each orientation [0, +45, -45, 90]. Minimum and maximum strain are observed to investigate the influence of macro ply thickness (Figure 73).

As observed, lower is the number of plies, lower is the mass but ply number has no influence on strain. Finally, 2 plies of each orientation can be used in GFEM.
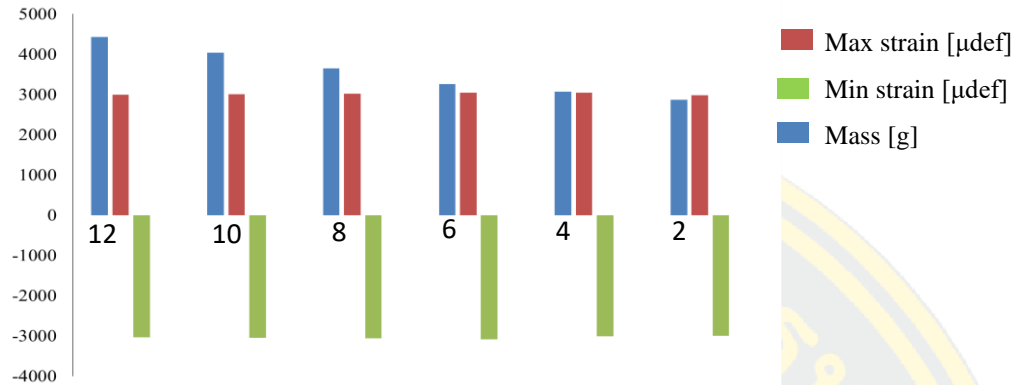

Figure 73: Macro plies comparison graph

4.7) Hollowing

In order to reduce the mass of the stiffeners hollowing has been used where the strain is smaller than $\epsilon_0 = 4047$ μDef. Therefore, if the result shows the area that has small strain hole will be done (Figure 74).
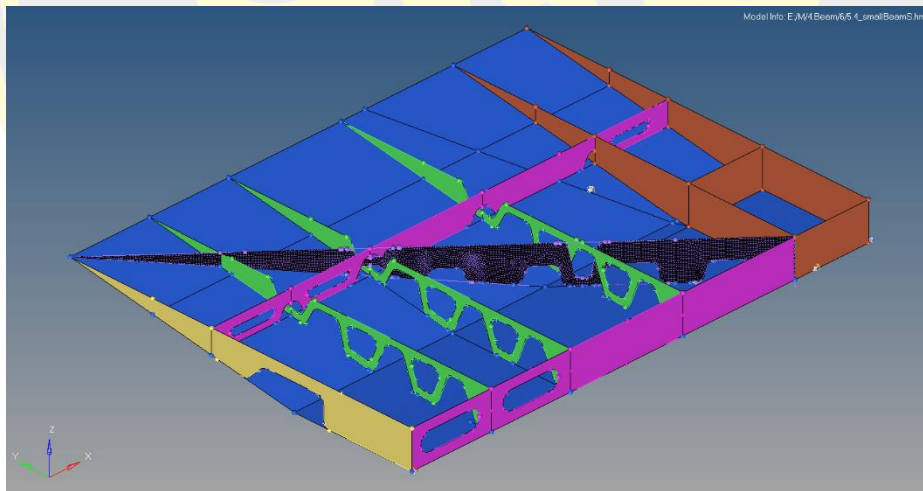

Figure 74: Hollowing the stiffeners

4.8) Reaction force

Calculation of The Flange

In the GFEM, no geometrical details have been used (no flanges, no corner…). In order to design the flange, Reaction Force need to be calculated. The flange size of each component can be calculated from analytical study (Figure 75). Flanges must be designed under bending and shear loadings.

Each interface between part are defined in order to get the RF that consists in 3 Forces (Fx, Fy, Fz) and 3 Moment (Mx, My, Mz) (Figure 76). The reaction force between components are extracted from GFEM and used to design each part.
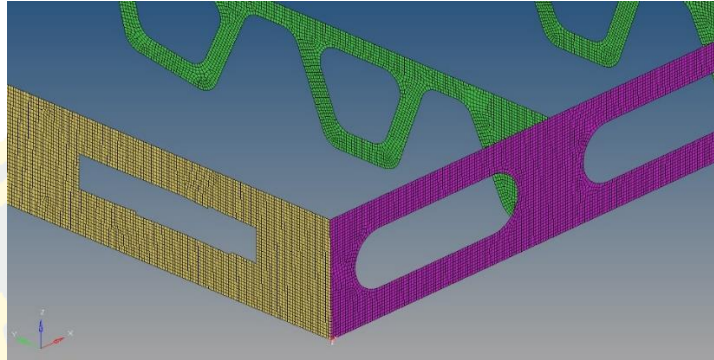

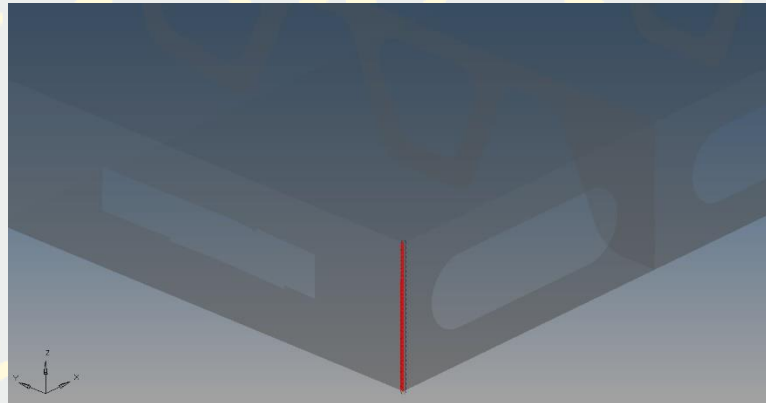*Figure 75: Reaction force on part with another components (Rib) in GFEM*

Figure 76: Reaction force consist in Fx Fy Fz Mx My Mz given by the software (FEM).

Finally, a mesh sensitivity study has to be performed in order to determine the optimized mesh. Indeed, if the mesh is too large, the results will not be accurate enough. If the mesh too small, the result will be accurate, but the running time will be too long. The goal is to find the balance between size and time different mesh size will be used and the running time and reaction force will be checked and compared.

4.9)   Calculation

From the GFEM Force Reaction (RF) between components are obtained (Figure 77). Thanks to the RF flanges can be designed by the mechanic of materials.
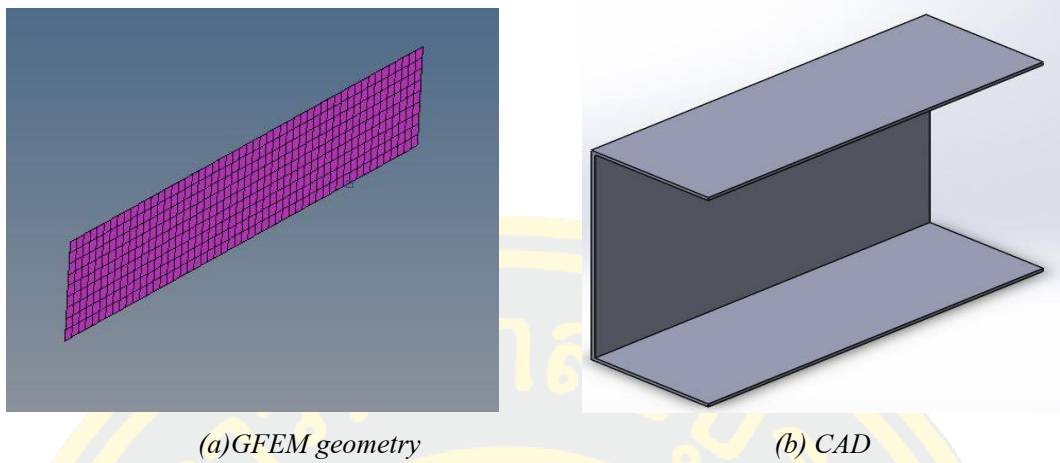
<table>
<tr><td>(a)GFEM geometry</td><td>(b) CAD</td></tr>
</table>

Figure 77: GFEM geometry (a) to CAD with volume (b)

The drag force creates in-plane and out-of-plane forces. The first one is shear and the second one bends the flanges (Figure 78)
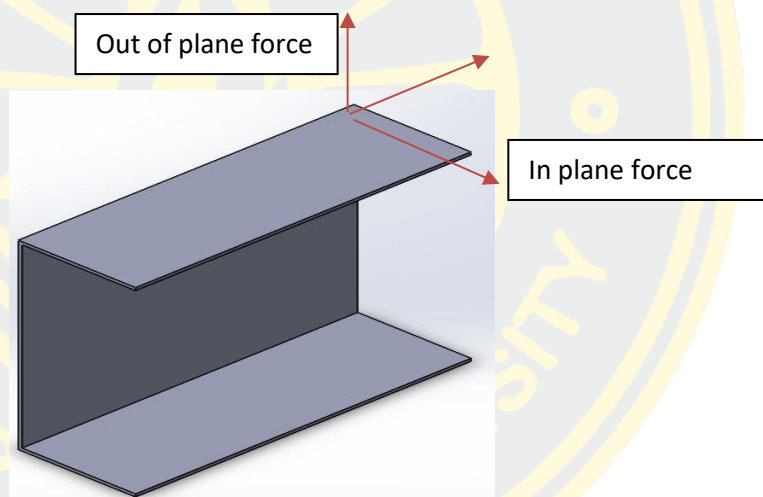

Out of plane force

In plane force

Figure 78: In plane and out of plane forces

in plane force

In plane force give shear force between 2 parts. In this case the epoxy bonding will fail.

$$\tau_{failure} = \frac{T}{S}$$

Where:

$\tau_{failure}$: shear stress failure of the bonding (MPa)

T: Sum of in-plane force = Shear force (N)

S: Surface of Flange (m^2)

$$S = L \cdot b$$

With:

L: Length given by geometry (m)

b: Width (m)

So, the width, b, is calculated from the shear stress failure of the epoxy bonding, τ_f:

$$b = \frac{T}{L \cdot \tau_f}$$

Then, the Reaction Force, RF, can be extracted from the GFEM. Each interface between parts are defined in order to get the RF that consists in 3 Forces (Fx, Fy, Fz) and 3 Moment (Mx, My, Mz). The reaction force between components are extracted from GFEM (Hypermesh) and used to design each part (Figure 79).

Figure 79: Example of reaction force between each component consist in 3 axes (Force and Moment)

Result of Shear force calculation (In-plane force)

Calculation results show that the flange width, b, is small due to the large length, L. However, from aerospace experience, the width must be largely bigger due to the manufacturing process. Indeed, bonding properties are related to the manufacturing quality (surface roughness, surface cleanness, surface impurities….). Therefore, the width, b, will be increased to 30 mm (Table 16).

Table 16: Calculation of Shear force that come from Reaction force (GFEM)

Components	Resultant of shear force [N]	Resultant of moment [N.mm]	Shear force from moment [N]	Total shear force [N]	b [mm]
Beam_S2_T	990.49	2290.57	995.90	1986.40	1.6
Beam_S3_T	78.78	-10688.5	-4647.18	-4568.39	3.8
Beam_BC4-1	313.19	39776.37	17294.07	17607.27	14.6
Beam_BC1_Low	2749.51	87667.54	25047.86	27797.38	23
Beam_BC2_Up	6495.59	138118.02	39462.29	45957.88	38.2
Beam_BC2_Low	1978.13	3986.24	1138.92	3117.06	2.5
Beam_BB-BC	5037.42	709433.11	202695.17	207732.59	173
Beam_T-BC1	2236.67	58688.07	25516.55	27753.22	23
Beam_BC4_Up	463.29	4771.06	1363.16	1826.45	1.5
Beam_Tfront-Up	6440.10	267495.18	76427.19	82867.30	69
Beam_BC4_Low	977.91	15915.44	4547.26	5525.18	4.6
Beam_S2-Low_4	3890.06	71443.15	31062.24	34952.30	29
Beam_S3-Up_1	1972.73	107855.50	30815.85	32788.59	27.3
Beam_BB_Up_1	11399.74	179717.59	51347.88	62747.62	52.2
Beam_BB_Up_3	6451.46	102040.72	29154.49	35605.95	29.6

Finally, due to the aerospace experience and rules width of the flange will be 30 mm.

Conclusion

In this chapter the objective has been propose the concept design of stiffeners instead of honeycomb. Model construction has been performed. Methods of the optimization were studied. Hollowing the stiffeners was explained. And reaction force was defined in order to calculate the flanges. The next step is to be going on detailed design.

CHAPTER 5: DETAILED DESIGN

5.1) Introduction

In detailed design will be focus on the detailed model and optimization of each ply. In a first step, detailed design from the optimization and flanges calculation On the GFEM will be performing and then boundary condition that applied on the model will be realized also loading and mesh. After that material which is used on this model will be detailed. Then, in detailed design, each ply of the components on spoiler will be optimized by the simulation program in order to reach the ply by ply optimization. After ply by ply optimization methodology of the process will be performing after that result of the model which is including with static and buckling result will be investigated. Aerospace design rules will be the next step in order to respect the aerospace manufacturing experience. Finally, the conclusion of the detailed design will be summarized.

5.2) Model Construction

From GFEM flanges were calculated, detailed design has been modelled with flanges, fillet, corner. In this case size of the flanges fillet and corner has been respected by aerospace design rules (Figure 80).
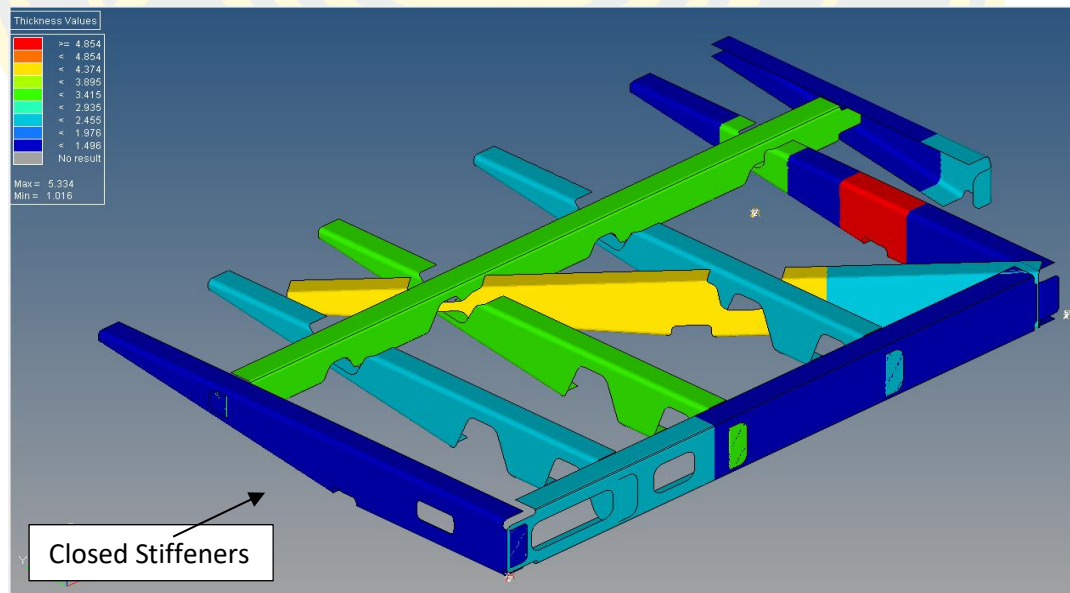
Figure 80: Detailed model after flanges calculation

5.3) **Boundary condition**

Due to the symmetry, the half spoiler will be performed in order to reduce the time of computing and. Therefore, symmetry constraint at the border will be created to decreasing time as mention above (Figure 81).
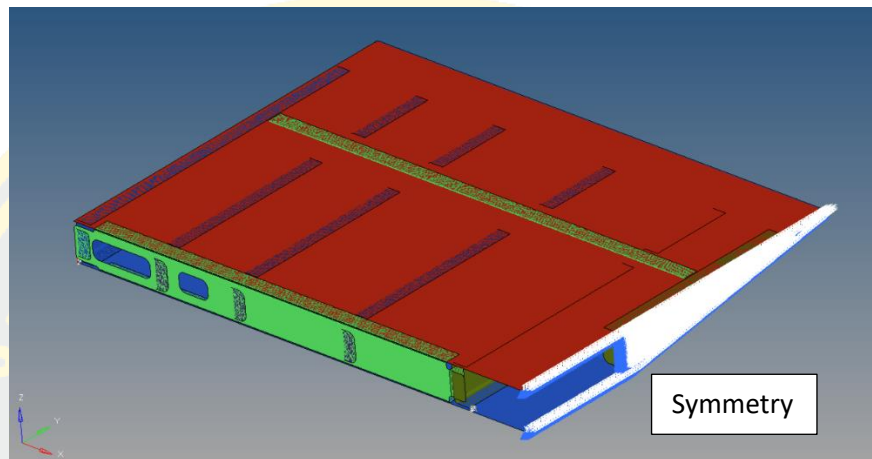
Figure 81: Half spoiler model

The half spoiler has two common boundary condition which is fix (Figure 82) and symmetry. Rotation mechanism is considered as rigid (Figure 83). Therefore, fix condition was applied. As mentioned above in "half spoiler" symmetry boundary condition was used in order to reduce the time on computing).
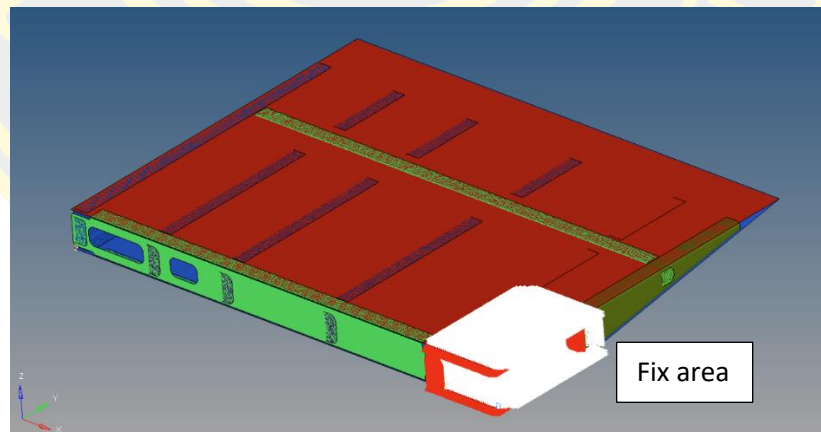
Figure 82: Fix area boundary condition
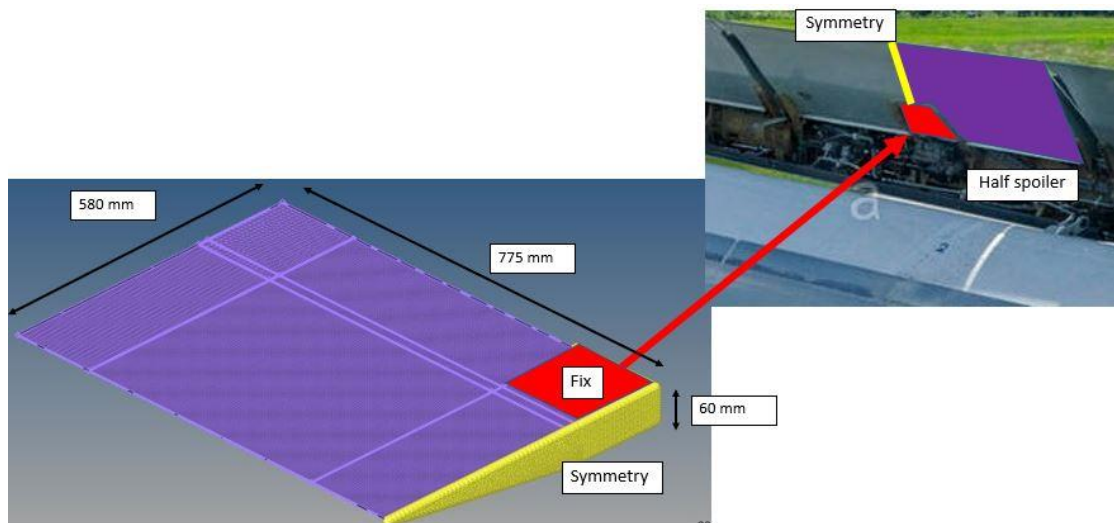
Figure 83: Rotation mechanism

5.4) Loading

The loading was applied on the upper surface of spoiler which is 15,395 N thanks to the calculation (Figure 84).
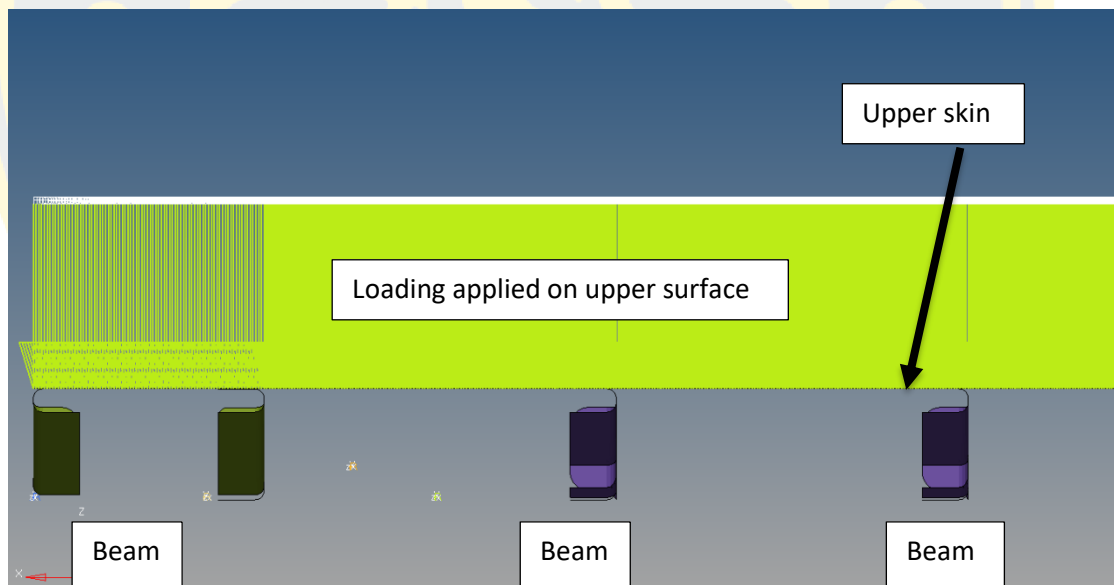
Figure 84: Load applied on upper surface on the half spoiler

5.5) Mesh

The model of spoiler in this thesis, mesh size 1.5 mm per element was selected in order to combine accuracy and computing time.
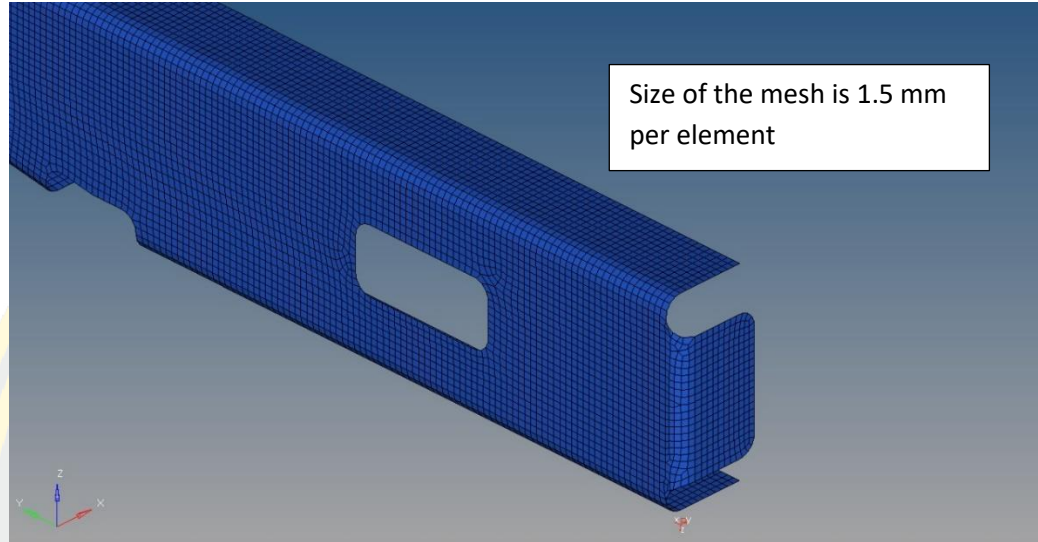
Figure 85: Fine mesh in Detailed design

5.6) Materials

CFRP IMA/M21E was used on this model in order to input the materials properties and damage tolerance on the simulation program. Especially, the damage tolerance has been used for design criterion (Figure 86).

Figure 86: IMA/M21E CFRP used on the model

5.7)   Laminate of components

Each ply of each component was created in order to check the result of each ply (Figure 87). Optimization is performed ply by ply by sequencing the ply stacking following aerospace rules. Laminates of each components (each stiffeners, each skins…) are detailed in the spoiler model (Figure 88 and 89).

Figure 87: Ply by ply created on the program
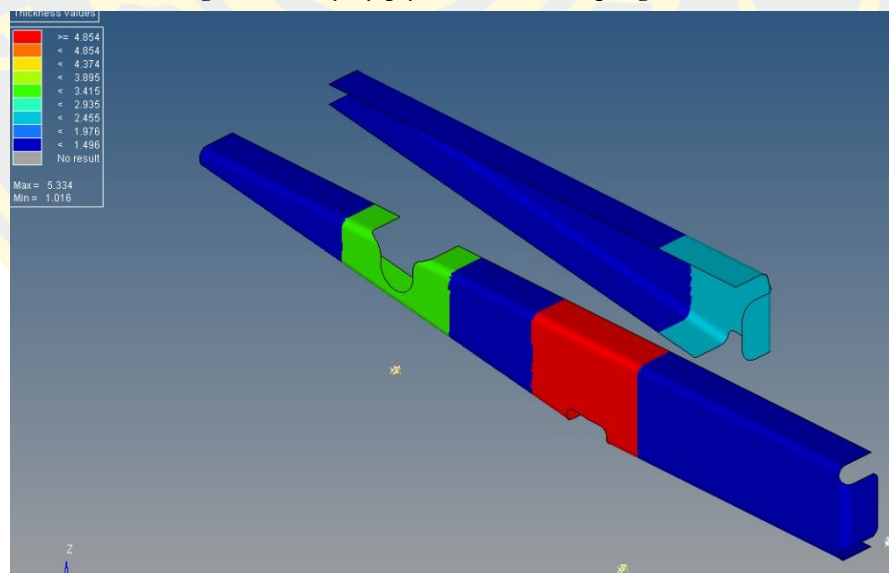
Figure 88:Location of the main ply and local patch

Figure 89: Stacking on the component with plies

5.8)   Methodology of detailed design

Detailed model with flanges was previously created where a first optimization was realized by adding local plies (Figure 80). Next optimization consists in ply by ply optimization in order to reduce the mass (Figure 90).

Detailed design	Ply by ply optimization

Figure 90: Methodology of detailed design

Ply by ply optimization is expressed into 2 parts. First, thickness will be reduced on each ply by ply simulation. Then, stacking sequence will be realized following aerospace rules. Detailed designed will be performed under static and buckling analysis. In static, strain will be observed as failure criteria, while in buckling force required to buckle will be investigated.

5.9)   Static result

Final optimization ply by ply results show that strain (-4000 μdef) do not exceed the allowable except at the boundary condition area (Figure 91). Due to the boundary condition it is not possible to conclude at this location and local analysis is required.
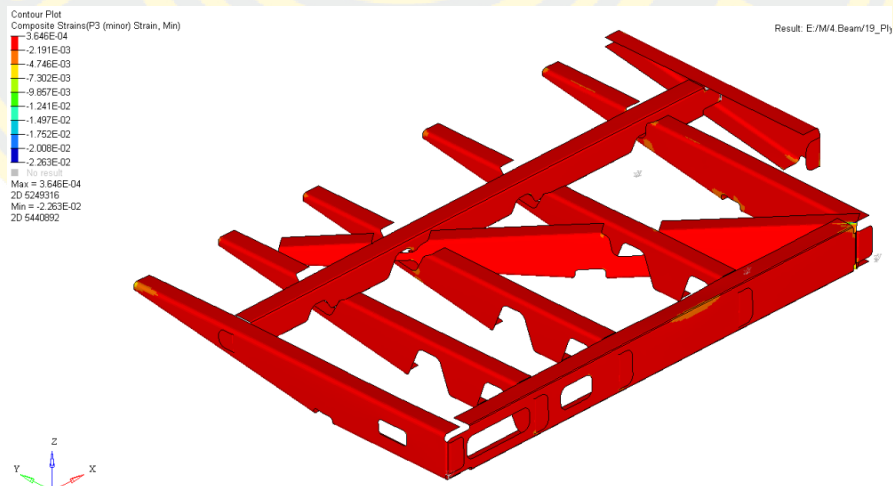
Figure 91: Static result

5.10)   Buckling result

First results show buckling of the lower skin (Figure 92) and therefore local plies have been applied to reinforce the structure. 4 plies have been added at the location described in the Figure 93 and 94. Therefore, the mass will be highly increased due to the local plies on the skins (Table 17).
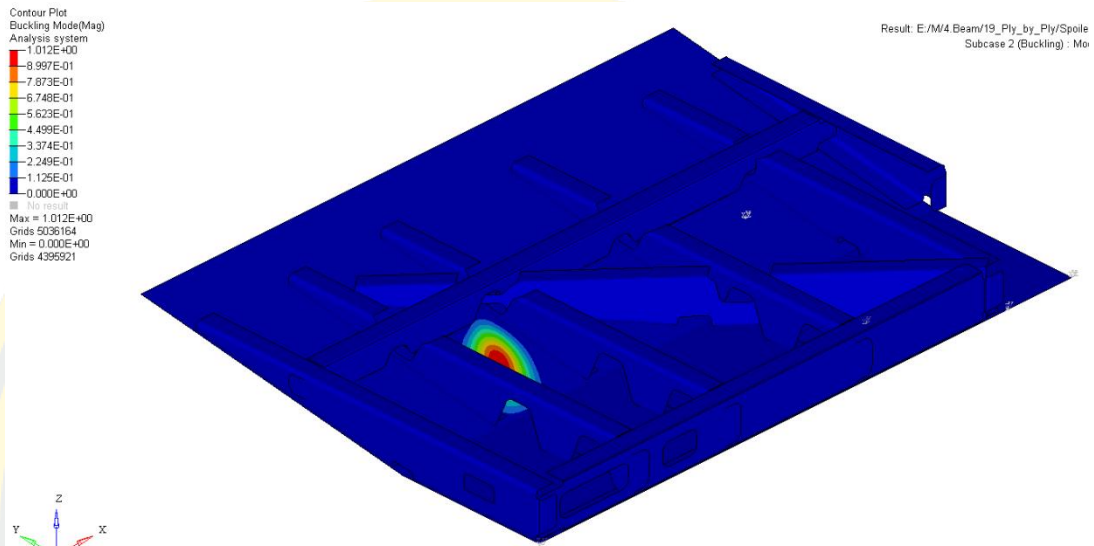
Figure 92: Buckling result
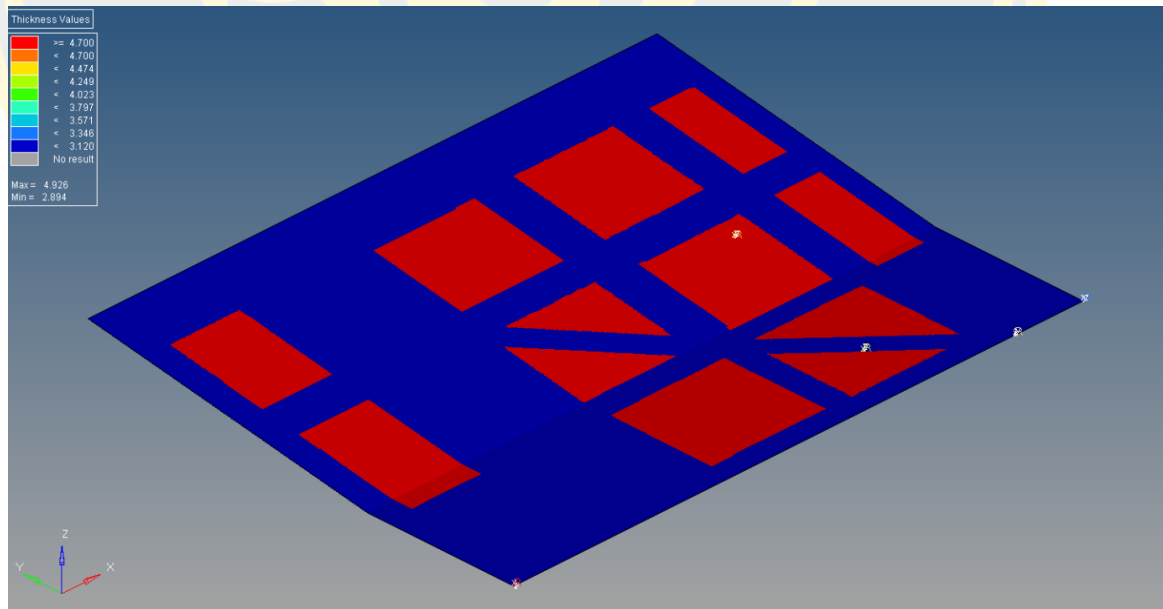
Figure 93: Full patch of the lower skin
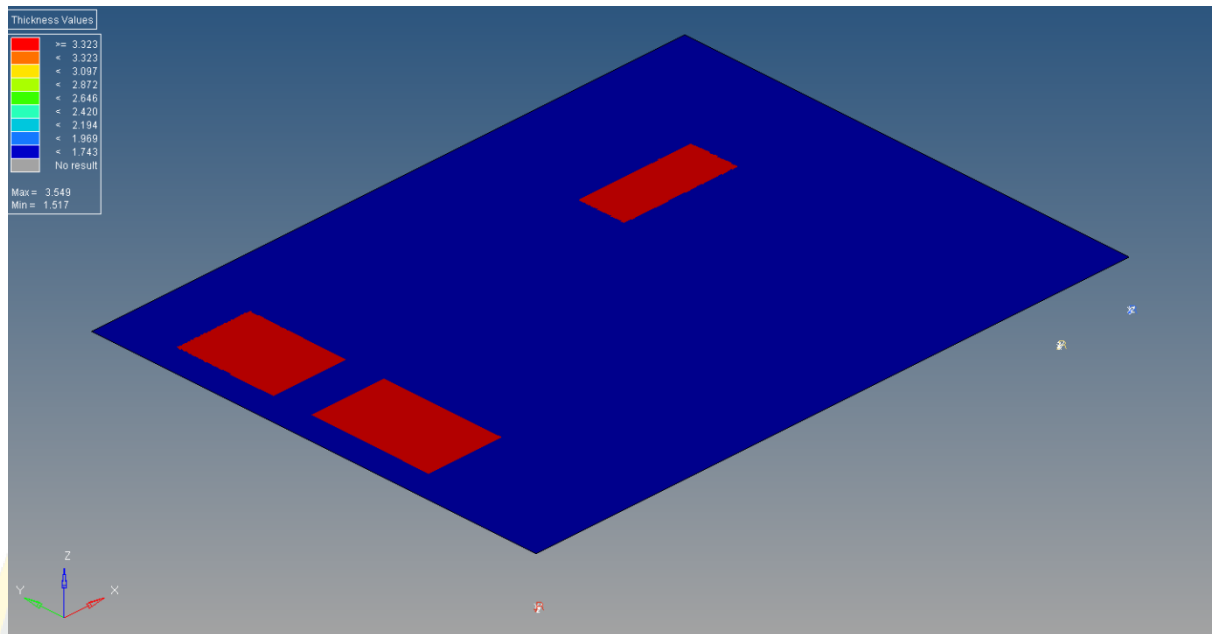
Figure 94: Full patch of the upper skin

Table 17: Comparison of mass before optimization between static and buckling

	Mass [kg]
Static	6.6
Buckling	7.9

5.11) Aerospace design rules

Aerospace design must follow a large number of rules in order to comply with aircraft manufacturer. These rules come from many years of experiences of the main aircraft manufacturer (Airbus and Boeing). These rules must be the most possible respected to avoid manufacturing problems, mechanical failure.

Stacking Sequence Rules

The following stacking sequence rules must be following to get especially orthotropic laminates or, otherwise, minimize coupling effect and help the manufacturing process.

Rules 1: Symmetry

The stacking sequence should be symmetric around the neutral axis: for each ply in direction $+\theta i$ at a distance Z of the middle plane, exists a ply in direction $+\theta i$ at a distance -Z, θi being the angle with regard to the main load direction

If perfect symmetry is not possible, the "asymmetry" shall be kept as close as possible to the middle plane. These cases should be analyzed to prevent manufacturing deformations (Table 18).

Table 18: Rule 1 - Symmetry (AIRBUS 2009)

45º	45º
90º	90º
135º	135º
0	0º
Middle	0º
0º	0º
135º	135º
90º	90º
45º	45º
OK	OK

Rules 2: Balanced

The laminate should be balanced: for each ply in direction $+\theta_i$ exists a ply in direction $-\theta_i$.

If perfect balance is not possible, the "Unbalance" shall be kept as close as possible to the middle plane. These cases should be analyzed to prevent manufacturing deformations (Table 19).

Table 19: *Rule 2 – Balancing (AIRBUS 2009)*

Angle	Number of Plies	
	20	20
0 º	10	10
45 º	4	6
135 º	4	2
90 º	2	2
	OK	Avoid

However, even for symmetrical and balanced laminates, other mechanical coupling can appear. These coupling can be minimizing with the following rules

Rule 3: plies orientation percentage

For solid laminate part the percentage of the plies laid-up in each direction should be comprised between 8 percent and 67 percent (Figure 95).

Resultant compression load due

Primary Load direction 0

Minimum 8
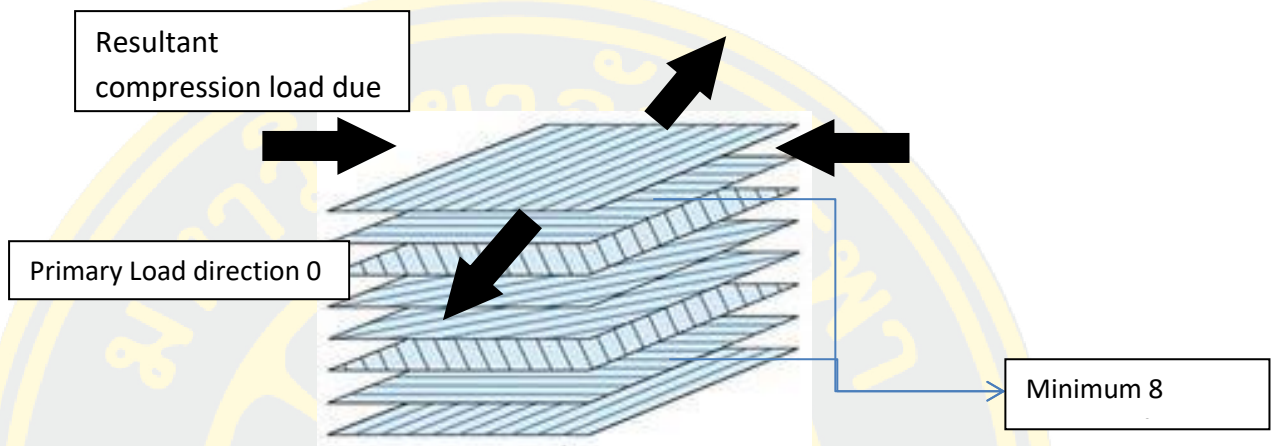
Figure 95: Rule 3 –Plies orientation percentage (AIRBUS 2009)

Rule 4: External Plies

External plies should never be in the direction of the main load. It is recommended to use a 45º/135º pair for the outer plies of the laminate. However, in certain application (CWB), a 90º external ply could be used (Table 20).

Table 20: Rule 4 – External plies (AIRBUS 2009)

45º	0º
135º	45º
0º	135º
135º	90º
45º	135º
90º	45º
Middle	Middle
90º	45º
45º	135º
135º	90º
0º	135º
135º	45º
45º	0º
OK	AVOID

Rule 5: Regular distribution of layer orientation

The layer with the same orientation should be uniformly distributed throughout the stacking sequence to minimize coupling effect and ensure a homogeneous stress distribution throughout the laminate (Table 21).

Table 21: *Rule: 5 Regular distribution of layer orientation (AIRBUS 2009)*

45º	45
135 º	135
90 º	90
135 º	90
45 º	90
0 º	135
45 º	45
135 º	0
90 º	45
45 º	135
135 º	135
0 º	45 º
135 º	0 º
45 º	135 º
90 º	45 º
Middle	Middle
OK	NOT PREFERED

5.12)   Result

Stacking proposed in detailed design (Figure 91) allow to avoid failure and buckling but do not respect aerospace rules. Therefore, more plies will be added on the model in order to respect aerospace design rules. The mass of the spoiler will be increased due to the added plies (Figure 94, 95 and 96).
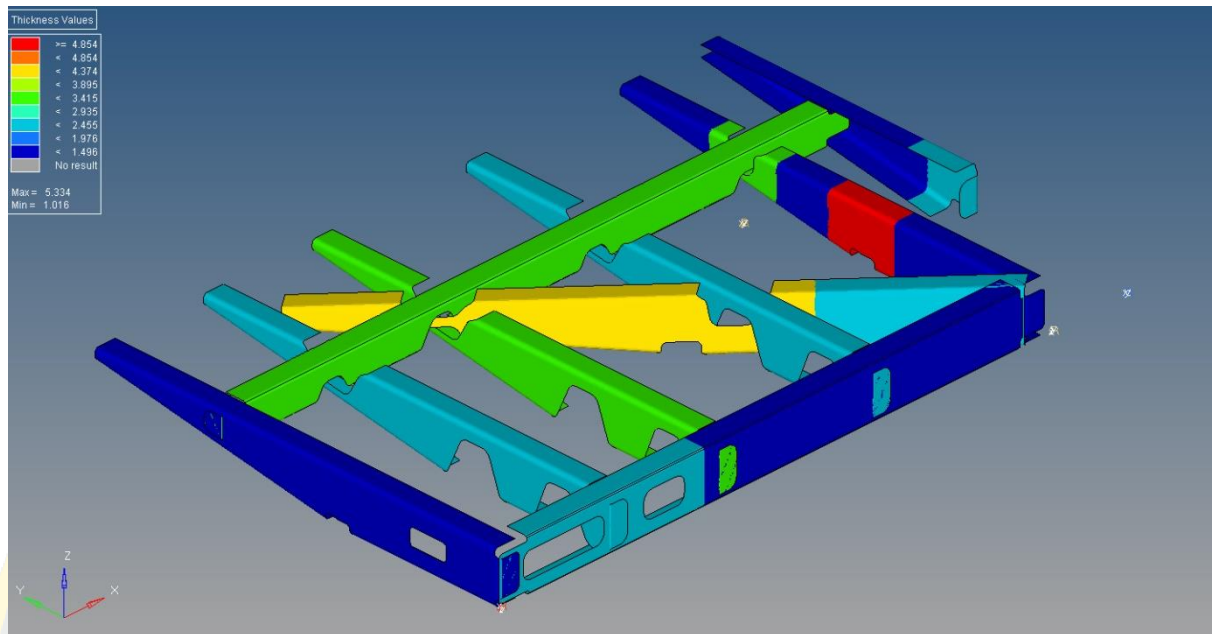
Figure 96: Full patch of the beam of the spoiler

As observed, the mass is 6.8 kg for static only that is lightly higher than the initial mass objective (Table 22). To avoid buckling a large number of plies are required locally that increases the mass to 7.7 kg. As more plies have been used on stiffeners, lower plies number are required for buckling resistance.

Table 22: Comparison of mass after optimization between static and buckling

Analysis	Mass [kg]
Static	6.8
Static + buckling	7.7

Conclusion

In this chapter the detailed design was performed by model construction, boundary condition, load applied and mesh. Methodology was followed by the process. Ply by ply optimization was performed by the result with laminates of each component and each ply also. Static and buckling has been studied. Aerospace design rules was thoroughly respected to be able to use for manufacturing process. Finally, the result after many aerospace rules and experience shows that more plies is necessary to avoid the buckling and to respect the rules. Ply patch is required on skins for buckling. So, the mass is increased.

Honeycomb can be replaced by stiffeners to avoid water retention and to simplify NDT maintenance but in term of mass, the use of stiffeners is not suitable.

CHAPTER 6: MANUFACTURING&TESTING

6.1) Introduction

This chapter will focus on two mains propose. Firstly, the prototype of stiffener will be manufactured by following the design proposed in the previous chapter. Secondly, the prototype of the stiffener will be mechanically tested at GALAXY LAB at GISTDA by using UTM machine. Testing result will be compared with local FEA to validated and optimized.

6.2) Manufacturing prototype

In a first step, preparing of materials that used for manufacturing will be shown by list of materials (Table 23). Secondly, process of manufacturing will be detailed by following the step.

6.2.1) List of materials

Table 23: List of materials used for manufacturing

Name of materials	Picture
Mold from COBRA	
Fixed bench	
Washer	
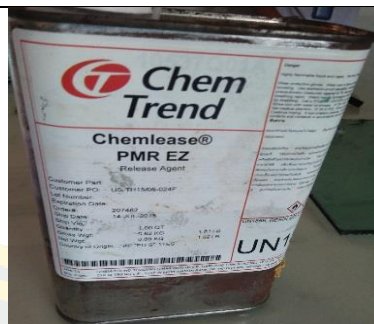
Chem Trend Release agent	
T-700 UD Carbon fiber	
Adhesive film AF3109-2U-0.35WT	
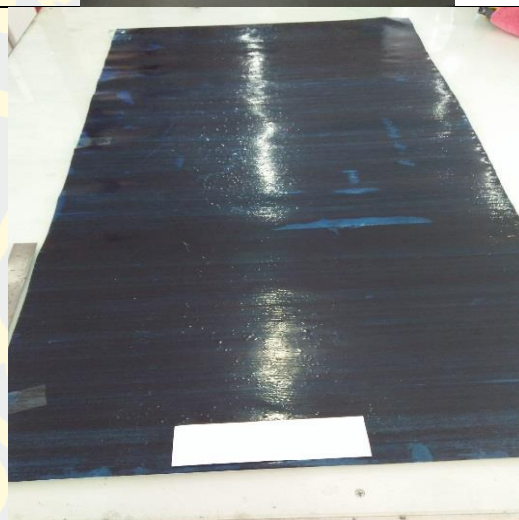
Bagging Flim	
Unperforate Release Film	
Breather	
Release Film Perforate	

Peel ply	
Sealant Tape	
MICROGARD® 1500 PLUS	

Safety gloves	
Cutter	
Roller	
Vacuum Pump	

Thermocouple Data Locker	
Curing Oven	

6.2.2) Manufacturing process

In a first step, stiffener mold was built and used to lay-up composite laminates and then bagging system was applied. Finally, stiffener prototype has been manufactured in oven following the temperature control given by the data sheet (Figure 97).

Figure 97: Step of manufacturing

Firstly, role of each materials (Table 23) will be detailed due to the different function. Secondly, requirements of aerospace standard will be explained due to safety of manufacture. Thirdly, stiffener can be built by following step of manufacture. Finally, stiffener will be checked by quality control by UT scan.

Role of each materials on the list

COBRA received stiffener CAD file to CNC the mold. Thanks to COBRA company mold of stiffener was built and can be used to manufacture the stiffener.

Chem Trend Release Agent used to clean the mold due to the dust in the air. However, the manufacturing process operated under clean room at GISTDA due to aerospace safety requirement.

T-700 UD carbon fiber was used in this manufacture process instead of IMA/M21 that is a reference used by AIRBUS because this material cannot be bought. Therefore, T-700 carbon fiber and Torey 120 ℃ Epoxy resin were used in aerospace and has been used in the research. Properties of T-700 is very closed to IMA/M21 properties. Finally, the differential properties of these two materials are 8% (Table 24).

Table 24 : Comparison of CFRP properties

Properties	*IMA*	T700
E_l (GPa)	154	125
σ_{12}(MPa)	105	90
σ_{lc}(MPa)	-1450	1570
σ_{lt} (MPa)	2610	2450

Method of sealing composite laminates before curing process (Figure 98). firstly, mold of stiffener is a base item and then lay-up composite laminated with 4 plies on it with basic stacking [0 45, -45,90]. Secondly, peel ply will lay upon the composite laminates it is necessary to use peel ply in order to separates part from bagging system. Thirdly, release film un-perforated will lay upon the peel ply to avoid resin for the part during lay-up process. Fourthly, to absorbs excess resin and protect the surface of laminate from vacuum pressure. Therefore, breather will be lay upon release film. In last step bagging film will applied to cover all of the system mentioned above and sealing with sealant tape and applied vacuum valve to control the pressure (Figure 99).

Figure 98: Demonstrate of vacuum system

Figure 99: Vacuum valve to control the pressure

Fixed bench and washer were used to fix the stiffener on the test bench (Figure 100). The stiffener will be attached with aluminum fixed bench by Adhesive film AF3109 by using curing oven for 1 hours due to data sheet of Adhesive film (Figure 101).
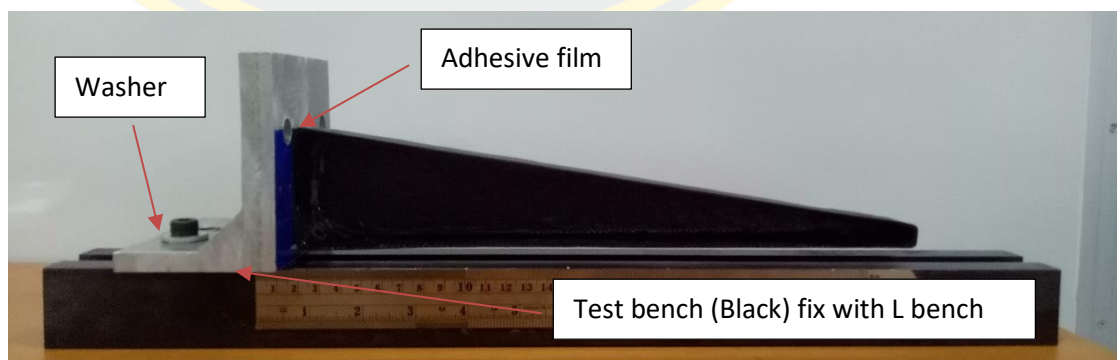
Figure 100: Stiffener attached with adhesive film
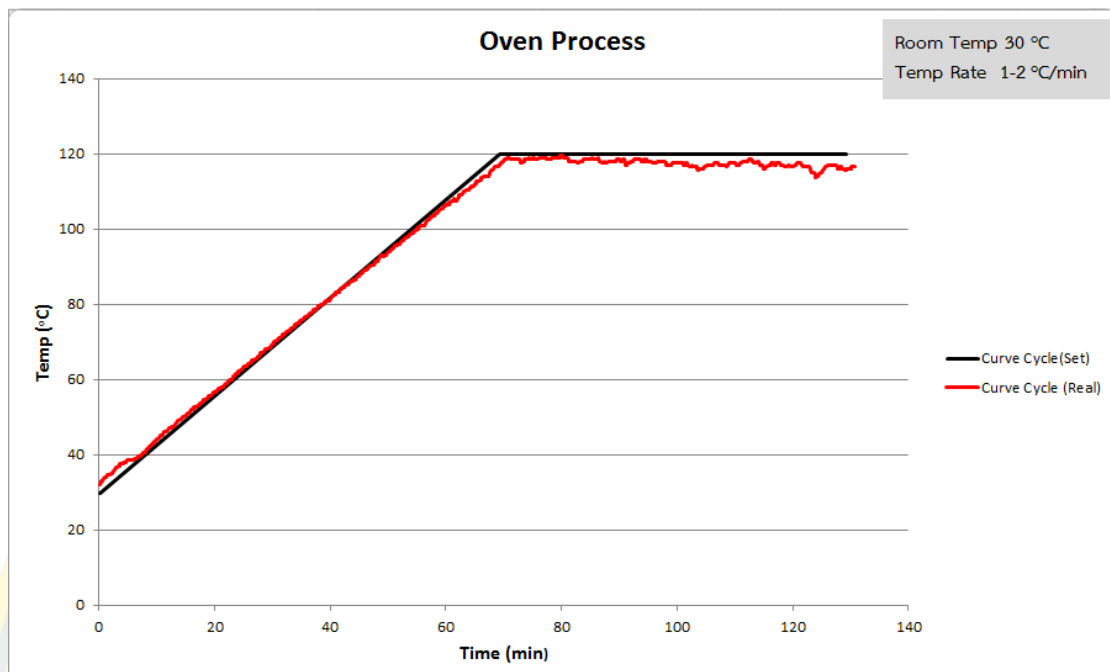
Figure 101: Curing cycle 1 hour for 120℃ of adhesive film

Aerospace standard manufacture requirement

Aerospace manufacturing required clean room to avoid the dust in the air instead of manufacture by normal room. To perform process in clean room safety guard, glove and shoes are required (Figure 102). Especially, aerospace standard ISO 17025 (Testing lab standard), AS9100 and NADCAP (Aerospace standard) were certificated at GISTDA laboratory.
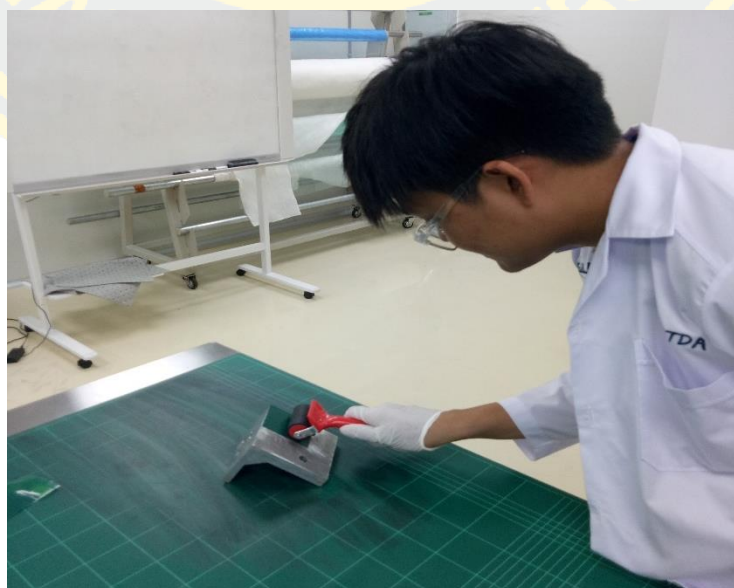
Figure 102: Safety equipment

Quality Control

Ultrasound is the most widely used technique for inspecting composite structures. There are a large variety of appropriate ultrasonic instruments available. Typically, ultrasound travels very well in composite laminated structures and it can detect anomalies quite easily. Unfortunately, in sandwich structures the ultrasound is extremely attenuated due to the inhomogeneity and low density of the core structure. Therefore, the use of ultrasound for sandwich structures requires more specialized features in instruments.

On microscopically homogenous materials (i.e. non-composite) it is commonly used in the frequency range 20 kHz to 20 MHz (Downes., 2003). With composite materials the testing range is significantly reduced because of the increased attenuation, so the operating frequency limit is usually 5 MHz or less (Downes., 2003). Ultrasonic pulse-echo is a well-established and widely used non-destructive testing technique. A pulse of ultrasonic energy, typically a few microseconds, is transmitted into the specimen in a direction normal to the surface. The pulse is reflected from good matrix-reinforcement boundaries and also from boundaries associated with flaws. Figure 103 shows a typical pulse-echo set-up for a submerged immersion test.
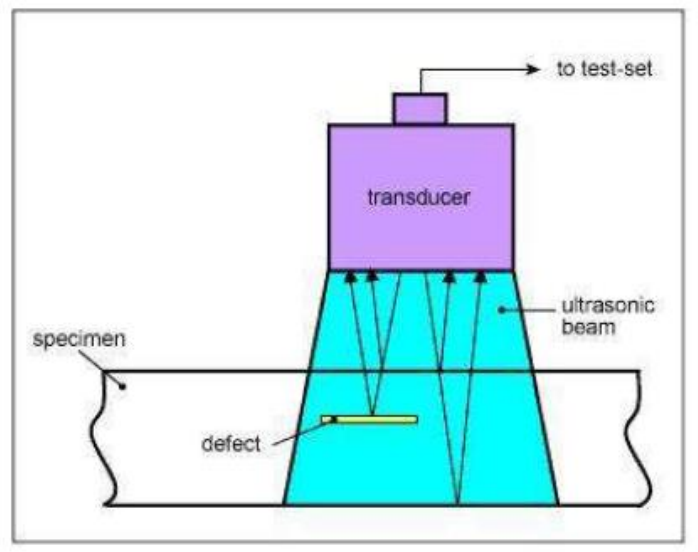
Figure 103: Immersion pulse-echo test with submerged specimen

Those signals which travel back towards the probe are detected and the position and size of a flaw is determined from the total pulse travel time and detected amplitude respectively. This is the 'A-scan' display and it consists of a series of peaks, the position of which along the horizontal axis can be calibrated in terms of the depth in the composite. The amplitude of each echo will give some indication of the size and nature of the reflector, which might be a flaw or a specimen boundary.
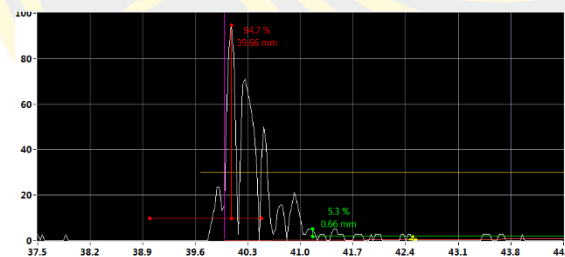
A-Scan
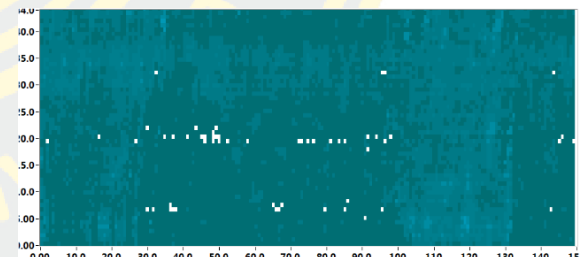
C-Scan
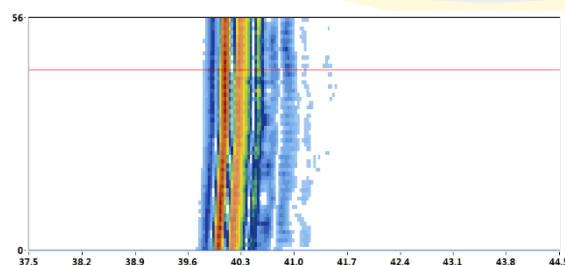
B-Scan
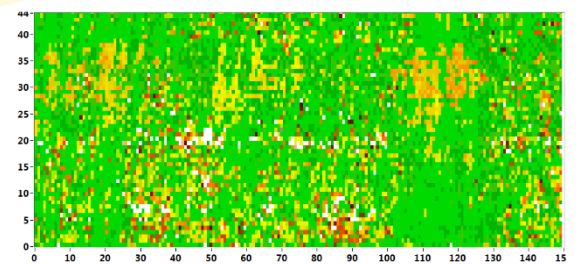
C-Scan

Figure 104 : Monitoring of result for UT-Scan

6.3)   Testing

In a first step, global view has been explained in order to summarize the process of testing. Then, the result of testing will be investigated and discussed. Therefore, local finite element analysis has been performed in order to check the boundary condition. Finally, result of FEA has been studied.

6.3.1)   Global view

From FEA results cannot be concluded at the boundary condition. Therefore, mechanical testing must be performed. Stiffener at the center of the spoiler bonded to the rotational feature is studied. The rotational feature (Figure 105) was considered as rigid. To test in the same condition, thick L steel bench in steel was used. L bench was bolted to a support that was fixed on the tensile machine. Rib was bended with constant velocity of 1 mm/min.
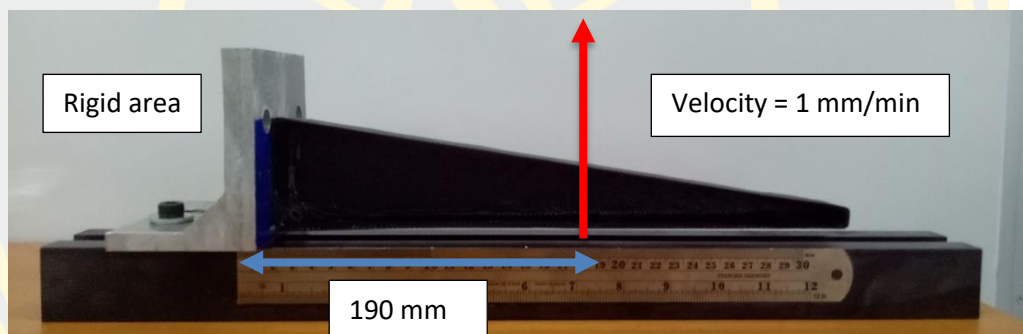
Figure 105: Global view of testing

Distributed force is applied on the spoiler. Due to the UTM used at GISTDA, concentrated load needs to be applied. In other hand, only bonding between rib and rotation feature must be checked (Figure 106). Therefore, moment at the bonding area will be compared between the test and the simulation.
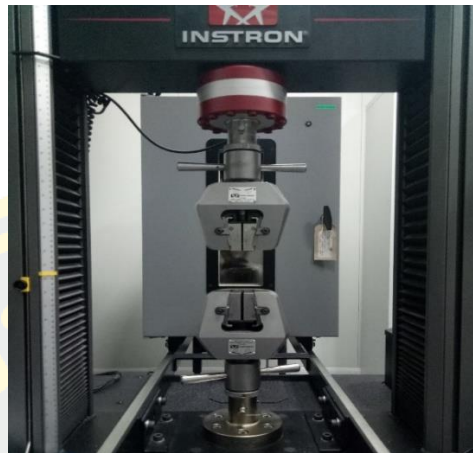
Figure 106: UTM in GISTDA Lab

6.3.2)   Results

Force-displacement is shown in Figure 107. Failure appears for a force of 120 N at the lower part of the bonding (Figure 108).
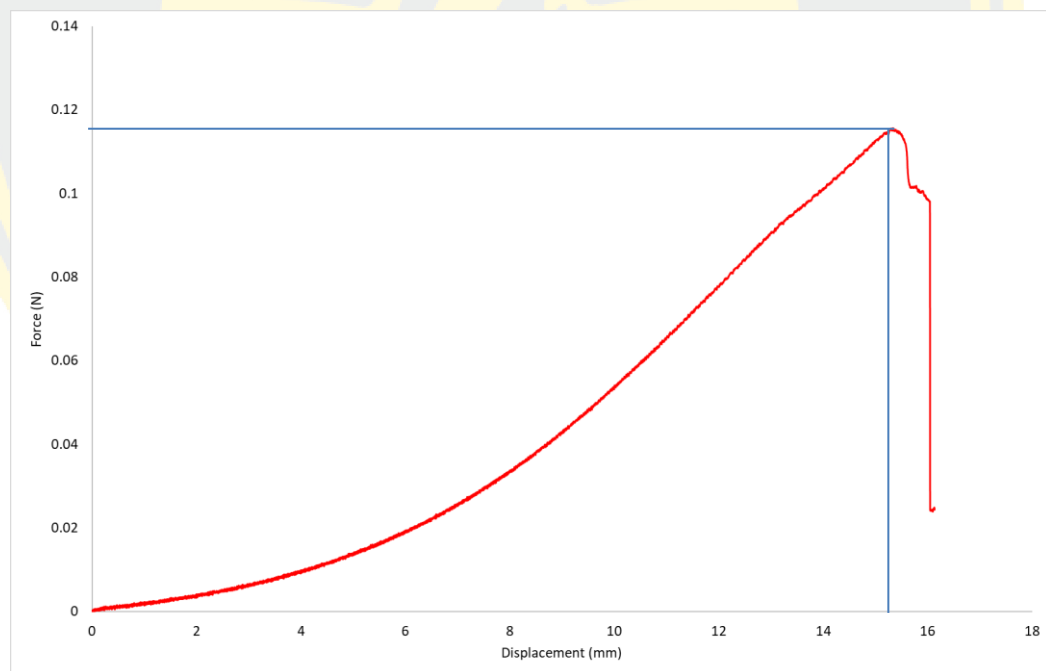
Figure 107: Force and Displacement of testing
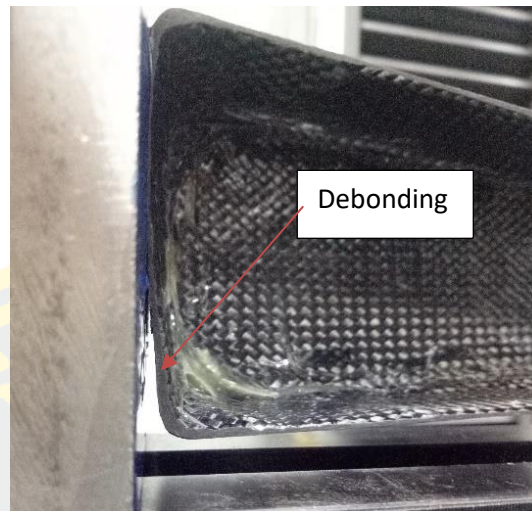
Figure 108: Debonding of the stiffener

From experiment the failure moment M_{exp} at the boundary condition is therefore:

$$M_{exp} = 120 \text{ N x } 190 \text{ mm} = 23 \text{ N.m}$$

6.3.3)   Discussion

M_{exp} must be compared with the failure given by the simulation using the distributed force on spoiler. From the simulation, the failure moment at the boundary condition M_f can be calculated by:

$$M_f = \frac{1}{2} P \cdot L$$

Where:

P: Force applied on the surface = $\frac{1}{2} \rho v^2 A$

A: Surface of force applied

V: Landing Velocity   =   86.64 m/s

ρ: Density of air   =   1.225 kg/m^3

L: Length of stiffener

The studied stiffener is one of the main stiffeners that support the load given by the drag force (Figure 109). These stiffeners are linked to the rotational feature. The moment and force applied on surface A can be considered to be fully supported by the main stiffeners. Therefore, the studied stiffener support only the load on the surface A_1.

Figure 109: Support area while force/moment applied

The force applied on the studied stiffener can be estimated by considering that only the surface, A_1, between the 2 stiffeners is used. Indeed, the force applied on the rest of the spoiler will be supported by the other stiffeners. The surface A_1 is therefore (Figure 110):

$$A_1 = 0.315 \times 0.1 = 0.0315 \text{ m}^2$$

Figure 110: Support area while force/moment applied in simulation

The moment given by this distributed force at the boundary condition is given by:

$$M_f = \frac{1}{2} \times \frac{1}{2}(86.64)^2(0.0315)(1.225) \times 0.315 = 29 \text{ N.m}$$

The failure moment given by the simulation is finally 29 N.m that is 20% higher than the value from experiment. The failure moment from experiment is lower than the value of the

simulation. Therefore, the proposed design fail. Finally, the bonding needs to be optimized to support the required moment. A first proposed optimization is to increase the contact surface of 20% given a value of 840 mm^2 (Figure 111).

Increase contact surface at least 840 mm^2
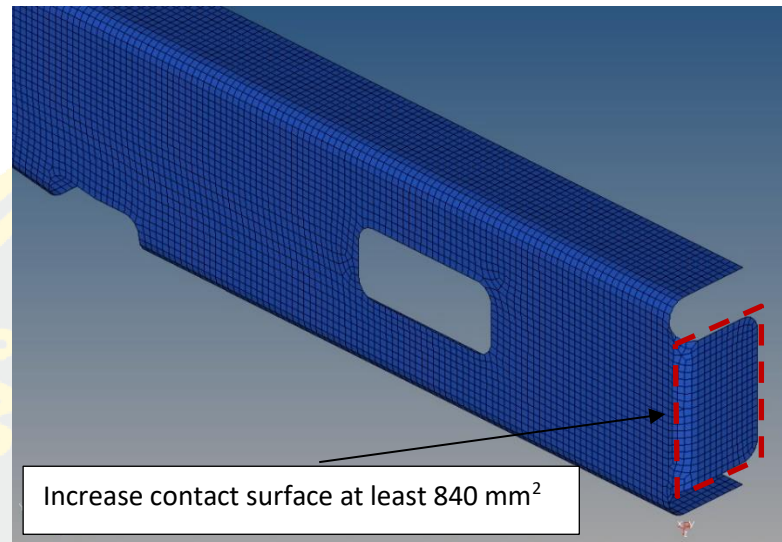
Figure 111: Contact surface proposal

6.3.4) Finite Element Analysis

In order to optimize the bonding, simulation needs to be used. In a first step model is built and validated by comparing the failure force between the model and the experiment. Then, the model can be used to optimize.

Model construction

The model consists of 3D components: L-Bench, Stiffener and Adhesive film (Figure 112). The L-Bench is considered as fixed with bolted. Steel is applied as properties for the L-Bench while epoxy resin is applied on the adhesive film. Properties are given Table 25. Steel and epoxy were considered as isotropic.

Table 25: Steel and epoxy resin properties

Properties	Steel	Epoxy
E (GPa)	220	36
σ (MPa)	370	34
ϑ	0.3	0.389
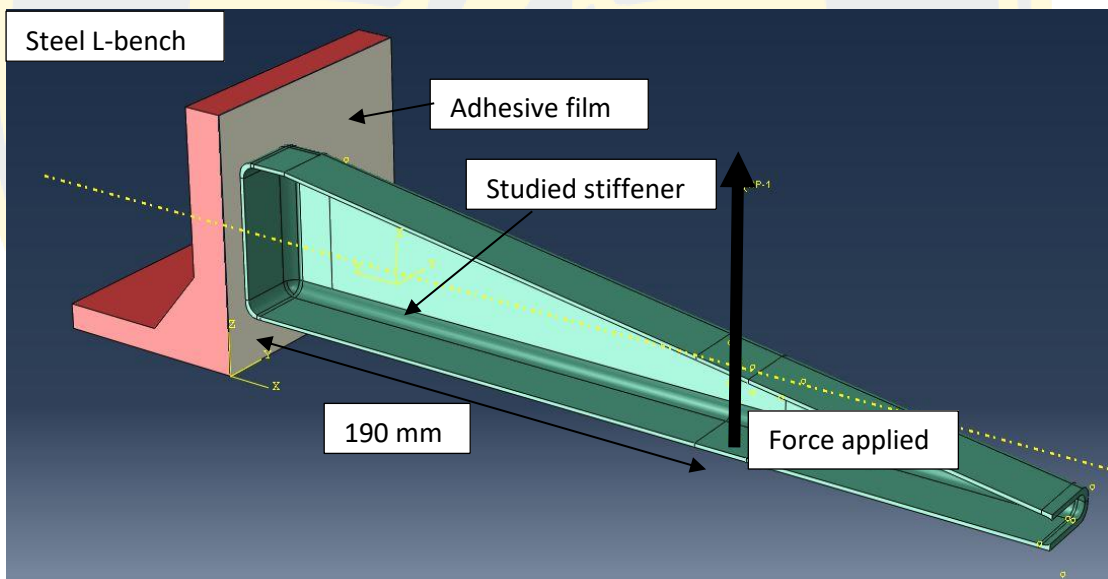
Figure 112: Model of experiment

Boundary condition

L-bench has been considered as fixed therefore fix boundary condition was applied at the bottom of the L-bench (Figure 112).
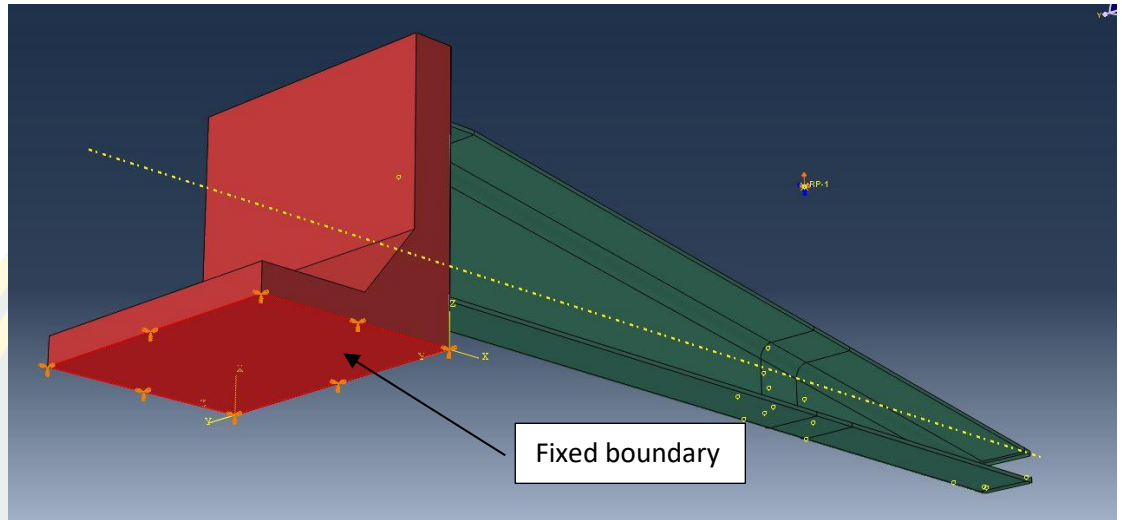
Figure 113: Fixed boundary on FEA

Mesh

Mesh was created on the model. In order to have a precisely result 1 mm of the mesh has been applied on the model (Figure 113).
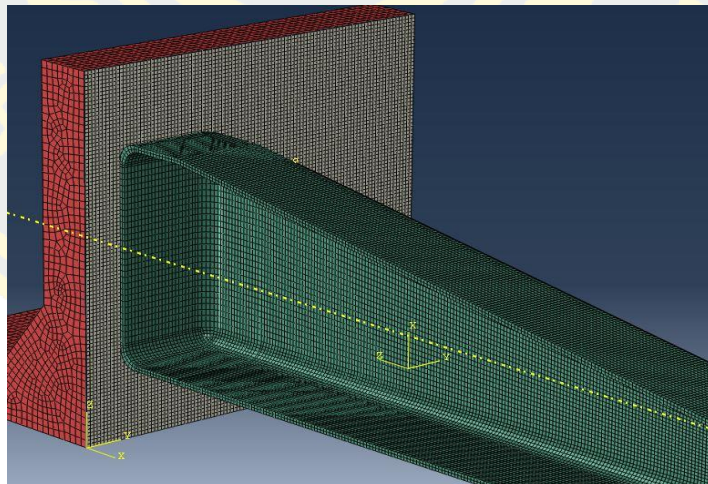
Figure 114: Mesh of the testing model

Load

As tensile test performed, displacement was applied. The displacement has been applied at the distance 190 mm from boundary condition (Figure 114).
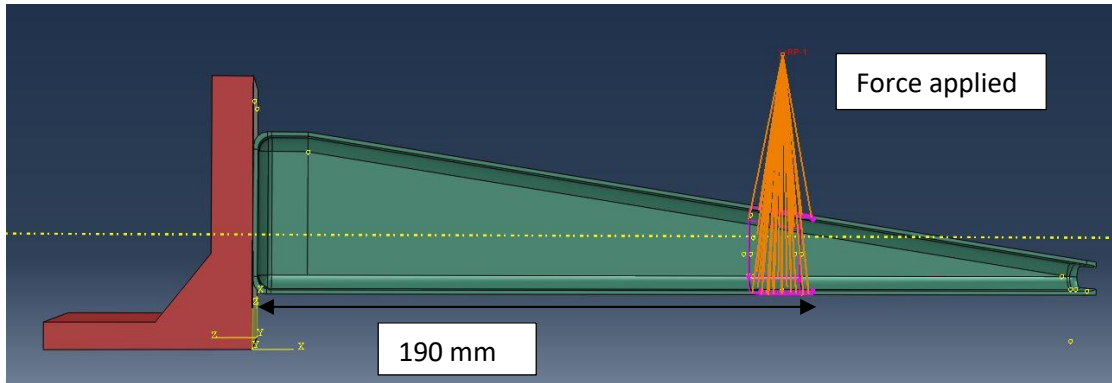
Figure 115: Load applied on the testing model

Contact surface

Contact surfaces were determined in order to give the contact surface of each component together. Tie contact was used. Firstly, the contact surface of adhesive film and L-bench was applied on the model (Figure 115). Secondly, the contact surface of adhesive film and stiffener was applied on the model also (Figure 116).
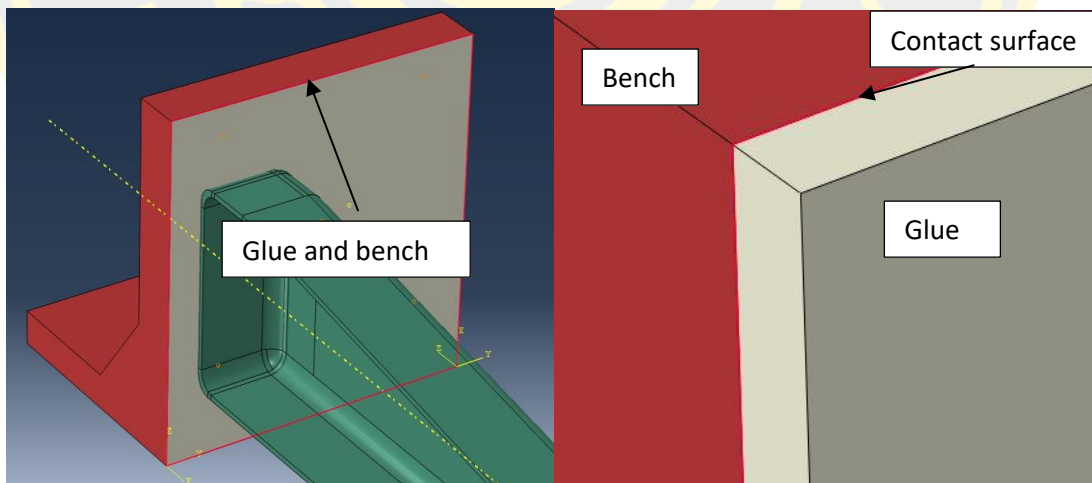
Figure 116: Adhesive film and L-bench contact
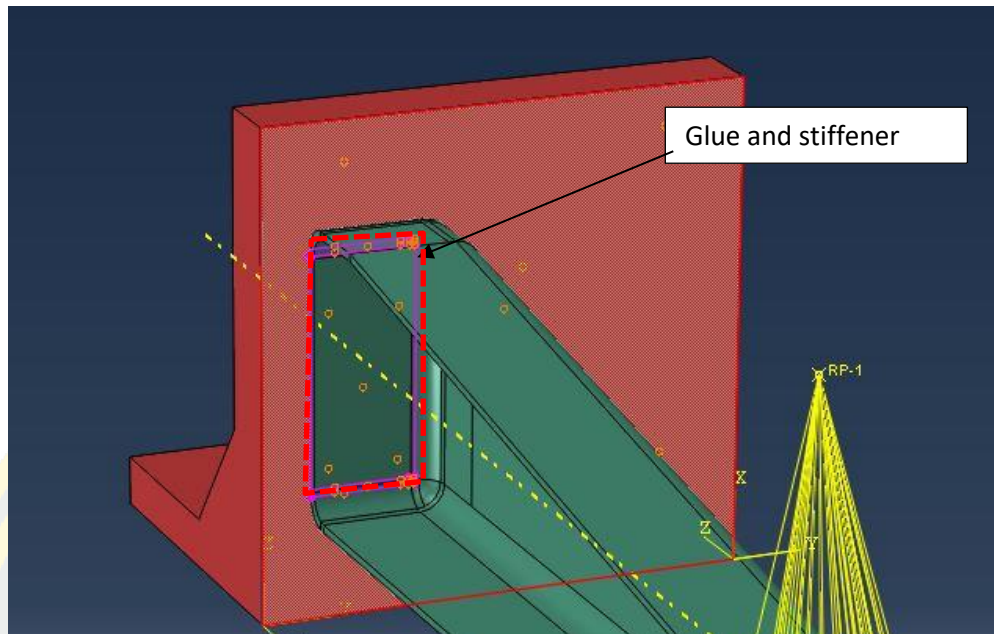
Figure 117: Adhesive film and stiffener contact

6.3.5)   Result of FEA

Result of finite element analysis will be expressed into 3 parts which is L-bench, adhesive film and stiffener. In a first step, result of L-bench will be detailed as von mises. Then, the bonding between adhesive film and stiffener will be investigated. Finally, the stress on the stiffener will be studied.

L-bench result

The result shown Von Mises of the L-bench is 5 MPa that is a really lower than steel yield strength ($\approx$ 220 GPa). Therefore, the boundary condition confirmed as rigid.
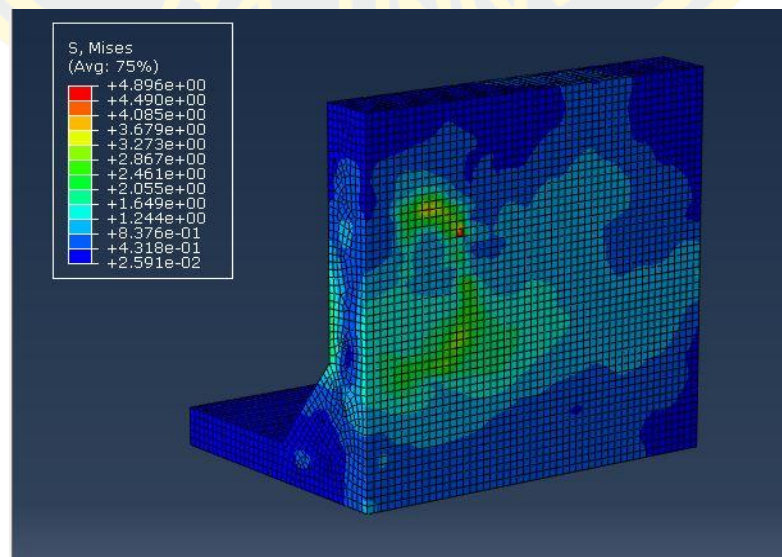
Figure 118: Result of L-bench

Adhesive film result

Failure appears on top and bottom of the epoxy film. In the model compression failure was allowed that is not possible experimentally. Therefore, the failure that appears on top of the film is not possible. Finally, the model predicts the failure the right location on the bottom.
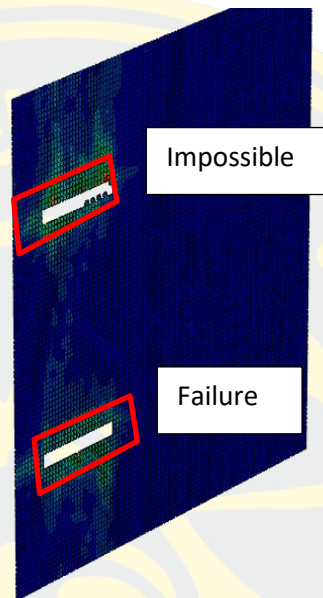
Figure 119: Result of adhesive film

The failure force obtained in the simulation is closed to the one measure experimentally (Table 26).

Table 26: Force between experimental and Finite element analysis

Experimental	FEA
120 N	130 N

The simulation matches the experiments in term of failure load and therefore can be used to optimize the bonding.

The model has been built and validated it can be used to optimize the contact by changing the surface area. Therefore, surface area has been increased and failure force has been extracted from the simulation. As it is time consuming to modifying the CAD of the stiffener under CATIA import in ABAQUS redo the mesh etc., so, by considering there is no influence of the contact surface on the mechanical behavior. Surface required to have 29 Nm of the failure moment can be calculated (Figure 119). Contact surface of 982 mm^2 is required to obtain 153 N to be applied force given by 29 Nm.
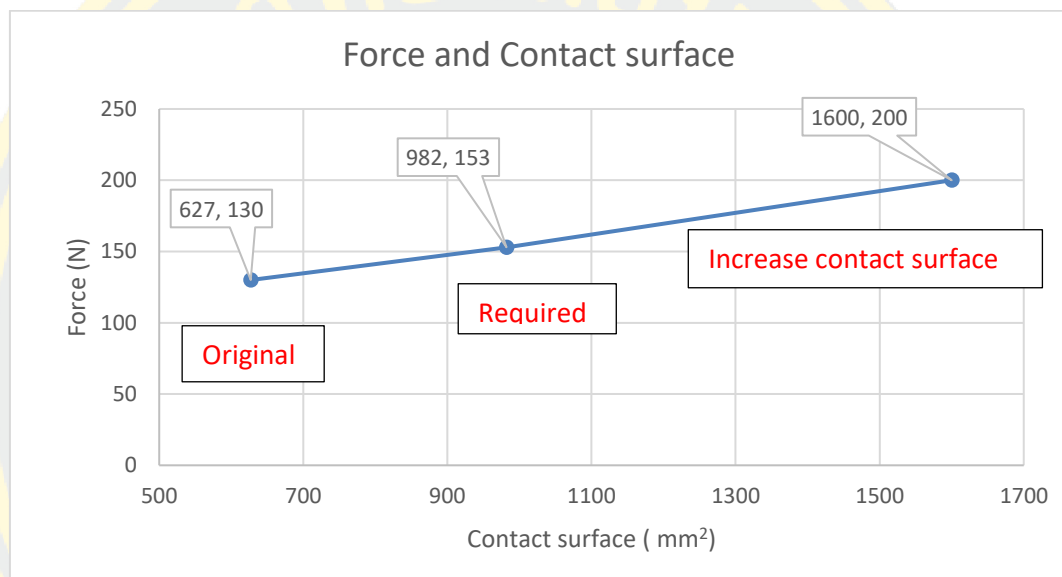
Figure 120: Force and required contact surface

Conclusion

In this chapter, manufacturing of prototype was performed by process of manufacture. Roles of all materials were used in this thesis has been detailed. Aerospace standard has been respected during manufacture process. Then, quality control was performed in order to check the quality of the stiffener. In case of testing process, global view of the test was detailed. The test result has been investigated and discussed. Local FEA has been performed in order to check the boundary condition and contact surface. FEA result prove L-bench as rigid body no failure on this component. Adhesive film result was found at the right location. Finally, the final optimization of the contact surface between adhesive film and stiffeners was investigated.

CHAPTER 7: CONCLUSION

Innovative of stiffeners spoiler has been proposed. The thesis focusses on static and buckling analysis only for Carbon epoxy prepreg Uni-Directional and for single aisle aircraft spoiler. While rotation feature was not considered. Different objective has been defined

- To analyze the case study. Loading and constrains applied on spoiler have been determined and calculated thanks to the literature. Moreover, aerospace design rules have been identified and composite limitation has been explained.

- To propose a innovative design of a spoiler for single aisle aircraft. Honeycomb is replaced by composite stiffeners in order to simplify the maintenance during the life cycle. The target is to be lightest as possible.

- To experimentally validate the simulation by comparing the results. A stiffener has been extracted and its design has been detailed. The prototype of the stiffener was manufactured and mechanically tested and results where compared with the numerical simulation.

Methodology has been proposed to reach the objectives. Firstly, conceptual design has been proposed after validation of the current spoiler. Topology has been used to determine the location of stiffeners. Secondly, preliminary design (GFEM) has been investigated. Global FEM has been studied to have first rough optimization where reaction force (RF) has been extracted to calculate the flange. Finally, detailed design has been realized under static and buckling.

By following thee aerospace stacking rules the mass of the optimized stiffener is finally higher than current spoiler. Indeed, buckling is the critical loading and more plies need to ne applied on the lower skin.

The prototype of stiffeners has been manufactured and test under static in order to validate the bonding between the stiffener and rotation feature. Simulation has been successfully proposed and used to optimize the bonding by increasing the bonding surface

Stiffeners spoiler is possible, but mass is higher than current honeycomb spoiler due to the buckling by using UD prepreg auto cleave process. In terms of manufacturing cost would be more expensive than honeycomb core spoiler but for water ingression during international flight is exempted by composite stiffeners spoiler. Technology to reduce the mass of the stiffener's spoiler can be used. Firstly, Resin Transfer Molding (RTM) process could be used. Indeed, RTM would

allow more complex geometry and shape specially to avoid the intersection between beam. Secondly, Thermoplastic carbon can be used to produce more complex shape.

REFERENCES

AIRBUS (2009). "Reference structure design principles for A350XWB Volume 2 general design principles ,Stacking Sequence Rules, Ply drop off, Bonding, Radius."

Bristow, J. W. and P. E. Irving (2007). "Safety factors in civil aircraft design requirements." Engineering Failure Analysis **14**(3): 459-470.

Campbell, F. C. (2010). "Structural Composite Materials." ASM International Technical Book Committee (2009–2010).

Chehroudi., B. (2016). "Composite Materials and Their Uses in Cars."

J.S.R, G. (2000). "Damage mechanisms and nondestructive testing in the case of water ingress in CF18 flight control surfaces."

John W. Rustenburg, Donal Skinn and D. O. Tipps. (August 1998). "Statistical Loads Data for Boeing 737-400 Aircraft in Commercial Operations."

John W. Rustenburg, Donald A. Skinn and D. O. Tipps. (2002). "Statistical Loads Data for the Airbus A-320 Aircraft in Commercial Operations."

LaPlante, G., A. E. Marble, B. MacMillan, P. Lee-Sullivan, B. G. Colpitts and B. J. Balcom (2005). "Detection of water ingress in composite sandwich structures: a magnetic resonance approach." NDT & E International **38**(6): 501-507.

LARSSON, R. (2016). "Methodology for Topology and Shape Optimization: Application to a Rear Lower Control Arm." Master's thesis in Applied Mechanics.

Rubem Matimoto Koide, Gustavo von Zeska de França and M. A. Luersen. (2012). "An ant colony algorithm applied to lay-up optimization of laminated composite plates."

Sadraey, M. "Spoiler design." Daniel Webster College.

V. Dattomaa, R. Marcucciob, C. Pappaletterec and G. M. Smithd. (2001). "Thermographic investigation of sandwich structure made of composite material." NDT&E International 34 (2001).

Verbart Alexander, Van Keulen Fred and L. Matthijs. (2015). "Topology Optimization with Stress Constraints." TU Delft.

BIOGRAPHY

NAME   Mr. Purith Polnikorn

DATE OF BIRTH   18 June 1994

PLACE OF BIRTH   Chonburi

PRESENT ADDRESS   114/13 หมู่.10 ต.ทุ่งสุขลา อ.ศรีราชา จ.ชลบุรี 20230

POSITION HELD   Research assistant at GISTDA

                               Project Engineer at Jinpao Precision Industry co. Ltd.

EDUCATION   Bachelor of Mechanical Engineering, Burapha University 2017

AWARDS OR GRANTS   Grant by GISTDA for Students fees and salary